FractalComs

Exploring the limits of Fractal Electrodynamics for the future telecommunication technologies
IST-2001-33055

Task 1.1 Final Report

Deliverable reference:	**D1**
Contractual Date of Delivery to the EC:	**July 31, 2003**
Author(s):	**Juan M. Rius, Jose María Gonzalez Arbesú, Jordi Romeu, Eugenia Cabot, Michael Mattes, Juan R. Mosig, Rafael Gómez, Amelia Rubio, Mario Fernadez Pantoja**
Participant(s):	**UPC, EPFL, UGR**
Workpackage:	**WP1**
Security:	**Public**
Nature:	**Deliverable**
Version: 1.0	**Date: July 3, 2003**

Total number of pages: 75

Abstract:

This deliverable describes the work done in task 1.1 to understand better the behaviour of electromagnetic fields and electric currents in pre-fractal domains, in order to acquire guidelines for the design of fractal-shaped antennas and microwave devices.

The conclusions are essentially that, as in any kind of antennas, the topology and the antenna geometry determine the radiation parameters. The fractal dimension of the limiting fractal object does not seem to play a significant role.

In order to design good miniature antennas, one have to take into account the electromagnetic coupling between the wire corners, the coupling between the feeder and the wire segments and the existing anti-parallel currents or wire loops.

Some non pre-fractal antennas that closely meet the design criteria, like the two-arm spiral, show excellent miniaturization properties.

It has been found also that high-directivity localized modes are not exclusive of pre-fractal antennas.

Keyword list: Pre-fractal geometries, miniature antennas, self-resonant antennas, resonant frequency, localized modes

TABLE OF CONTENTS

RELATED WP AND TASKS (FROM THE PROJECT DESCRIPTION)

WP1: Theory of fractal electrodynamics.

Task 1.1: Understanding fractal electrodynamics phenomena

- *Deliverables:* Report D1

Objective: Understand better the behaviour of electromagnetic fields and electric currents in fractal domains, in order to acquire guidelines for the design of fractal-shaped antennas and microwave devices.

Since the whole report of work done in task 1.1 is very extensive, the first section presents a brief summary; section 2 presents the conclusions and section 3 the antenna design guidelines that can be derived from the conclusions. The remaining sections include the complete reports of the research done in this task. The figure and table numbering is reset at each section.

1. SUMMARY

1.1. On the Influence of Fractal Dimension and Topology on Radiation Efficiency and Quality Factor of Self-Resonant Pre-fractal Wire Monopoles

Preliminary studies on small pre-fractal antennas [Puente et al., "The Koch monopole: a small fractal antenna", IEEE Trans. on Antennas and Propag., 48 (11), pp. 1773–1781] showed that fractal dimension might play a role in the radiation efficiency and quality factor of electrically small antennas. Its influence on the radiation pattern of small antennas is not of such importance because all electrically small monopoles have, essentially, the same radiation pattern. Nevertheless, until the work presented here no practical evidence has revealed a relation between fractal dimension and antenna parameters for self-resonant antennas.

The influence of fractal dimension on the behaviour of monopole antennas in terms of efficiency and quality factor has been investigated. Also, the role of the shape of pre-fractal monopoles with the same fractal dimension is analysed. This research has been carried out on 2D self-resonant pre-fractal wire monopoles and through the use of radiation efficiency and quality factor maps versus electrical size of the antennas at resonance.

The conclusions of this work are based on both measurements and simulations. It has been shown that manufacturing technology is able to fabricate highly iterated pre-fractal antennas and the preliminary measurements agree with simulated results for low-iteration pre-fractals.

Influence of fractal dimension:

Influence of radiation efficiency and quality factor on pre-fractal antennas has been analysed through the design of pre-fractal structures that in the limit converge to fractal

curves of dimension 1.26 (Koch), 1.58 (Sierpinski Arrowhead) and 2 (Hilbert and Peano).

The simulation results show that increasing the number of pre-fractal iterations means a reduction on radiation efficiency and an increase on quality factor. The increase of fractal dimension, although making better space filling curves, builds larger monopoles with lower efficiencies and higher quality factors even for the first iterations.

Prototypes of the simulated structures have been printed on a fibreglass substrate with standard techniques used for the manufacturing of printed circuits for electronic boards. All of the monopoles are designed as self-resonant antennas, so they do not need any external load to cancel out the reactive part of their input impedance. Conclusions from the measurements of the printed antennas are nor different from simulations.

Influence of topology:

The influence of topology on the radiation efficiency and quality factor of small self-resonant pre-fractal wire monopoles with the same fractal dimension has been investigated. Several iterated function systems (IFS) could be used to design fractals with the same fractal dimension. So far, the consequence of changing the topology of a fractal without changing the fractal dimension of the curve has not been analysed before FractalComs project.

Several designs of Sierpinski antennas are simulated, all of them with fractal dimension 1.58 but having different IFS initiators and, therefore, different topology. Also, several designs of self-resonant wired pre-fractals with fractal dimension 2 are analysed: the Hilbert and 3 designs of the Peano curve have been used.

Results for both families of pre-fractals (fractal dimension 1.58 and 2) reveal the same behaviour when the shape of the fractal defines a long wire (like the Hilbert monopole, variants 2 and 3 of the Peano curve and the Sierpinski Arrowhead monopole): the increase on iteration means an increase on quality factor, a decrease on efficiency, and a reduction of the electrical size of the antenna at resonance. When the topology is defined by loops (delta and Y- wired Sierpinski monopole, and Peano monopole) the increase on iteration number means a reduction of quality factor, an increase in radiation efficiency and a trend to stagnation on a Euclidean structure (a rhombic monopole in the case of the Peano curves, or a triangular antenna in the case of the Sierpinski monopoles). Convergence to these limits is faster as the number of loops of the monopole structure increases.

The above structures have been not only simulated, but also fabricated as printed monopoles using conventional printed circuit techniques. The measured results show a reduction of η and an increase on Q when increasing the iteration and fractal dimension of large wire antennas. When pre-fractal structures include loops, larger radiation efficiencies and smaller quality factors are found with increasing fractal dimension and iteration. Nevertheless, high miniaturization is not easily achieved using pre-fractal loops. Quick stagnation of performances and trends to certain Euclidean structures (triangular and rhombic monopoles) are also observed in the measurements for these cases.

1.2. Study of 3D pre-fractals

The 3D Hilbert monopole has been modelled. Its performance in terms of efficiency, quality factor and electrical size at resonance has been simulated and, finally, the first three iterations of the pre-fractal have been manufactured with patience. Figure 1 shows the wire models analysed by the simulation software.

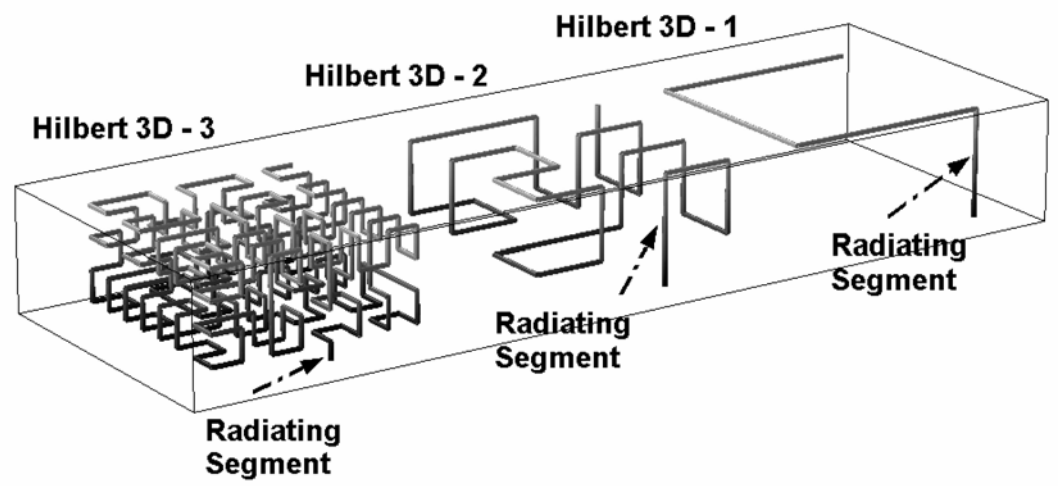

Figure 1. Simulated 3D Hilbert antennas in a monopole configuration. The first segment is the main contribution to radiation.

The computed current distribution along the wire suggests that the first segment, connected to the feeder and perpendicular to the ground plane, is the main source of radiation, while the rest of the antenna behaves as a load.

Table 1 summarizes the computed parameters for these 3D models, showing that while the ratios of miniaturization are remarkable, the loss efficiencies and the quality factors achieved are unpractical. The extremely low value of the radiation resistance agrees with the hypothesis that only the feeding segment of the pre-fractal radiates as an electrically very small monopole, and the rest of the structure is a capacitive load that reduces the input reactance, and therefore, the resonant frequency.

Antenna	Total Wire Length (cm)	Electric Size at Resonance, *ka*	Resonant Frequency (MHz)	Radiation Resistance at Resonance (Ohms)	Input Resistance at Resonance (Ohms)	Efficiency (%)	Quality Factor	Fundamental Limit, Q
Hilbert 3D-1	61,78	0,71	127,5	2,47	3,24	76,6	126	4
Hilbert 3D-2	184,99	0,25	51,4	0,16	1,67	9,4	2091	70
Hilbert 3D-3	642,61	0,10	21,0	0,01	3,07	0,5	31966	1088

Table 1. Computed performance of the first three iterations of a 3D Hilbert monopole.

1.3. On the resonant frequency of pre-fractal miniature antennas

Wire antennas miniaturization is usually based in packing a long wire inside a small volume. It has been already shown that the resonant frequency of the Koch monopole decreases as the number of fractal iterations increases. However, it has been found later that some non-fractal configurations that enclose a long wire into a finite volume also lead to a similar or better reduction in the resonant frequency, compared to the straight monopole having the same enclosing volume. In all cases, the resonant frequency is higher than that of a straight monopole of the same wire length.

This work investigates further in the dependence of the resonant frequency with the monopole geometry, in order to acquire guidelines for the design of self-resonant small antennas, in which an increase of the wire length effectively leads to a reduction in the resonant frequency.

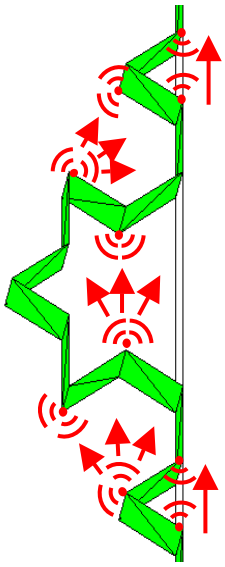

Fig. 2: Shorcuts

Hypothesis:

The observed behaviour is due to the coupling between sharp angles at curve segment junctions. These angles radiate a spherical wave with phase centre at the vertex (Fig. 2). Each angle not only radiates, but also receives the signal radiated by other angles. As a consequence, part of the signal does not follow the wire path, but takes "shortcuts" that start at a radiating angle. The length of the path travelled by the signal is, therefore, shorter than the total wire length. The higher iteration number in the Koch antenna, the more angles it has and the closer to each other they are, so the more signal takes shortcuts and the less signal follows the whole curve path.

Numerical simulations in the frequency and time domains lead to the following conclusions, that fully support the shortcut or coupling hypothesis:

- The resonant frequency increases if the strip width is increased.
- Pre-fractal antennas of the same class and IFS iterations have shorter electrical height at resonance if the physical size of the antenna is larger.
- The reduction factor in the resonant frequency from K_i to K_{i+1} monopoles of size h is the same as the reduction factor from K_{i+1} to K_{i+2} monopoles of size sh, where s is the IFS scale factor.

Comparison with other pre-fractal and non-prefractal monopoles:

The coupling or shortcut hypothesis is also valid for other kinds of pre-fractal or non-fractal miniature monopoles. Different kinds of miniature wire monopoles having the same wire length exhibit different length of signal leaps –or shortcuts- between wire angles, resulting in a different amount of coupling signal that takes the shortcut. For that reason, these antennas have different resonant frequency while having the same monopole height h and the same wire length.

Two pre-fractal monopoles of different fractal dimension in the limit and two non-fractal antennas have been analysed (Fig. 3). The generalized Koch and the wide zigzag configurations, for equal wire length, show longer signal leaps –or shortcuts- than the Koch or the narrow zigzag. The longer signal leaps, the less amount of coupling signal that takes the shortcut, the longer path followed by the signal and the lower resonant frequency.

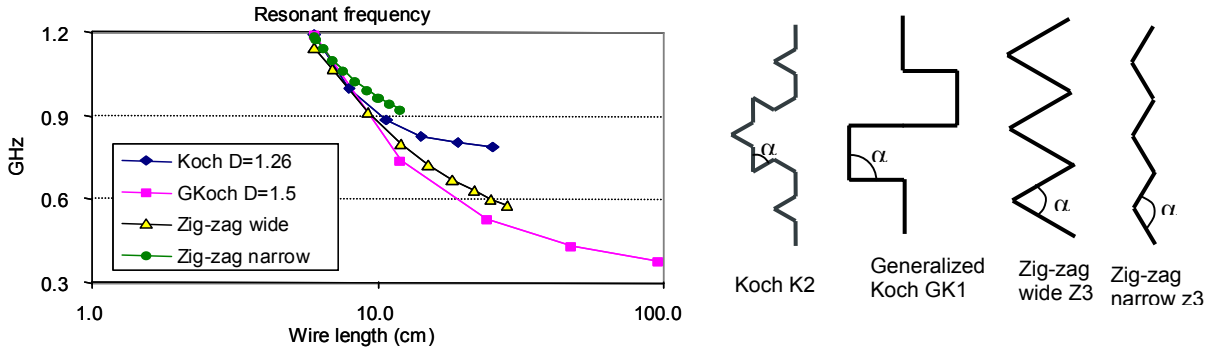

Figure 3: Resonant frequency as a function of the wire length. The antennas have been modeled as extrusion-strips of 1-mm width. Each marker in the plot corresponds to an IFS iteration in the pre-fractal geometries or the number of meanders in the zig-zags.

1.4. Benchmarks for pre-fractal antenna performance

In order to develop accurate numerical tools for pre-fractal antennas, well-defined non-fractal benchmarks must be first considered. Two Euclidean structures that have been found to posses properties that were considered exclusive of pre-fractal antennas are the meander printed line and the two-arm spiral.

High-gain localized modes: the meander line

The meander-line printed antenna has been carefully studied in order to see if it has high-gain localized modes, like the pre-fractal Koch-island patch, or not. The objective here is to assess if the localized modes are exclusive of pre-fractal structures, or not.

The meander antenna is a rectangular printed patch with N gaps of infinitesimal width parallel to two sides of the rectangle. The N gaps transform the rectangular patch in a line with N meanders.

The meander antenna has been compared with the original patch without the gaps:

- At low frequencies, below the patch resonance, the current follows the meander line. The input impedance of the meander behaves as that of the equivalent line. This is useful for antenna miniaturization, because it presents almost the same resonance frequency that unwrapped line and occupies much less space.
- At high frequencies (for example 4th resonance of the patch) the meanders couple one with the other and the antenna behaves more like a patch with gaps. Hot spots or "localized modes" appear at the end of the gaps (Fig. 4). The ones at the top of the antenna are in phase, and the ones at the bottom are also in phase, but in counter-phase with the ones at the top.

- For higher frequencies complex resonance phenomena appear due to EM coupling between the parallel lines. Further studies are needed in order to understand these complex phenomena.

Since localized modes have been known since the 60's and outside the scope of fractal or pre-fractal structures, **we can conclude that localized modes are not exclusive of pre-fractal antennas**.

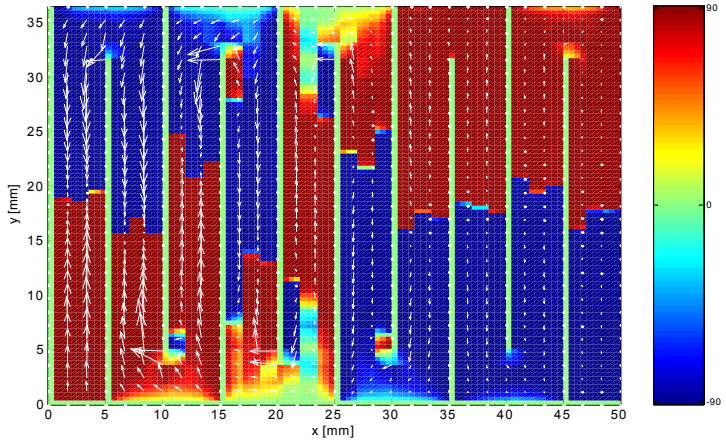

Fig. 4: Higher order mode at the printed meander line antenna. The colour scale shows the phase and the arrow length the magnitude of the imaginary part of the electric current.

Miniature antenna: The two-arm spiral.

A study of a two-arm square microstrip spiral antenna backed by a ground plane has been made (Fig. 5).

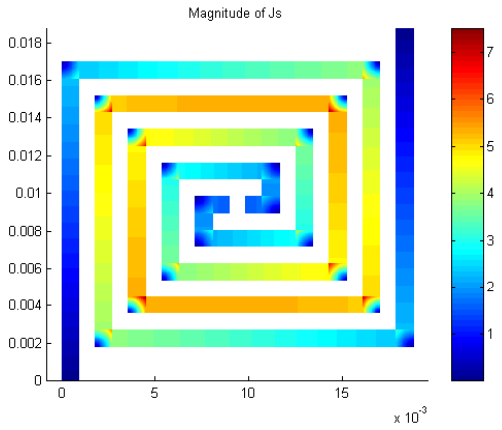

Fig. 5: Current magnitude at the first resonance of a four-turn two-arm spiral antenna.

A spiral presents interesting properties from the geometric point of view, namely self-similarity and infinite length in a finite surface, properties shared by fractal objects. Having chosen a polygonal spiral rather than a Archimedean one is due to the fact that polygonal spiral fits better in a given surface, achieving a more efficient utilization of given area, a principle to take into account when miniaturizing antennas.

Taking as working surface a square of side SL=1.875cm, different iterations of a spiral have been studied and compared with two straight dipole configurations: the dipole of length equal to the unwrapped spiral length and the longer dipole that would fit in the reference square, having as length the diagonal of the square.

Table 2 shows that the spiral antenna has a resonant frequency almost as low as the straight dipole of same wire length. According to the guidelines derived from the shortcuts or couplings study in preceding section, this is due to the weak electromagnetic coupling between angles, between the feeder and the strip or between parallel strip segments with opposite current. Unlike pre-fractal antennas, the resonant frequency scales almost linearly with the inverse of strip length while keeping the wire enclosed by a small square.

	Resonant freq. [GHz]
Spiral 4-turns	1.77
Straight dipole unwrapped spiral	1.6
Straight dipole diagonal	11.6

Table 2: Resonant frequency of a 4-turn two-arm spiral, the straight monopole of equal length and the longer monopole that would fit in the reference square

The spiral antenna constitutes a very good benchmark to judge pre-fractal antennas as provides a tough challenge offering excellent miniaturization while keeping a reasonable frequency behaviour.

2. CONCLUSIONS

- When the number of IFS iterations (order of the pre-fractal) increases beyond a certain threshold, the change in radiation patterns and input impedance of the antenna tends to zero. In other words**,** there is no use in increasing the number of IFS iterations. Convergence is usually achieved between 4 and 6 iterations. This value depends largely on the size, wire radius or strip width and topology of the antenna.
- The increase of fractal dimension, although making better space filling curves, builds larger monopoles with lower efficiencies and higher quality factors even for the first iterations, at least for wire structures without loops.
- Topology has a stronger influence than fractal dimension on the behaviour of planar pre-fractal wire monopoles, in particular on the losses efficiency.
- When the wire geometry contains no loops, each IFS iteration increases the length and bending of the wires, and as a consequence ohmic losses and the amount of stored energy on the surrounding of the antenna increases (this means lower radiation efficiencies and higher quality factors). While the ratios of miniaturization are remarkable, achieved efficiencies and quality factors are unpractical. The low radiation resistances are due to the presence of anti-parallel currents that cancel the radiation of each other.
- Wire geometries containing loops do not have anti-parallel currents. Although they do not achieve a large degree of miniaturization, as the number of loops inside the structure increases, efficiency and fractional bandwidth (inverse of quality factor) seem to increase with the order of the pre-fractal (number of IFS iterations).
- It has been observed that radiation resistance results are dependent on the length of the feeding segment of the monopole, which seems to be the main source of radiation, while the rest of the structure behaves as a capacitive load that reduces the resonant frequency.
- The hypothesis of electromagnetic coupling –or shortcuts- between corners fully explains why the resonant frequency of pre-fractal antennas is much larger than what could be expected from the wire length only, and why it stagnates as the number of IFS iterations increases.
- As a result of the electromagnetic coupling hypothesis, some guidelines for the design of small antennas have been derived. An antenna design that follows these guidelines, the two-arm spiral antenna, has the smallest possible size for a given resonant frequency.
- The design of wire small antennas using pre-fractal geometries has the advantage of using an easily programmable IFS algorithm to pack a long wire into a given volume. However, the mere fact of being a pre-fractal object does not imply that the degree of miniaturization and antenna parameters are optimum. As in any other kind of antenna, it is in fact the antenna geometry what determines the radiation behaviour. The previous conception that “fractal antenna” is equivalent to “optimum miniaturization and bandwidth” is perhaps a misunderstanding of the well-known

Hansen's statement: "To obtain performance closer to the minimum Q curve the spherical volume must be used more effectively".

- Some pre-fractal antennas have a slightly smaller electrical size than its conventional counterparts while maintaining their main radiation parameters (quality factor and loss efficiency). This has been assessed for planar monopole configurations.

3. GUIDELINES FOR THE DESIGN OF MINIATURE MONOPOLES

As a conclusion of the work in this task and very recent work available in the literature, the following guidelines can established for the design of miniature wire antennas:

1- In order to reduce signal coupling –or shortcuts- between wire angles, the distance between those angles must be as large as possible, and the angles α the larger possible.

2- In order to reduce the signal coupling between the feeder and the wire segments, the most possible wire length must be perpendicular to the electric field radiated by the feeder.

3- In order to reduce coupling between wire segments, parallel wire segments with opposite (anti-parallel) currents very close to each other must be avoided.

An example of wire antenna that closely follows these guidelines is a two-arm spiral. The resonant frequency of a square spiral is inversely proportional to the wire length, while keeping the wire enclosed by a small square.

4. ON THE INFLUENCE OF FRACTAL DIMENSION AND TOPOLOGY ON RADIATION EFFICIENCY AND QUALITY FACTOR OF SELF-RESONANT PRE-FRACTAL WIRE MONOPOLES

4.1. Introduction

The influence of fractal dimension and topology on the radiation efficiency and quality factor of small monopoles has been investigated through the design of 2D self-resonant prefractal wire monopoles.

Why wire monopoles?

- because monopole configurations are easy to fabricate;
- because monopoles do not need baluns to balance currents on the arms of the antenna;
- because wire monopoles are fabricated with wires, but also with strips supported on a dielectric substrate;
- because wire monopoles are simple structures and the conclusions obtained with wires are easily extended to all kind of antennas.

Why 2D prefractal structures?

- because they are easily fabricated with the standard technology used for printed circuit manufacturing;
- because it is simple and quick to check the correct manufacturing of prototypes;
- because conclusions obtained for 2D prefractals are also easily extended to 3D structures.

Sections 4.3 and 4.4 briefly shows the results obtained from simulated bidimensional prefractal wire monopoles computed with Numerical Electromagnetics Code [NEC, 1981]. This software, although not suitable for the analysis of fractal (nor prefractal) structures, was used to make a first approach to self-supporting prefractal wire structures. Their results do not take into account the presence of the dielectric substrate that supports the strip structure really fabricated, nor the presence of a limited size ground plane. Nevertheless, results from NEC are quite accurate to be considered a reference.

In section 4.5, the simulated structures that were fabricated are shown. A first set of measurements carried out using the Wheeler cap method is also presented. While a properly dimensioned cap is going to be acquired in order to get more accurate results, a small cylindrical cap was used at first. Results with this cap are in perfect agreement with the trends from simulations.

Conclusions are summarized at section 4.6 of this report.

4.2. Glossary

D: fractal dimension;
DWS-*i*: Delta Wired Sierpinski monopole of iteration *i*;
H-i: Hilbert monopole of iteration *i*;
K-*i*: Koch monopole of iteration *i*;
K1S-*i*: Koch-1 wired Sierpinski monopole of iteration *i*;
P-i: Peano monopole of iteration *i*;
Pv2-i: Peano variant 2 monopole of iteration *i*;
Pv3-i: Peano variant 3 monopole of iteration *i*;
Q: quality factor;
SA-i: Sierpinski Arrowhead monopole of iteration *i*;
YWS-*i*: Y-Wired Sierpinski monopole of iteration *i*;

η: radiation efficiency.

4.3. Influence of fractal dimension

Influence of radiation efficiency and quality factor on prefractal antennas is analysed through the design of prefractal structures with different stages of growth of fractals with fractal dimension ranging from 1.26 to 2. These antennas make better use of space than any other geometrical structures, but no practical research (apart from [Puente, 1998], [Puente-Baliarda, 2000], [Gianvittorio, 2002]) has been carried out to reveal that fractal geometries really improve the behaviour of common small antennas in terms of quality factor.

Simulations are the first step to a deeper study on the influence of fractal dimension on radiation efficiency and quality factor. Structures with fractal dimension 1.26, 1.58 and 2 are selected: Koch monopoles (K), Sierpinski Arrowhead monopoles (SA) and Hilbert monopoles (H), respectively. Peano monopoles (Pv2) are also simulated as fractal structures with fractal dimension 2. These monopoles, that we call *variant* 2, are not strictly fractals because they are slightly altered to avoid crossings among wires and make the structure more suitable for miniaturisation.

Simulated antennas are all resonant at 800 MHz and *virtually* fabricated with copper wire of radius 0.2 mm. Their radiation efficiency and their quality factor at resonance are summarised at table 1, together with their electric size k_0a, being k_0 the wavelength number at resonance and a the radius of the smallest sphere that encloses the antenna (and its image, because the designed structures are monopoles). The performance of a conventional $\lambda/4$ monopole is also shown as reference to compare results.

Antenna	D	k_0a	Q	η
λ/4 monopole at 0,8 GHz	1,00	1,49	7,1	99,2
K-1	1,26	1,24	10,3	98,7
K-2	1,26	1,09	13,0	98,1
K-3	1,26	1,01	15,0	97,3
K-4	1,26	0,99	15,1	96,4
SA-1	1,58	1,08	11,7	98,5
SA-2	1,58	0,78	25,3	96,6
SA-3	1,58	0,63	38,6	93,7
SA-4	1,58	0,53	55,0	89,3
SA-5	1,58	0,49	66,4	83,3
Pv2-1	2,00	0,72	34,7	94,8
Pv2-2	2,00	0,45	99,5	76,8
H-2	2,00	0,57	53,0	90,9
H-3	2,00	0,40	114,6	76,2
H-4	2,00	0,33	204,5	52,0

Table 1. Simulated results of electric size k_0a, radiation efficiency η and quality factor Q at resonance of Koch monopoles, Sierpinski Arrowhead monopoles, Peano monopoles (variant 2) and Hilbert monopoles compared with the performance of a $\lambda/4$ monopole.

Figures 1 and 2 show how the increasing order of the prefractal means a reduction on radiation efficiency and an increase on quality factor. The increase of fractal dimension, although making better space filling curves, builds larger monopoles with lower efficiencies and higher quality factors even for the first iterations. It is worth emphasizing that in the figures the dashed lines join the behaviour of prefractals of the same family, for instance, Koch monopoles or Sierpinski Arrowhead monopoles. The fundamental limitation for the quality factor (in the case of linear polarization) established by Chu [Chu, 1948] and reexamined by McLean [McLean, 1996] is also displayed in figure 2.

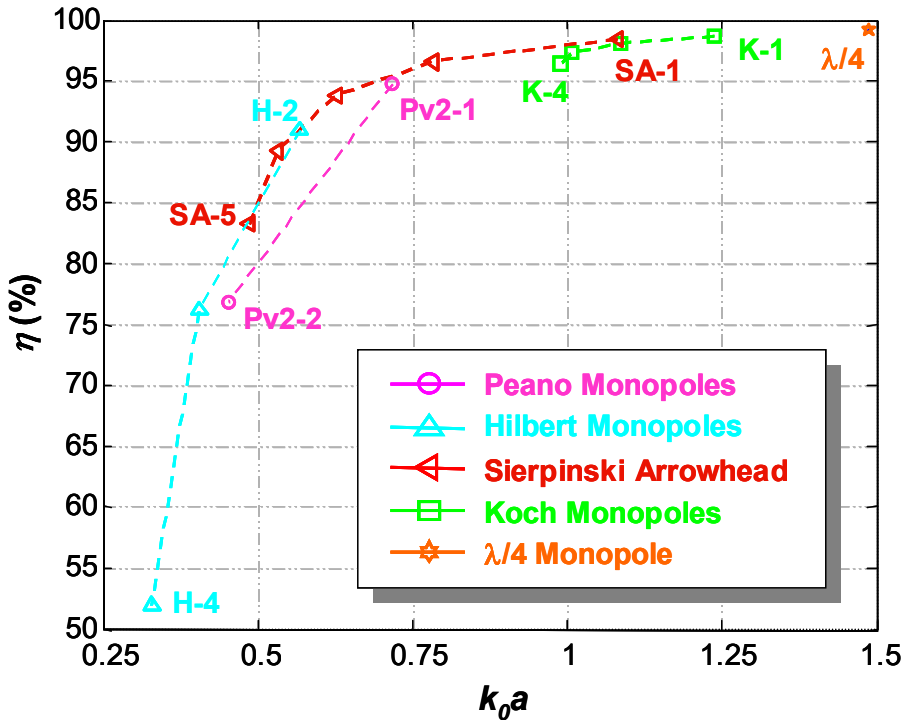

Figure 1. Simulated radiation efficiency (η) of some prefractal curves: Koch monopole, Sierpinski monopole, Peano monopole, Hilbert monopole and λ/4 monopole.

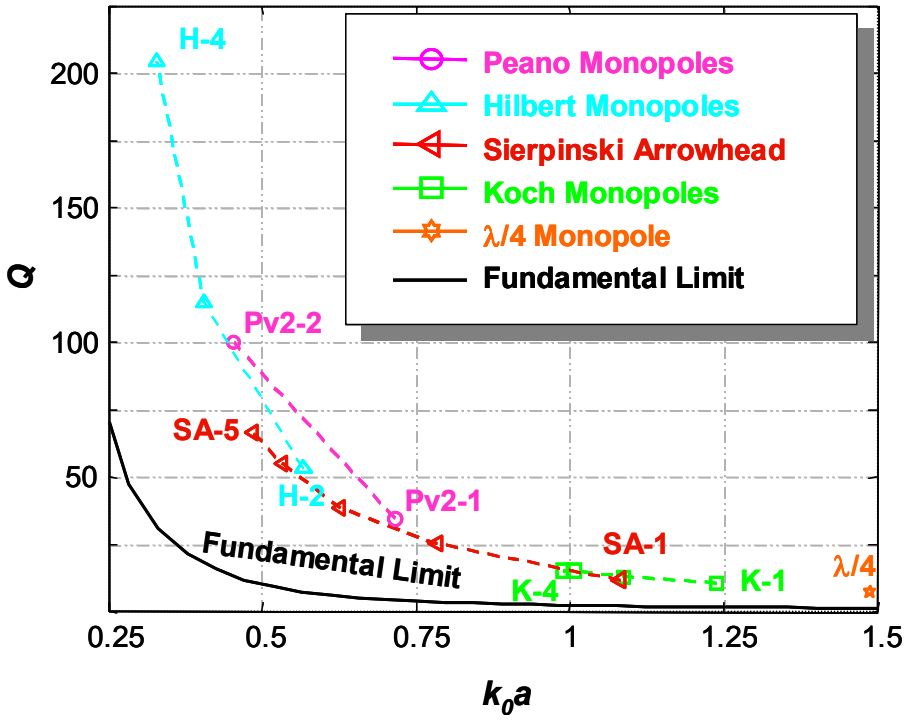

Figure 2. Simulated quality factor (Q) of some prefractal curves: Koch monopole, Sierpinski monopole, Peano monopole, Hilbert monopole and λ/4 monopole.

4.4. Influence of topology

The influence of topology on the radiation efficiency and quality factor of small self-resonant prefractal wire monopoles with the same fractal dimension is investigated. Several iterated function systems could be used to design fractals with the same fractal dimension. So far, the consequence of changing the topology of a fractal without changing the fractal dimension of the curve has not been analysed.

To investigate this relation several designs of Sierpinski antennas are simulated, all of them with fractal dimension 1.58. Also, several designs of self-resonant wired prefractals with fractal dimension 2 are analysed. Hilbert curves and 3 designs of Peano curves have been used. As mentioned, one of them (Peano variant 2), though strictly not a fractal, is slightly altered to construct a wired monopole able to achieve higher compression ratios.

Monopoles of fractal dimension 1.58 are all made resonant at 1200 MHz, while monopoles of fractal dimension 2, with the exception of Peano monopole, are made resonant at 800 MHz to have *manufacturable* dimensions. Monopoles are simulated with thin copper wires of 0.06 mm-radius. All of them are connected to their feeding point through a 2 mm length wire.

Figure 3 shows the simulated results of efficiency (left) and quality factor (right) for the fractals of fractal dimension 1.58. Results for the prefractals with fractal dimension 2 are displayed in figure 4. Results for both types of fractals reveal the same behaviour when the shape of the fractal defines a long wire (like the Hilbert monopole, variants 2 and 3 of the Peano curve and the Sierpinski Arrowhead monopole): the increase on iteration means an increase on quality factor, a decrease on efficiency, and a reduction of the electrical size of the antenna at resonance. When the topology is defined by loops (delta and Y- wired Sierpinski monopole, and Peano monopole) the increase on iteration number means a reduction of quality factor, an increase in radiation efficiency and a trend to stagnation on a Euclidean structure (a rhombic monopole in the case of the Peano curves, or a triangular antenna in the case of the Sierpinski monopoles). Convergence to these limits is faster as the number of loops of the monopole structure increases.

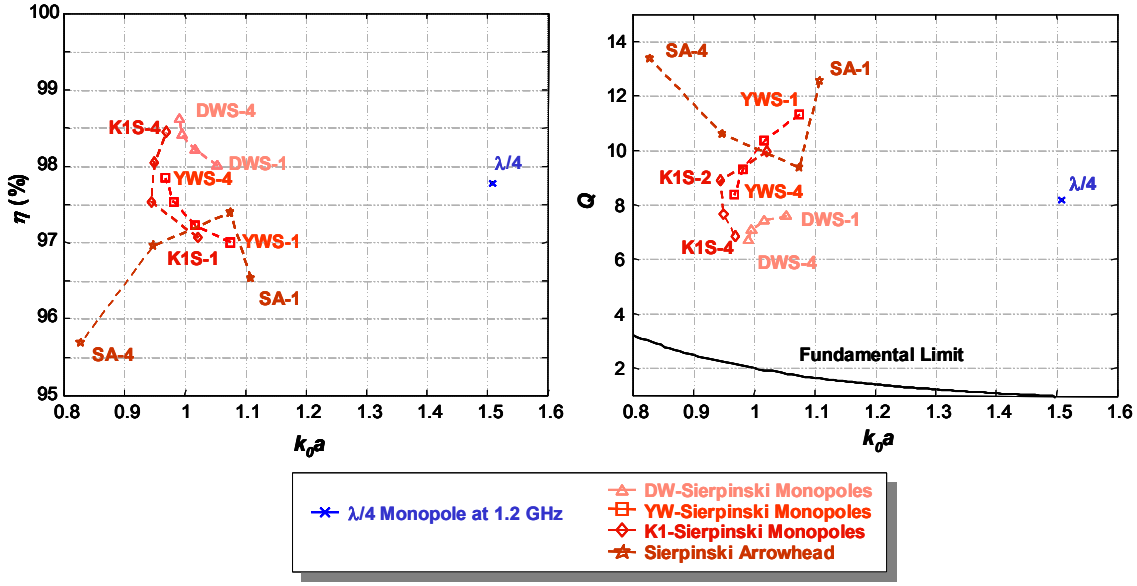

Figure 3. Simulated results of prefractals with fractal dimension 1.58 compared with a conventional λ/4 monopole: efficiency (η) at left, and quality factor (Q) at right.

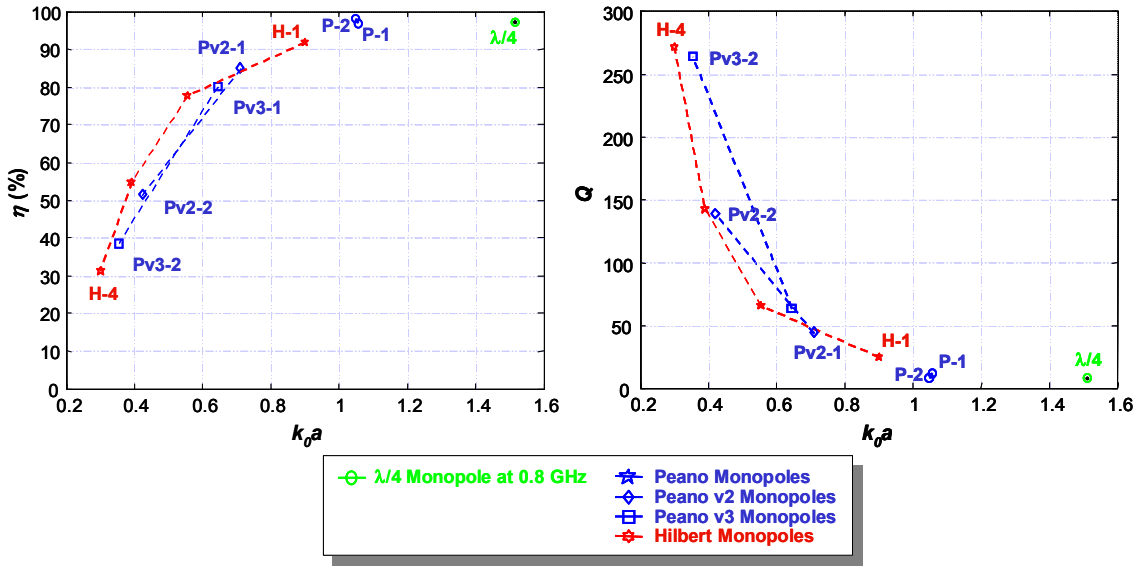

Figure 4. Simulated results of prefractals with fractal dimension 2 compared with a conventional λ/4 monopole: efficiency (η) at left, and quality factor (Q) at right.

Table 2 summarizes the performance of these self-resonant monopoles at resonance, including their electric size, their efficiency and their quality factor.

Antenna	D	k_0a	Q	η
λ/4 monopole at 0,8 GHz	1,00	1,51	8,7	97,3
λ/4 monopole at 1,2 GHz	1,00	1,51	8,2	97,8
P-1	2,00	1,06	11,9	97,3
P-2	2,00	1,05	8,1	98,1
Pv2-1	2,00	0,71	43,2	85,1
Pv2-2	2,00	0,42	141,6	51,9
Pv3-1	2,00	0,64	63,5	80,3
Pv3-2	2,00	0,35	264,4	38,6
H-1	2,00	0,90	24,4	91,8
H-2	2,00	0,56	65,3	77,6
H-3	2,00	0,39	142,1	54,8
H-4	2,00	0,30	270,9	31,2
DWS-1	1,58	1,05	7,6	98,0
DWS-2	1,58	1,01	7,4	98,2
DWS-3	1,58	1,00	7,1	98,4
DWS-4	1,58	0,99	6,7	98,6
YWS-1	1,58	1,07	11,3	97,0
YWS-2	1,58	1,02	10,3	97,2
YWS-3	1,58	0,98	9,3	97,5
YWS-4	1,58	0,97	8,4	97,8
K1S-1	1,58	1,02	10,0	97,1
K1S-2	1,58	0,94	8,9	97,5
K1S-3	1,58	0,95	7,7	98,1
K1S-4	1,58	0,97	6,9	98,5
SA-1	1,58	1,11	12,5	96,5
SA-2	1,58	1,07	9,4	97,4
SA-3	1,58	0,95	10,6	97,0
SA-4	1,58	0,83	13,4	95,7

Table 2. Simulated results of electric size k_0a, radiation efficiency (η) and quality factor (Q) at resonance of several monopoles with fractal dimension 1.58 and 2 compared with a $\lambda/4$ monopole (with fractal dimension 1).

4.5. First prototypes and preliminary results

Influence of fractal dimension

Simulated structures of section 4.1 have been printed on a fibreglass substrate (FR4) with standard techniques used for the manufacturing of printed circuits for electronic boards. The strips that configure the monopole are 0.35 mm wide (and 35 μm thick) and are welded to an SMA connector attached to the 800 x 800 mm^2 ground plane through a 5 mm strip.

All of the monopoles are designed as self-resonant antennas, so they do not need any external load to cancel out the reactive part of their input impedance. All of them are resonant at ~780 MHz, being slightly deviated from the designed resonant frequency due to the presence of the substrate and the fact that the monopoles are constructed with strips and not with wires as simulated with NEC. Figure 5 shows the fabricated monopoles compared with a coin of 10 euro cents.

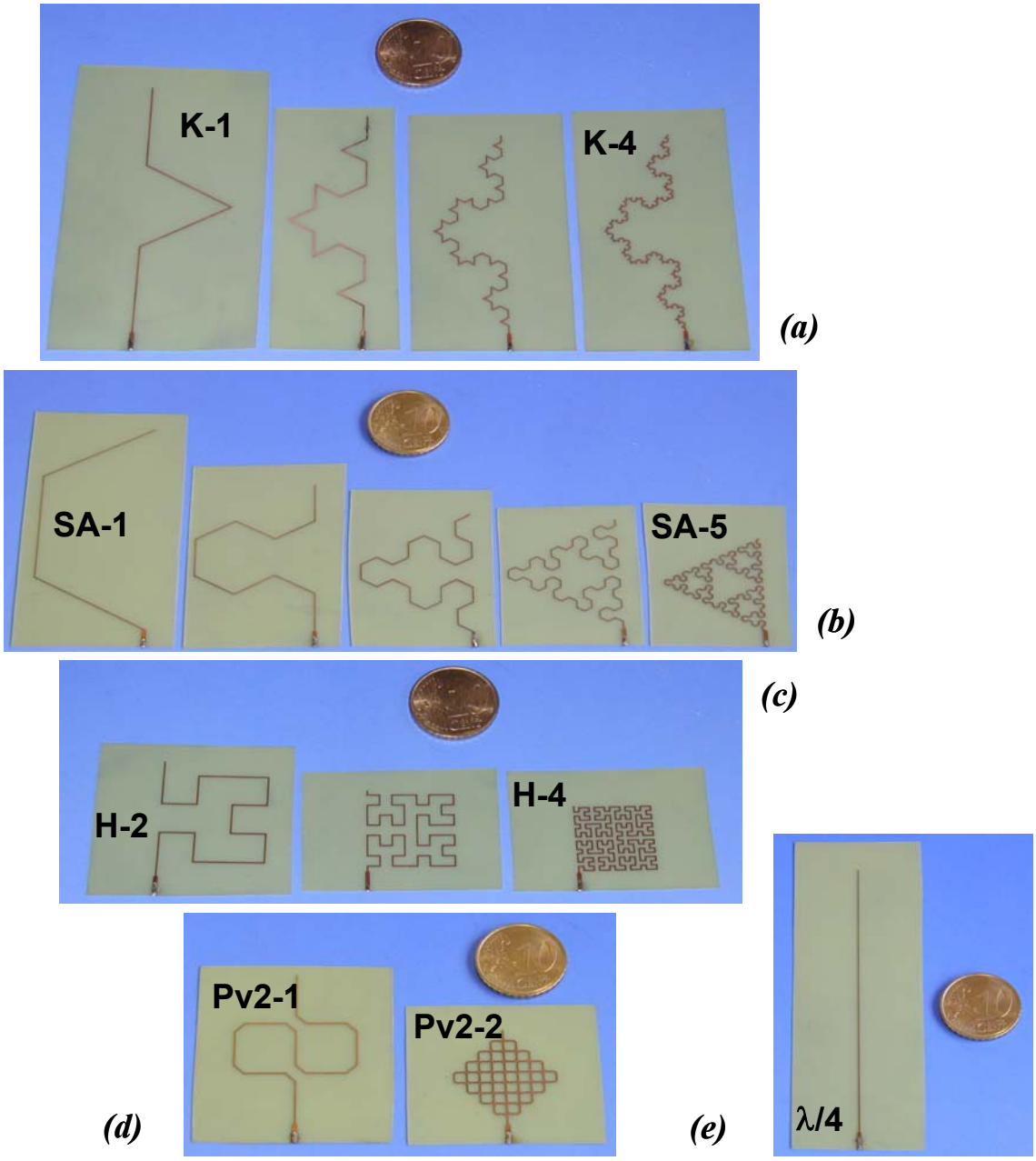

Figure 5. Printed monopoles used for the investigation on the influence of fractal dimension on radiation efficiency and quality factor: (a) Koch monopoles; (b) Sierpinski Arrowhead monopoles; (c) Hilbert monopoles; (d) Peano variant 2 monopoles; and (e) λ/4 monopole.

Preliminary results of radiation efficiency and quality factor have been measured using the Wheeler cap method with a 120 mm-high cylindrical cap of 30 mm-radius. Table 3 and figures 6 and 7 summarizes the measured results. Though the cap is small we are confident about the results thanks to previous experiences on small caps that do not fulfil the distance a criterion ($a \geq \lambda/2\pi$) between the antenna centre and the walls of the caps. Also, the measured trends agree with simulations of previous sections and with the values expected for a $\lambda/4$ Euclidean monopole. More accurate measurements will result when a wider cap is acquired and used.

Conclusions from the measurements of the printed antennas are nor different from simulations. Fractal dimension makes possible the design of miniaturized antennas (observed from the reduction of the product k_0a with the increasing iteration and the increasing fractal dimension) but with higher and higher quality factors and smaller and smaller radiation efficiencies at self-resonance.

Antenna	D	k_0a	Q	η
$\lambda/4$ monopole of 82,4 mm height	1,00	1,36	7,7	92,7
K-1	1,26	1,15	10,2	91,1
K-2	1,26	0,98	16,3	85,6
K-3	1,26	0,95	14,0	86,9
K-4	1,26	0,94	14,2	86,7
SA-1	1,58	1,00	12,8	89,8
SA-2	1,58	0,75	25,0	81,4
SA-3	1,58	0,62	39,4	72,5
SA-4	1,58	0,52	59,3	63,3
SA-5	1,58	0,49	65,1	56,6
Pv2-1	2,00	0,70	33,3	75,6
Pv2-2	2,00	0,45	108,3	42,3
H-2	2,00	0,58	49,9	68,2
H-3	2,00	0,46	101,1	45,9
H-4	2,00	0,38	178,1	28,0

Table 3. Measured results of electric length k_0a, radiation efficiency η and quality factor Q at resonance of several monopoles with fractal dimension 1.26, 1.58 and 2 compared with a $\lambda/4$ monopole with fractal dimension 1.

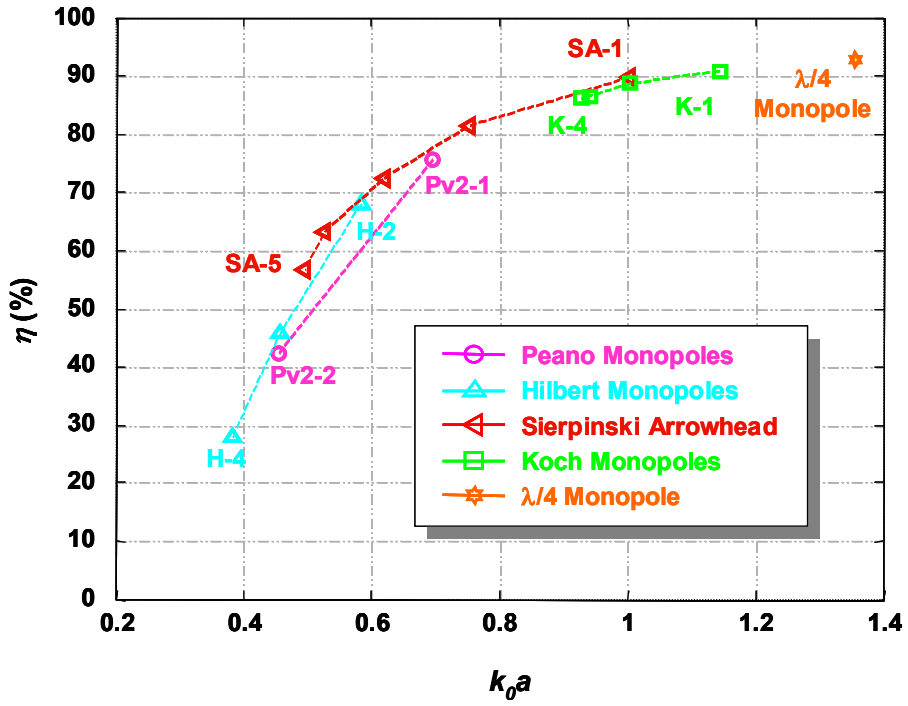

Figure 6. Measured radiation efficiency (η) of some prefractal curves: Koch monopole, Sierpinski monopole, Peano monopole, Hilbert monopole and λ/4 monopole.

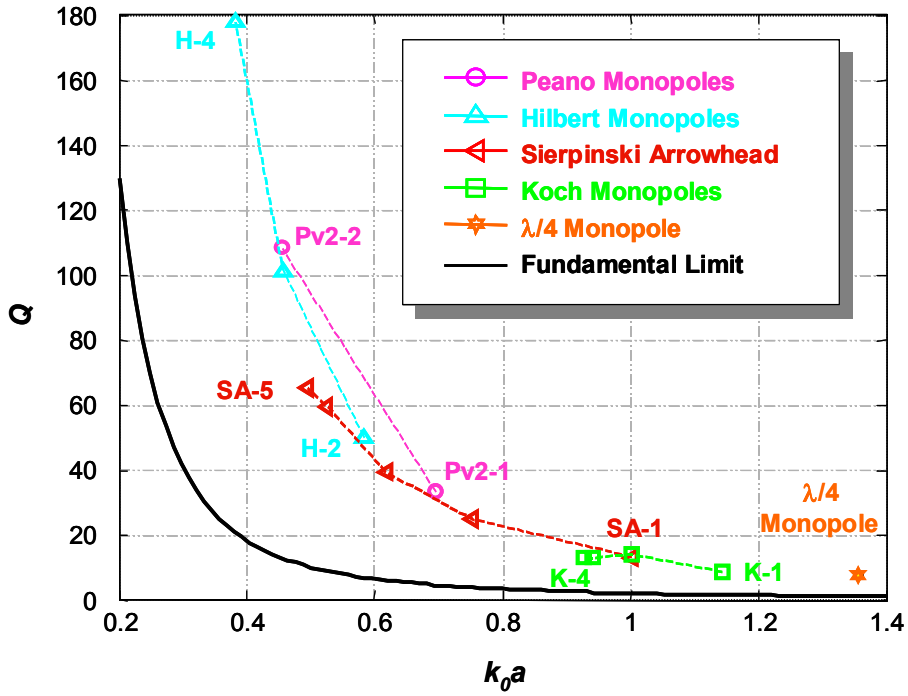

Figure 7. Measured quality factor (Q) of some prefractal curves: Koch monopole, Sierpinski monopole, Peano monopole, Hilbert monopole and λ/4 monopole.

Influence of topology

Fractals with fractal dimension 1.58 and 2 are fabricated as microstrip monopoles using conventional printed circuit techniques. Monopoles are fabricated with 0.35 mm strips and welded to the feeding pin of an SMA connector attached to the 800 x 800 mm^2 ground plane using a 2 mm high pedestal. Figures 8 and 9 show the manufactured prefactals of fractal dimension 1.58 and 2, respectively.

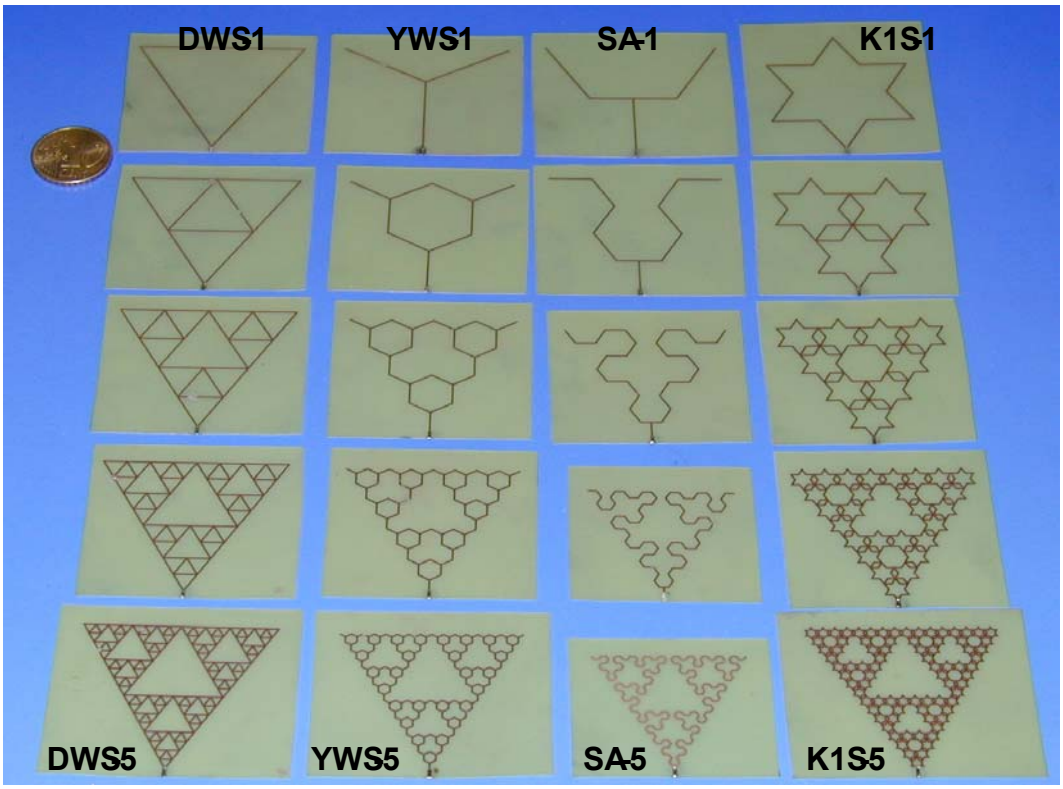

Figure 8. Manufactured prefractals with fractal dimension 1.58 compared with the size of 10 euro cents. From left to right and by columns: Delta-Wired Sierpinski monopoles (DWS); Y-Wired Sierpinski monopoles (YWS); Sierpinski Arrowhead monopoles (SA); and Koch-1 Sierpinski monopoles (K1S).

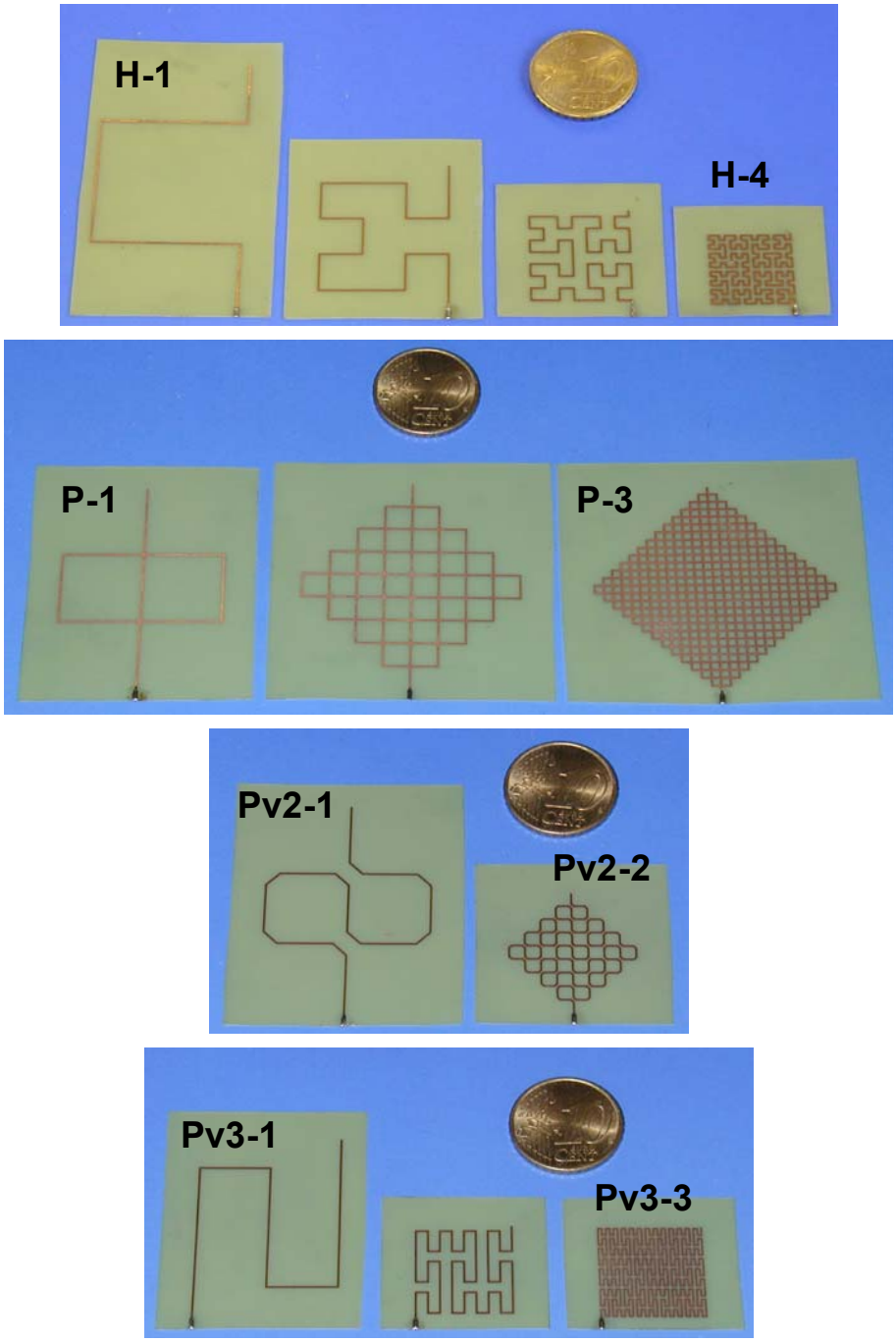

Figure 9. Manufactured prefractals with fractal dimension 2 compared with the size of 10 euro cents. From top to bottom: Hilbert monopoles (H); Peano monopoles (P); Peano variant 2 monopoles (Pv2) and Peano variant 3 monopoles (Pv3).

All of the self-resonant prefractal monopoles were designed to be resonant around 780 MHz and 1000 MHz. The resonant frequency was selected according to the size of the monopole. It is preferred not to increase the width of the area covered by the monopole more than 50 mm due to mechanical limitations in the measurement process. The monopoles are preliminary characterized in terms of their radiation efficiency and quality factor using the Wheeler cap method with the small cylindrical cap described at section 4.1. Figures 10 and 11 show their behaviour in terms of radiation efficiency and quality factor and table 4 summarizes the measured results. The prefractal antennas are

compared with a conventional $\lambda/4$ monopole, rhombic, square and triangular monopoles to show trends on their behaviour. Figure 12 shows the manufactured Euclidean antennas.

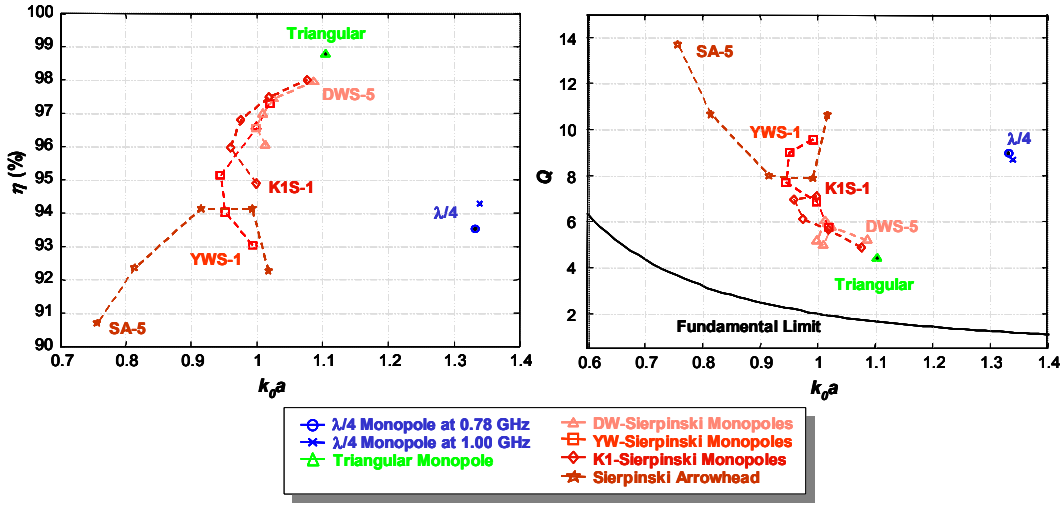

Figure 10. Measured results of prefractals with fractal dimension 1.58 compared with a conventional λ/4 monopole and a triangular monopole: radiation efficiency (η) at left, and quality factor (Q) at right.

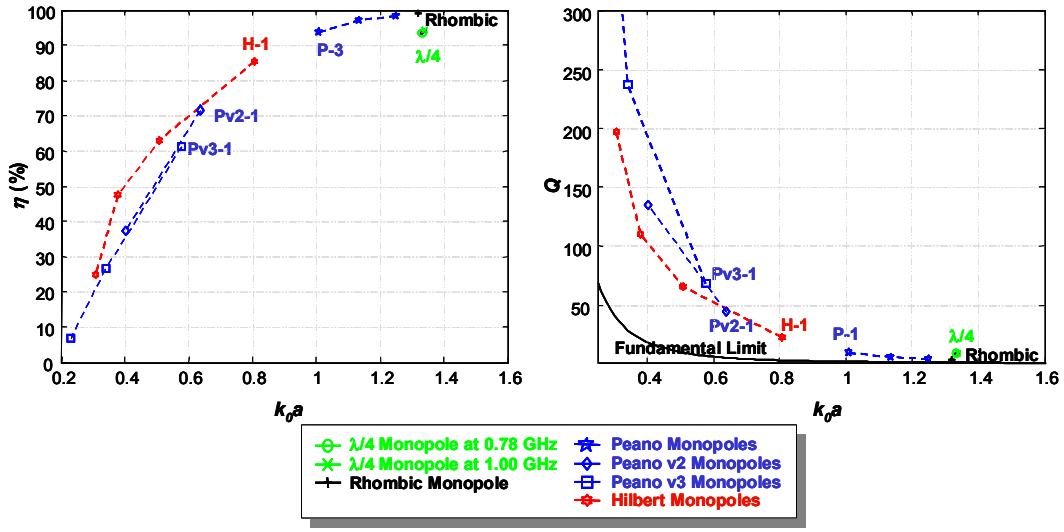

Figure 11. Measured results of prefractals with fractal dimension 2 compared with a conventional λ/4 monopole and a rhombic monopole: radiation efficiency (η) at left, and quality factor (Q) at right.

Antenna	D	k_0a	Q	η
λ/4 monopole of 90,8 mm	1,00	1,33	9,0	93,5
λ/4 monopole of 60,3 mm	1,00	1,34	8,7	94,3
Rhombic mon. of 49,3 mm height	1,00	1,32	3,7	99,0
Triangular mon. of 48,5 mm height	1,00	1,10	4,4	98,8
Square mon. of 57 mm side	1,00	1,57	2,5	98,3
DWS-1	1,58	1,01	6,1	96,1
DWS-2	1,58	1,00	5,2	96,6
DWS-3	1,58	1,01	5,0	97,0
DWS-4	1,58	1,02	5,8	97,4
DWS-5	1,58	1,09	5,2	97,9
YWS-1	1,58	0,99	9,6	93,0
YWS-2	1,58	0,95	9,0	94,0
YWS-3	1,58	0,94	7,7	95,1
YWS-4	1,58	1,00	6,8	96,6
YWS-5	1,58	1,02	5,8	97,3
K1S-1	1,58	1,00	7,1	94,9
K1S-2	1,58	0,96	7,0	96,0
K1S-3	1,58	0,97	6,1	96,8
K1S-4	1,58	1,02	5,7	97,5
K1S-5	1,58	1,08	4,9	98,0
SA-1	1,58	1,02	10,6	92,3
SA-2	1,58	0,99	7,9	94,1
SA-3	1,58	0,92	8,0	94,1
SA-4	1,58	0,81	10,7	92,4
SA-5	1,58	0,76	13,7	90,7
Pv2-1	2,00	0,64	44,3	71,6
Pv2-2	2,00	0,40	134,9	37,3
Pv3-1	2,00	0,58	68,7	61,2
Pv3-2	2,00	0,34	237,2	26,6
Pv3-3	2,00	0,23	625,4	6,9
P-1	2,00	1,01	9,5	93,8
P-2	2,00	1,13	5,5	97,1
P-3	2,00	1,25	4,6	98,4
H-1	2,00	0,81	22,8	85,5
H-2	2,00	0,51	65,3	63,0
H-3	2,00	0,38	110,4	47,6
H-4	2,00	0,31	196,8	25,0

Table 4. Measured results of electric size k_0a, radiation efficiency (η) and quality factor (Q) at resonance of several monopoles with fractal dimension 1.58 and 2 compared with a $\lambda/4$ monopole, a triangular monopole and a rhombic monopole. Main dimensions of triangular, rhombic and square monopoles do not include the 2 mm pedestal where the feeding pin was welded.

Gathering together all the results, such as figures 13 and 14, shows a reduction of η and an increase on Q is observed when increasing the iteration and fractal dimension of large wire antennas. When prefractal structures include loops larger radiation efficiencies and smaller quality factors are found with increasing fractal dimension and iteration. Nevertheless, high miniaturization is not easily achieved using prefractal loops. Quick stagnation of performances and trends to certain Euclidean structures (triangular and rhombic monopoles) are observed too in these cases.

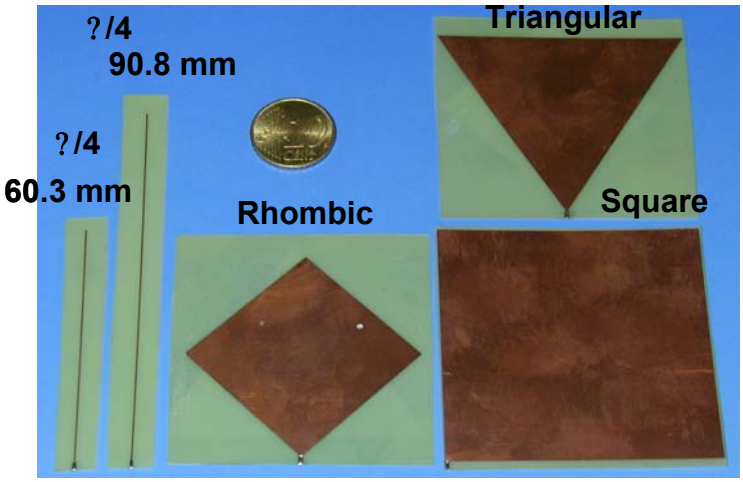

Figure 12. Manufactured Euclidean structures.

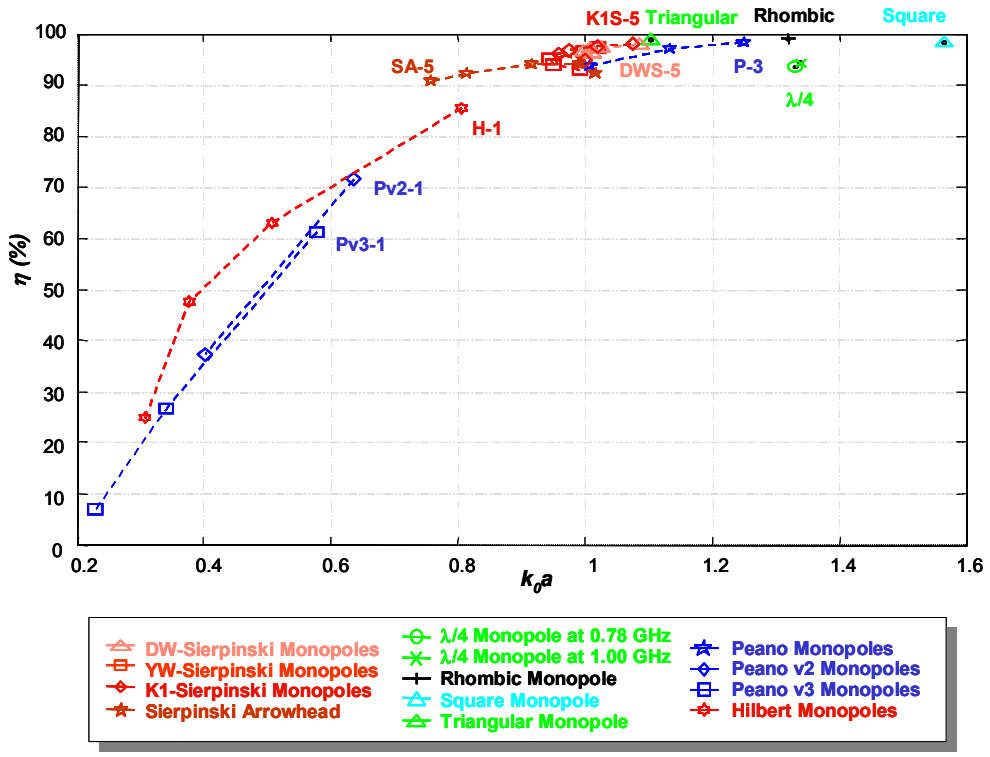

Figure 13. Measured radiation efficiencies of prefractals with fractal dimension 1.58 and 2 compared with conventional λ/4, triangular, square and rhombic monopoles.

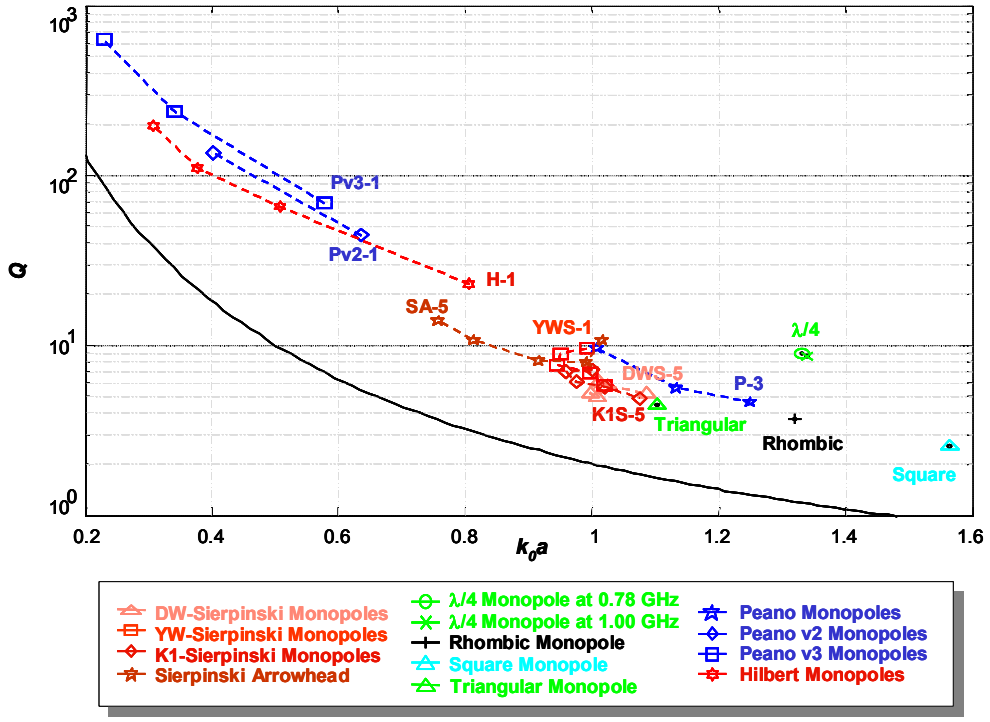

Figure 14. Measured quality factors Q of prefractals with fractal dimension 1.58 and 2 compared with conventional λ/4, triangular, square and rhombic monopoles.

4.6. Conclusions

The conclusions from the work presented in this section are:

- prefractal monopoles with higher iteration orders (than simulated) are achievable with the conventional printing technology used for the electronics boards manufacturing;
- topology seems to influence efficiency more than fractal dimension;
- as the number of loops inside the structure increase, efficiency and fractional bandwidth (inverse of quality factor) seem to increase too with the increasing order of the prefractal;
- when there is no loop each iteration increases the length and bending of the wires, and as a consequence ohmic losses and the amount of stored energy on the surrounding of the antenna increases (this means lower radiation efficiencies and higher quality factors);
- it has been observed that results are slightly dependent on the length of the feeding pin of the monopole: prefractals seem to be good capacitive loads. This point deserves further research.

4.7. References

[Chu, 1948] Chu, L.J.: ”Physical limitations of omni-directional antennas”, Journal of Applied Physics, 1948, 19, pp. 1163-1175.

[McLean, 1996] McLean, J. S.: “A re-examination of the fundamental limits on the radiation Q of electrically small antennas “, IEEE Transactions on Antennas and Propagation, May 1996, 44, (5), pp. 672-676.

[Gianvittorio, 2002] Gianvittorio, J.P., and Rahmat-Samii, Y.: “Fractal Antennas: a novel antenna miniaturization technique, and applications”, *IEEE Antennas and Propagation Magazine*, vol. 44, no. 1, pp. 20-36, Feb. 2002.

[NEC, 1981] Burke, G.J. and Poggio, A.J.: “Numerical Electromagnetics Code (NEC) - Method of Moments”, Lawrence Livermore Lab. Livermore, CA, Rep. UCID18834, Jan. 1981.

[Puente, 1998] Puente, C.; Romeu, J.; Pous, R.; Ramis, J.; Hijazo, A.: “Small but long Koch fractal monopole”, Electronics Letters, 8 Jan. 1998, 34, (1), pp. 9 –10.

[Puente-Baliarda, 2000] Puente-Baliarda, C.; Romeu, J.; Cardama, A.: “The Koch monopole: a small fractal antenna”, IEEE Transactions on Antennas and Propagation, November 2000, 48, (11), pp. 1773–1781.

5. ANALYSIS OF 3D PRE-FRACTAL SMALL ANTENNAS: THE 3D HILBERT MONOPOLE

According to a naïve interpretation of Hansen's statement: "To obtain performance closer to the minimum Q curve the spherical volume that encloses the antenna must be used more effectively" [1], one may think that 3D monopoles are expected to reach lower values for the quality factor because they pack more wire length into the enclosing sphere.

Nevertheless, previous experiences with planar electrically small self-resonant pre-fractals showed that both the quality factor and the loss efficiency achieve worst values when increasing the fractal dimension of the monopoles. Since increasing the fractal dimension is equivalent to increase the wire length for the same size of the enclosing sphere, we cannot expect a-priori that 3D pre-fractals exhibit much better bandwidth and radiation properties than their 2D counterparts.

The 3D Hilbert monopole has been modelled, its performance in terms of efficiency, quality factor and electrical size at resonance have been computed and, finally, the first three iterations of the pre-fractal have been manufactured with patience.

Figures 1 and 2 show, respectively, the wire models and the normalized current distribution along the wire computed by the simulation software.

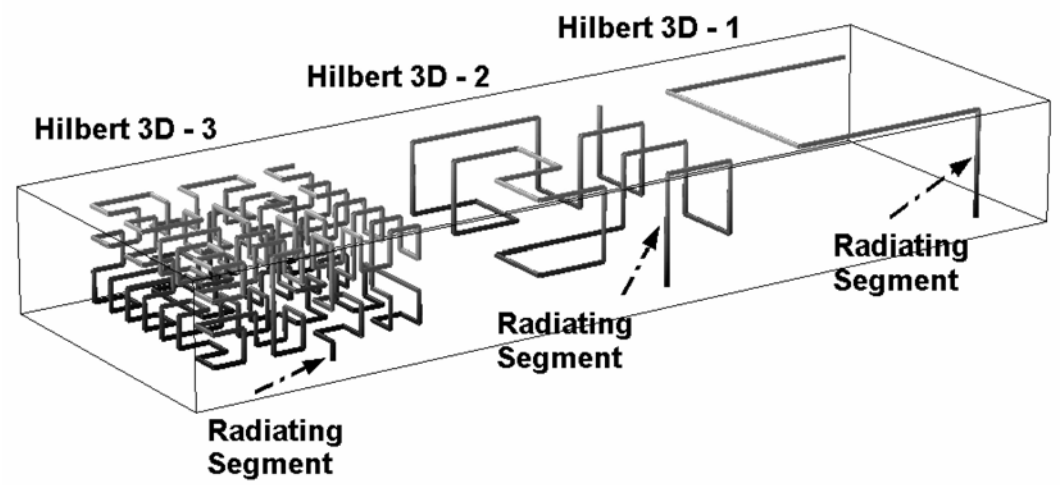

Figure 1. Simulated 3D Hilbert antennas in a monopole configuration. The first segment is the main contribution to radiation.

The current distribution along the wire is not very different from a sinusoidal one, and reflects that, as the number of iterations increases, the current in the first segment tends to be more uniform. A feasible explanation is that the first segment, connected to the feeder and perpendicular to the ground plane, is the main source of radiation, while the rest of the antenna behaves as a load.

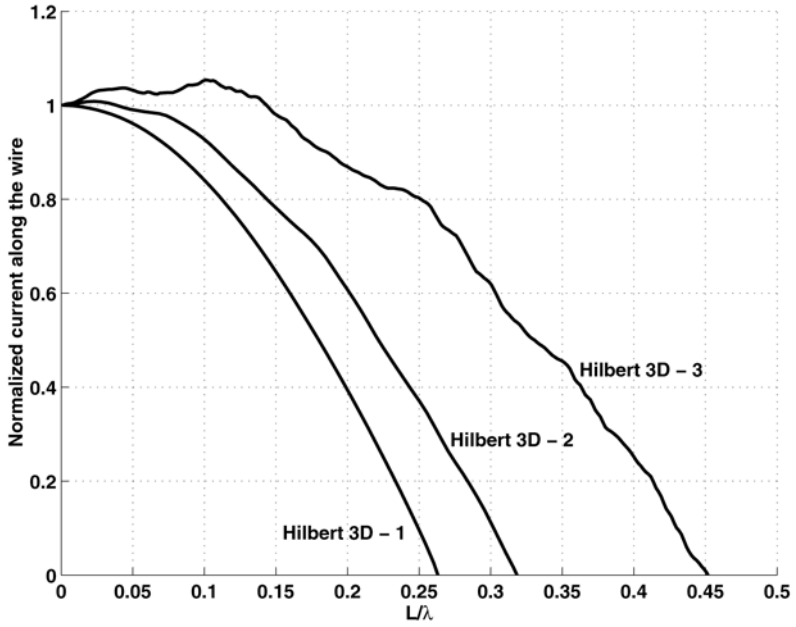

Figure 2. Normalized current distribution along the wire for the first three iterations of the 3D Hilbert monopoles.

Table 1 summarizes the computed parameters for these 3D models, showing that while the ratios of miniaturization are remarkable, the loss efficiencies and the quality factors achieved are unpractical. The extremely low value of the radiation resistance agrees with the hypothesis that only the feeding segment of the pre-fractal radiates as an electrically very small monopole, and the rest of the structure is a capacitive load that reduces the input reactance, and therefore, the resonant frequency.

Antenna	Total Wire Length (cm)	Electric Size at Resonance, *ka*	Resonant Frequency (MHz)	Radiation Resistance at Resonance (Ohms)	Input Resistance at Resonance (Ohms)	Efficiency (%)	Quality Factor	Fundamental Limit, *Q*
Hilbert 3D-1	61,78	0,71	127,5	2,47	3,24	76,6	126	4
Hilbert 3D-2	184,99	0,25	51,4	0,16	1,67	9,4	2091	70
Hilbert 3D-3	642,61	0,10	21,0	0,01	3,07	0,5	31966	1088

Table 1. Computed performance of the first three iterations of a 3D Hilbert monopole.

Simulations have been carried out modelling the monopoles as copper wires with 0.4 mm diameter and 89.8 mm height. The simulation software used is the well-known NEC2 code, based on the Method of Moments (MoM) discretization of the thin-wire Electric Field Integal Equation (EFIE). To avoid the inconveniences of the thin-wire reduced kernel approximation, the enhanced kernel formulation of NEC2 has been used instead.

Figure 3 shows the manufactured monopole prototypes and their dimensions.

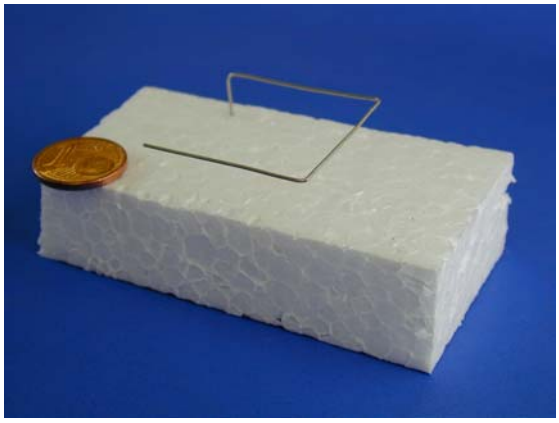

1st iteration

h=15 mm
s=27 mm

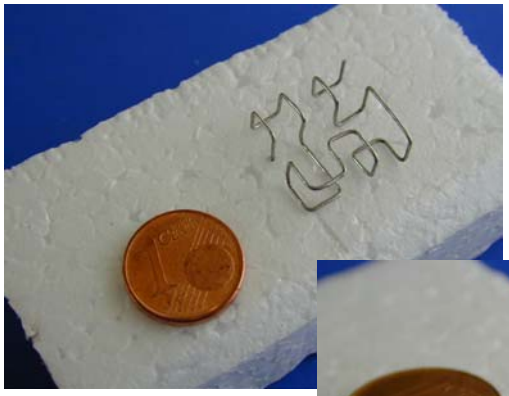

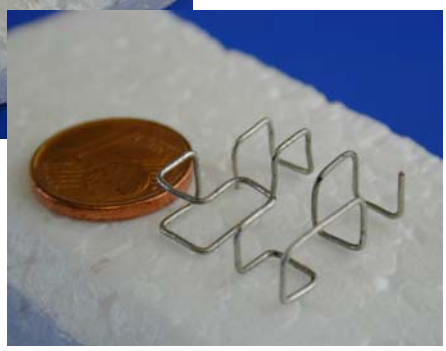

2nd iteration

h=5 mm
s=17 mm

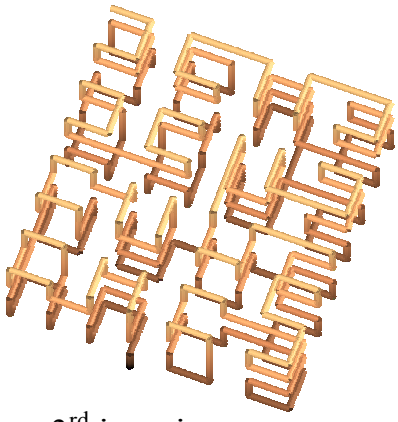

3rd iteration

h=10 mm
s=23 mm

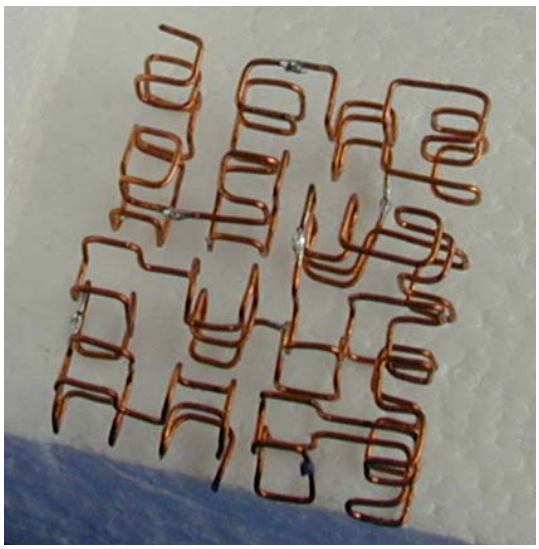

5.1. References

[1] R.C. Hansen, "Fundamental Limitations in Antennas", *Proceedings of the IEEE*, Vol. 69, No. 2, pp.170-182, February 1981.

6. ON THE RESONANT FREQUENCY OF PRE-FRACTAL MINIATURE ANTENNAS

6.1. Introduction

Some fractal geometries have complex, highly convoluted shapes. This property can be used to build pre-fractal antennas with arbitrarily wire length enclosed in a finite surface or volume. In principle, it is expected that the longer wire length, the lower resonant frequency. The Koch pre-fractal monopole shown in Fig. 1 is a well-studied example of such objects. It is a pre-fractal antenna generated by an iterated function system (IFS) that in the limit converges to the Koch fractal curve [Peitgen].

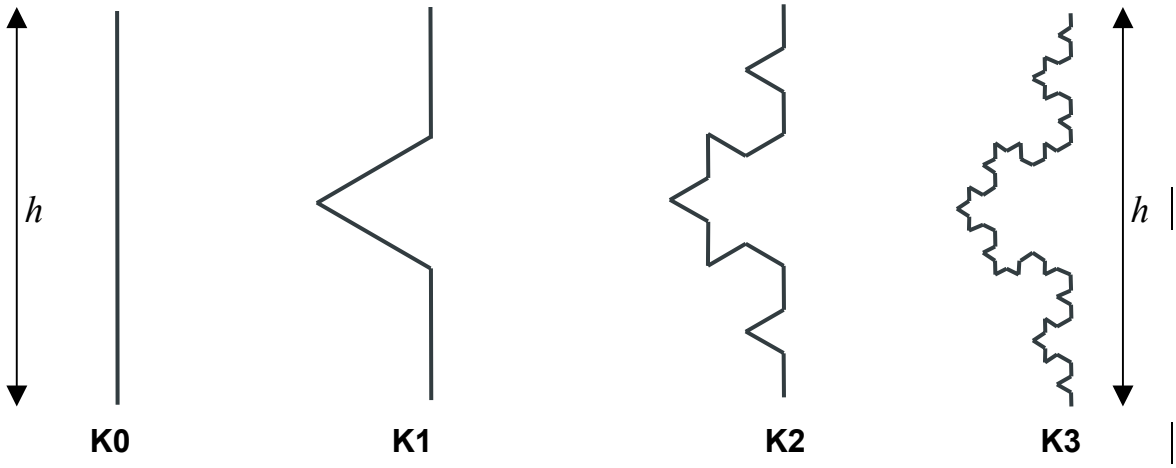

Fig. 1. Iterative construction of the Koch fractal curve. The height of the monopole is h.

It has been already shown that the resonant frequency of the Koch monopole decreases as the number of fractal iterations (K1, K2, K3...) increases [Puente-88]. However, other authors showed later that some non-fractal configurations that enclose a long wire into a finite volume also lead to a similar or better reduction in the resonant frequency, compared to the straight monopole having the same enclosing volume [Best-02a].

A close look at the results in [Puente-88] reveals that the resonant frequency of a Koch monopole is higher than that of a straight monopole of the same wire length (Fig. 2). At each iteration, the wire length of the Koch antenna is increased in a factor 4/3, and therefore it might be naively expected that the resonant frequency would be reduced in a factor ¾. It is not so, as can be clearly seen in [Puente-88] results and in Fig. 2. In fact, the reduction factor in the resonant frequency of the Koch antenna as the iteration number increases tends monotonically to one.

One possible explanation for this behaviour has been found recently for the Hilbert pre-fractal antenna [Best-02b]: a high degree of coupling between parallel wire segments with opposite current vectors causes a significant reduction in the effective length of the total wire, and therefore an increase in the resonant frequency.

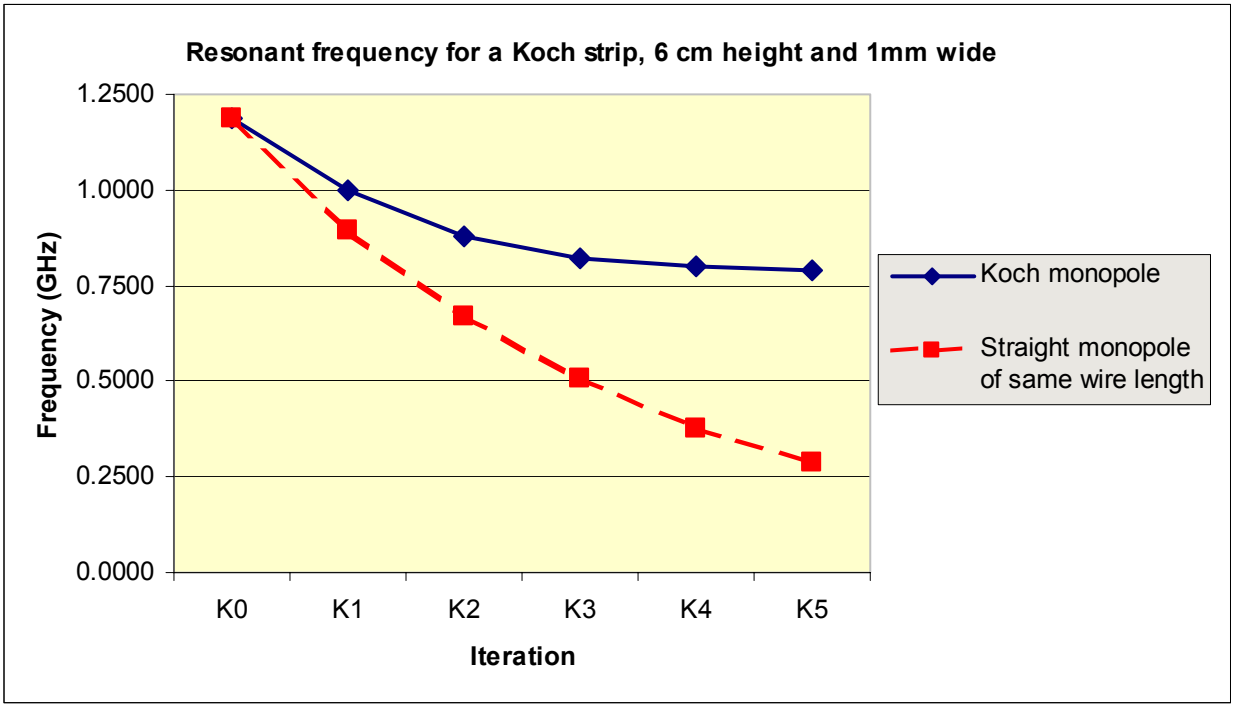

Figure 2: Resonant frequency of Koch strip monopoles, from iteration 0 to 5, compared with the straight monopole of height equal to the wire length of the Koch pre-fractal. The Koch monopoles are strips obtained as extrusion of the Koch curve (Fig. 5), 6cm-height and 1mm-wide. The results have been obtained by numerical simulation using Method of Moments (see section 3).

The aim of this report is to investigate further in the dependence of the resonant frequency with the monopole geometry, in order to acquire guidelines for the design of self-resonant small antennas, in which an increase of the wire length effectively leads to a reduction in the resonant frequency.

6.2. Hypothesis

The observed behaviour is due to the coupling between sharp angles at curve segment junctions. These angles radiate a spherical wave with phase centre at the vertex (Fig. 3). Each angle not only radiates, but also receives the signal radiated by other angles. As a consequence, part of the signal does not follow the wire path, but takes "shortcuts" that start at a radiating angle. The length of the path travelled by the signal is, therefore, shorter than the total wire length.

This hypothesis agrees with the fact that the resonant frequency of a Koch monopole corresponds to a straight monopole much shorter than the Koch curve length (Fig. 2). The higher iteration number in the Koch antenna, the more angles it has and the closer to each other they are, so

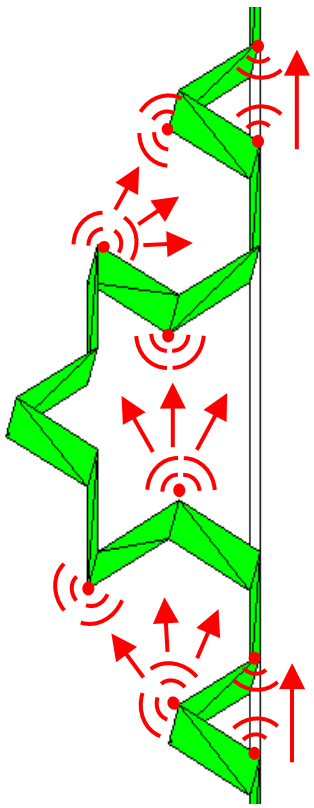

Fig. 3: Signal coupling at angles.

the more signal takes shortcuts and the less signal follows the whole curve path. It can be noticed in Fig. 2 that the resonant frequency reduction between K4 and K5 is negligible, although the curve length increases in a factor 4/3. The reason is that the signal follows the shortcuts and the length of the path followed by the signal is the same. This hypothesis will be verified by numerical simulations in the frequency and time domains.

6.3. Numerical Simulations

Wire antennas can be analysed using integral equation methods (IE) in conjunction with Method of Moments (MoM) discretization [Harrington]. The numerical electromagnetics code (NEC) [Burke] is a well-known example of computer code that can deal with these problems efficiently. NEC, as most wire-modeling codes, assumes that the current is constant around the wire circumference, which is not the case in problems having non-collinear wire segments very close to each other [D7 Final report Task 3.2]. Moreover, highly iterated pre-fractal antennas have wire segments of length comparable to the wire diameter, which either break the commonly used thin-wire approximation or lead to problems with the exact kernel integration around the wire circumference [D7 Final report Task 3.2].

For the above reasons, we propose here to model highly iterated pre-fractal antennas as a strip instead of as a wire. This is in agreement with the fact that, in practice, the antenna prototypes are built using printed strip technology. The strip can be easily meshed in triangle, rooftop or quadrangular basis functions, leading to an accurate MoM discretization of the EFIE if enough integration points are used on each triangle [D6 Final report Task 3.1].

We have considered two kinds of strips:

- **Planar strips**: Usual strips contained in a plane (Fig. 4), like printed antennas.
- **Extrusion strips**: Strips obtained by extrusion of the pre-fractal curve in the direction perpendicular to the plane containing the curve (Fig.5).

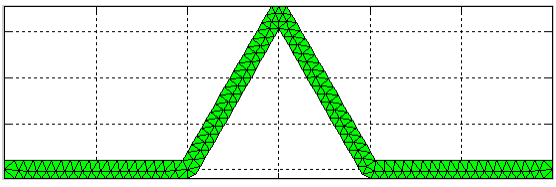

Fig. 4. One iteration planar-strip Koch antenna, discretized in triangular patches.

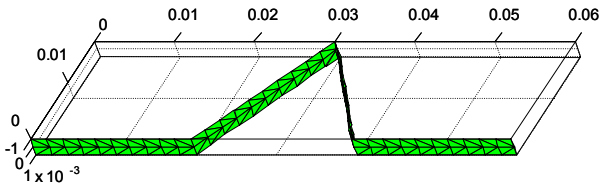

Fig. 5.One iteration extrusion-strip Koch antenna, discretized in triangular patches.

For low-iteration Koch antennas, both kinds of strips lead to the same antenna resonant frequency if the strip width is the same (Table I).

On the other hand, for high-iteration pre-fractals, in planar strips the width of the strip interferes with the strip angles, while in extrusion strips it does not. Obviously, the effect is less noticeable for thinner strips (Table I). Therefore, the geometry of a highly

iterated planar strip losses the main properties of fractals (auto scaling and fractal dimension), while extrusion strips preserve these properties.

For the above reasons we propose here to **use extrusion strips and not planar strips in the verification of the signal coupling hypothesis**.

Software	NEC wire	NEC wire	FIESTA wire	FIESTA wire	FIESTA strip	FIESTA strip
Model	thin-wire kernel	extended kernel	thin-wire kernel	eq. radius kernel	planar strip	extrusion strip
Radius / width	**0.5/π (mm)**	**0.5/π (mm)**	**0.5/π (mm)**	**0.5/π (mm)**	**0.5 mm**	**0.5 mm**
K-0	1.202	1.202	1.238	1.238	1.195	1.196
K-1	0.987	0.987	0.993	0.993	0.988	0.990
K-2	0.866	0.866	0.864	0.863	0.858	0.859
K-3	0.799	0.799	0.785	0.783	0.787	0.783
K-4	0.773	0.773	0.772	0.763	0.762	0.750
K-5			0.782	0.758		0.736

Software	NEC wire	NEC wire	FIESTA wire	FIESTA wire	FIESTA strip	FIESTA strip
Model	thin-wire kernel	extended kernel	thin-wire kernel	eq. radius kernel	planar strip	extrusion strip
Radius / width	**1/π (mm)**	**1/π (mm)**	**1/π (mm)**	**1/π (mm)**	**1 mm**	**1mm**
K-0	1.194	1.194	1.232	1.232	1.185	1.188
K-1	0.993	0.993	1.001	1.001	0.994	0.997
K-2	0.890	0.890	0.875	0.875	0.880	0.881
K-3	0.842	0.842	0.833	0.828	0.828	0.821
K-4	0.831	0.832	0.867	0.824	0.821	0.799
K-5			0.877	0.774		0.788

Table I: Resonant frequency (GHz) of wire, planar strip (Fig. 4) and extrusion strip (Fig. 5) Koch monopoles. Height is 6cm and the strip width 1mm or 0.5mm. The wire models have a radius equal to the strip width over π.

Two computer software codes have been used to analyze the wire model: NEC-2 and FIESTA; with three different integral equation kernel formulations: thin-wire approximation, extended kernel and thin-wire with equivalent wire radius [Imbrialle]. Taking the extrusion-strip results as a reference, the wire model error grows rapidly after iteration K3 (NEC) or K4 (FIESTA).

Planar- and extrusion-strips have resonant frequencies that differ less than 1% for one (K1), two (K2) or three (K3) pre-fractal iterations. For four iterations (K4), the pre-fractal curve segment length is 0.75mm, comparable to the strip width. The error in the K4 1mm strips is 2.7% and in the 0.5mm strips 1.6%. Five-iterations (K5) planar strips cannot be build, since the segment length (0.25mm) is too small compared with the strip width.

6.4. Numerical Verification in the Frequency Domain

The numerical verification in the frequency domain of the coupling -or shortcut- effect hypothesis will be based on three conjectures. These conjectures will be true if the shortcut effect hypothesis is true.

Strip width

It is known that, for a straight monopole antenna, the resonant frequency slightly decreases if the monopole diameter –or strip width- is increased. Our first conjecture is the opposite, that is, **the resonant frequency of a pre-fractal antenna increases if the strip width is increased**.

The reason is very simple: the wider the monopole, the more coupling and, thus, a larger fraction of the signal takes the shortcuts between the pre-fractal curve angles. The result is a shorter signal path length and, therefore, higher resonant frequency.

The numerical simulation in Fig. 6 completely corroborates the conjecture.

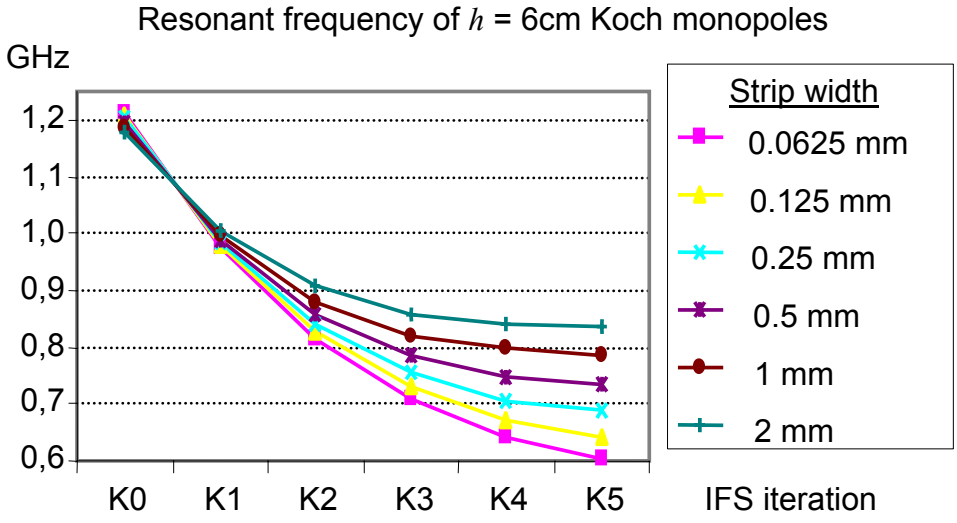

Figure 6: Resonant frequency of extrusion-strip Koch monopoles of different widths. The monopole height is 6 cm. It can be observed that for highly convoluted pre-fractal antennas, the resonant frequency increases with the strip width, due to the coupling effect.

Monopole size

The electrical height (h/λ_{RES}) of a resonant straight monopole is approximately 0.235 or 0.24. In a pre-fractal monopole, the resonant frequency decreases for each new IFS iteration (Fig. 2 and 6), and therefore the electrical height is shorter.

The second conjecture is that pre-fractal antennas of the same class and the same number of IFS iterations have **shorter electrical height at resonance if the physical size of the antenna is larger**. The obvious reason is that larger antennas have longer distance between pre-fractal curve angles and, therefore, the coupled signal that follows the shortcuts between angles is weaker.

To verify the conjecture, the electrical height at resonant frequency, h/λ_{RES}, has been numerically computed for Koch monopoles of different sizes. The results in Fig. 7 completely corroborate the shortcut effect hypothesis.

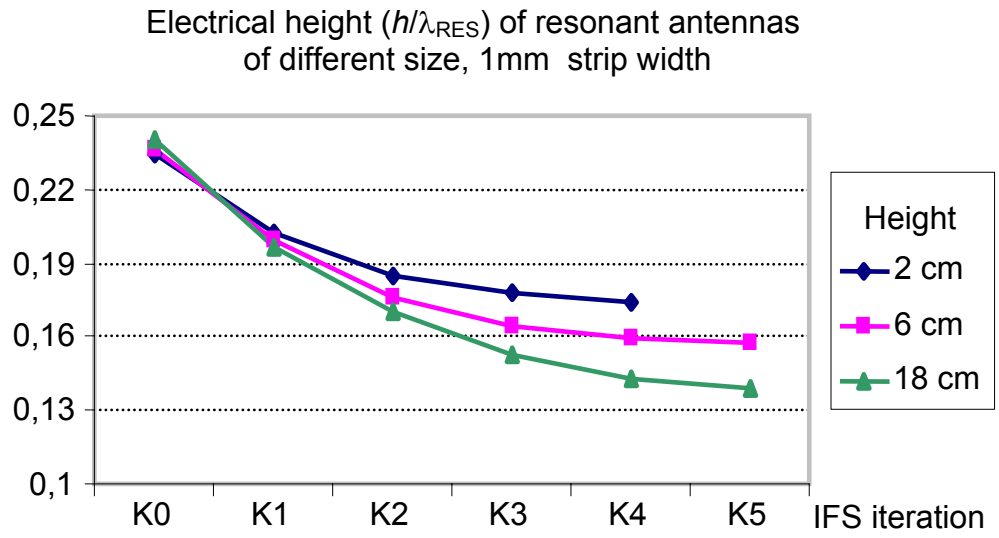

*Figure 7: Electrical height at resonance (*h/λ_{RES}*) of extrusion-strip Koch monopoles of different sizes. The strip width is 1mm. It can be observed that for highly convoluted pre-fractal antennas, the electrical height at resonance decreases for larger monopoles because there is less coupling.*

Pre-fractal small details

The length of coupling leaps –or distance between pre-fractal curve angles- of a i-th iteration Koch monopole (K_i) of size *h* is the same as the length of coupling leaps of a K_{i+1} monopole of height 3*h*, where 3 is the IFS scale factor.

The third conjecture is that **the reduction factor in the resonant frequency from K_i to K_{i+1} monopoles of size *h* is the same as the reduction factor from K_{i+1} to K_{i+2} monopoles of size *sh*, where *s* is the IFS scale factor**, equal to three for the Koch antenna.

To verify this conjecture, the reduction factor in the resonant frequency has been numerically computed for 1mm wide extrusion-strip Koch monopoles, iterations K1 to K5. The results in Table II completely corroborate the shortcut effect hypothesis.

Height	K1-K2	K2-K3	K3-K4	K4-K5
2 cm	0,92	0,96	0,98	
6 cm	0,88	0,93	0,97	0,98
18 cm	0,86	0,90	0,94	0,98

Table II: Reduction factor in the resonant frequency from K_i to K_{i+1} Koch monopoles of different sizes. It can be observed that, for example, the reduction factor from K3 to K4 of a 2cm monopole (0.98) is the same as the reduction factor from K4 to K5 of a 6cm monopole, where 6cm is equal to 2cm times the IFS scale factor (3).

6.5. Numerical Verification in the Time Domain

Near fields

The Near fields in the vicinity of a single-iteration Koch monopole have been computed in the time domain for very short-pulse excitation (Fig. 8). The antenna has been modeled as a thin wire using DOTIG code from University of Granada.

It can be noticed that the sharp angles of the pre-fractal curve become the centre of spherical wave radiation, which corroborates the coupling or shortcut effect hypothesis.

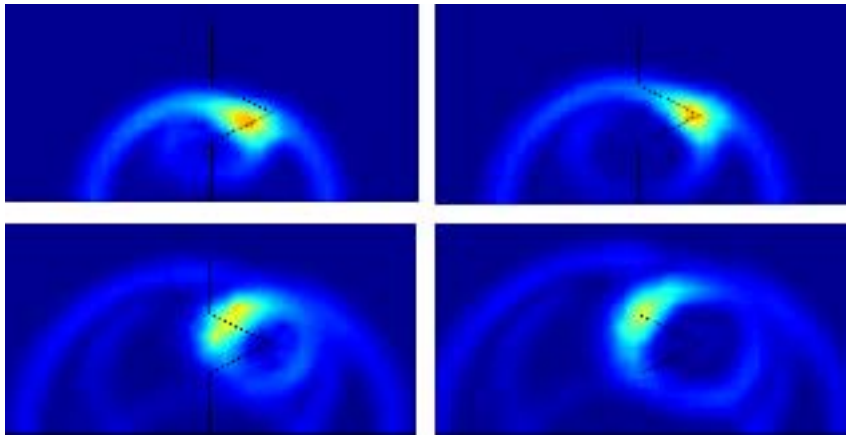

Figure 8: Near fields in the time domain in the vicinity of a single-iteration Koch monopole (K1) with short-pulse excitation. The sharp angles of the pre-fractal curve become the center of spherical wave radiation, which corroborates the coupling or shortcut effect hypothesis.

Space-time diagram

For a short-pulse excitation, the space-time diagram shows the current magnitude at a given time and space position along the wire. Fig. 9 is the space-time diagram corresponding to a 1m-height K2 monopole. The antenna has been modeled as a thin wire using DOTIG code from University of Granada.

In Fig. 9, the space axis (vertical) is scaled in pre-fractal curve segments, that is, one unit is the length of one segment in the pre-fractal curve (see picture of the K2 monopole below). The time axis (horizontal) is scaled in segments / light-speed, that is, one unit is the time that light takes to travel one segment distance.

The shortcut between angles 1 and 3 is shown in **blue** colour. The distance between these angles is one segment. The space-time diagram shows that the signal reaches the segment between angles 2 and 3 at t = 2 segments-light, that is, one segment-light after a spherical wave is launched at angle 1.

Similarly, the shortcut between angles 2 and 6 is shown in **red** colour. The distance between these angles is $\sqrt{3}$ =1.73 segments. The space-time diagram shows that the signal reaches angle 6 at t = 3.7 segments-light, that is, 1.7 segments-light after a spherical wave is launched at angle 2 (t = 2 segments-light). The signal reaches angle 5 a bit later than angle 6, because the distance between angles 2 and 5 is a bit longer than between angles 2 and 6.

The shortcut between angles 5 and 9 is shown in **green** colour. The distance between these angles is again $\sqrt{3}$ =1.73 segments. The space-time diagram shows that the signal reaches angle 9 at t = 5.7 segments-light, that is, 1.7 segments-light after a spherical wave is launched at angle 5 (t = 4 segments-light). The signal reaches angle 11 a bit later than angle 9, because the distance between angles 5 and 11 is a bit longer than between angles 5 and 9. It can be noticed also that the signal reaches angle 10 much later than angles 9 or 11, because the distance to angle 5 is longer.

The space-time diagram also shows that the signal is reflected at the end of the monopole, and it reaches back the feeding point at a time that is half the period at the resonant frequency, T_{RES} / 2.

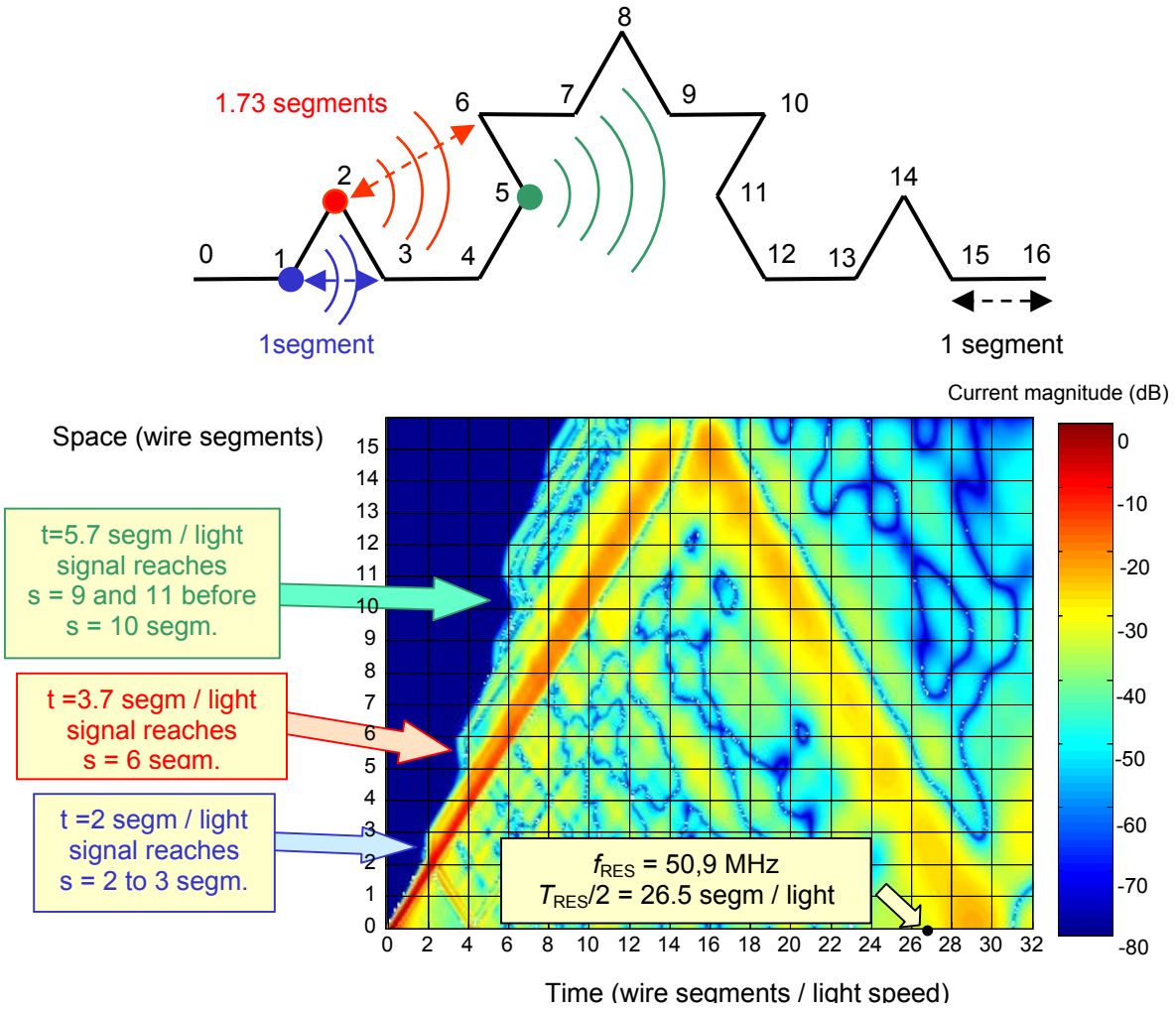

*Figure 9: Space time-diagram for short-pulse excitation in a 1m-height K2 monopole. The antenna has been modeled as a thin wire using DOTIG code from University of Granada. The signal shortcuts from angles 1 to 3 (**blue** color), 2 to 6 (**red** color) and 5 to 9 (**green** color) can be clearly observed.*

Another important effect is the coupling between the feeder and the wire segments of a very small antenna. Fig. 10 shows the space-time diagram for a K2 monopole excited by a wide Gaussian pulse whose maximum spectral component is such that the monopole is a electrically small antenna at that frequency. The feeder-wire segments coupling can be clearly seen in Fig. 10, and they play a significant role in the behavior of electrically short pre-fractal antennas. The feeder-shortcut effects take place mainly at segments with a specific orientation tangential to the electric field radiated by the feeder, which are indicated with arrows in Fig. 11. In consequence, it is clear that the orientation of the segments in the pre-fractal antennas plays also an important role that has to be taken into account in the design of self-resonant small antennas.

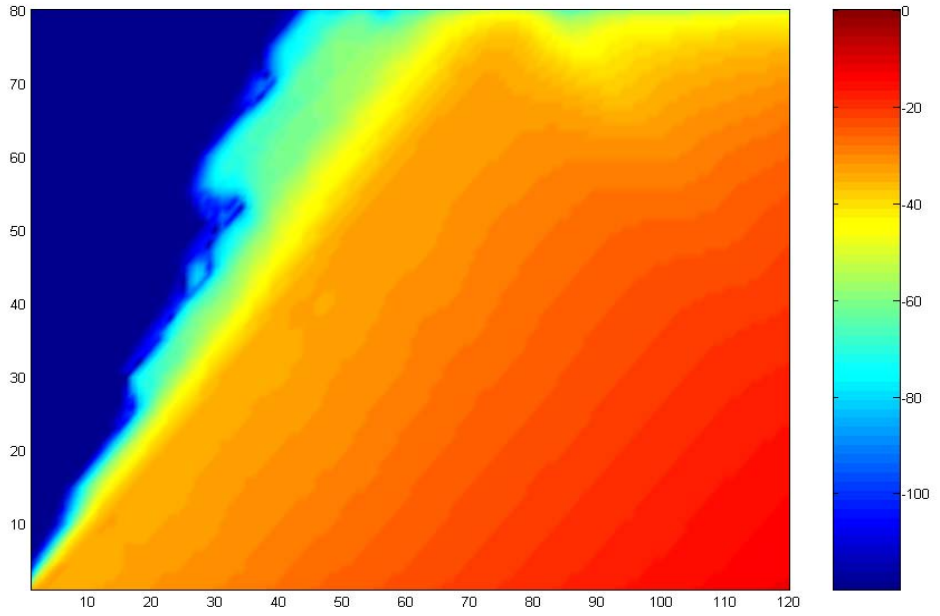

Fig 10: Space time diagram for an electrically small K2 monopole.

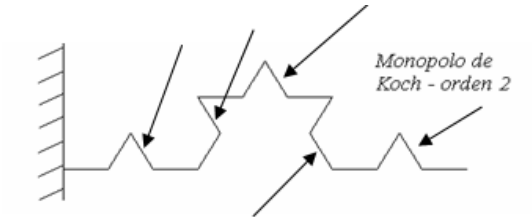

Fig. 11: Wire segments in a K2 monopole that couple with the field radiated by the feeder.

6.6. Comparison with other pre-fractal and non-prefractal monopoles

We can expect reasonably that the coupling or shortcut hypothesis is also valid for other kinds of pre-fractal or non-fractal miniature monopoles. As a consequence, the three conjectures that have been used to verify the hypothesis will be also true in these cases. However, different kinds of miniature wire monopoles having the same wire length exhibit different length of signal leaps –or shortcuts- between wire angles, resulting in a different amount of coupling signal that takes the shortcut. For that reason, these antennas will have different resonant frequency while having the same monopole height *h* and the same wire length.

Fig. 12 shows different monopole configurations that have been analysed. There are two pre-fractals: the conventional Koch antenna and a generalized version. In the limit of infinite IFS iterations, they converge to fractal curves of fractal dimension respectively equal to 1.26 and 1.5. There are also two non pre-fractal configurations: both are zigzag antennas of different meanders size.

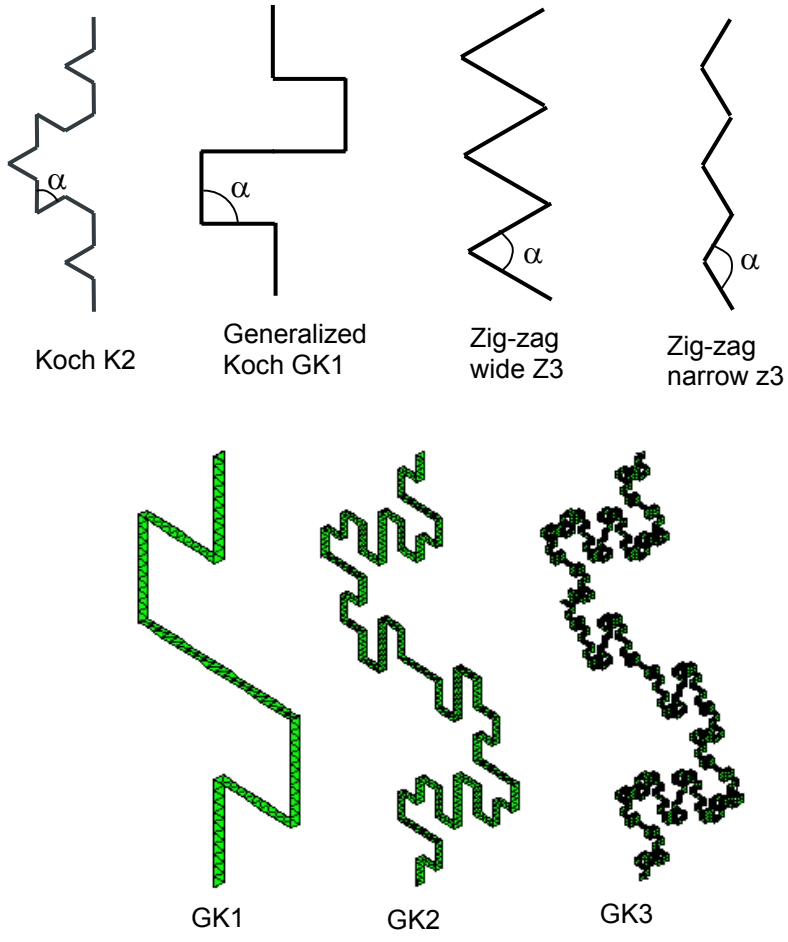

Figure 12: Different pre-fractal and non pre-fractal configurations analyzed: The Koch antennas with different number of IFS iterations will be denoted as K1, K2,..; the generalized Koch as GK1, GK2,...; the wide zig-zag as Z1, Z2..., where Zn has n meanders, and similarly the narrow zig-zag as z1, z2, ...

Figure 13 compares the resonant frequency of the four-monopole families as a function of the wire length. The antennas have been modeled as extrusion-strips of 1mm width. The wide zigzag antenna performs significantly better than the Koch monopole, while the narrow zigzag is slightly worse. It is remarkable that the other pre-fractal antenna based on a generalized Koch IFS mapping, has the lowest resonant frequency.

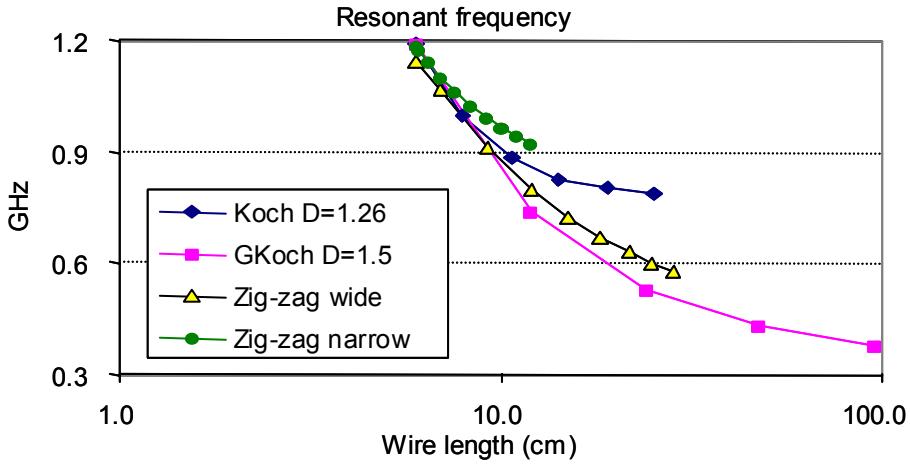

Figure 13: Resonant frequency as a function of the wire length. The antennas have been modeled as extrusion-strips of 1-mm width. Each marker in the plot corresponds to an IFS iteration in the pre-fractal geometries or the number of meanders in the zig-zags.

The reason can be found in the fact that the generalized Koch and the wide zigzag configurations, for equal wire length, show longer signal leaps –or shortcuts- than the Koch or the narrow zigzag (Figure 14). The longer signal leaps, the less amount of coupling signal that takes the shortcut, the longer path followed by the signal and the lower resonant frequency.

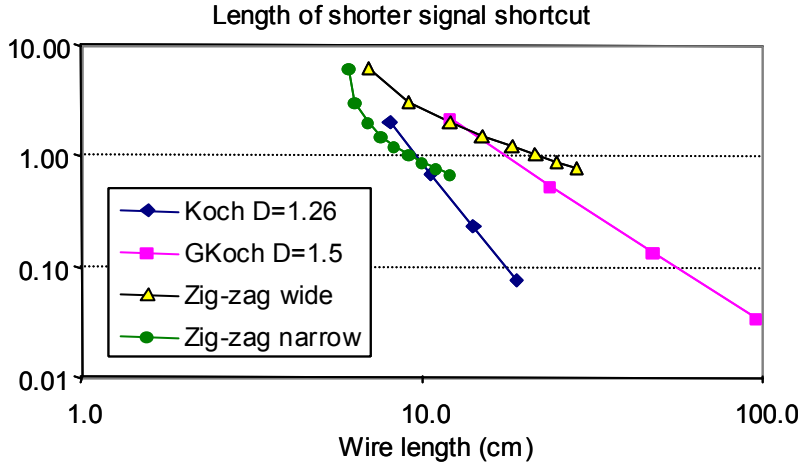

Figure 14: Length of shorter signal shortcut for the four families of monopoles, equal to the smallest distance between wire angles.

However, according to Fig. 14, the wide zigzag should perform better than the generalized Koch. In practice, it is the opposite (Fig. 13). The reason for this behaviour

relies on the fact that the strength of the coupling depends not only on the distance between the coupled curve angles, but also on the value of the angles α: the lower α angle, the larger magnitude of the coupled signal. Since an angle of α=180º defines a straight wire, and therefore there is no coupling, and an angle of α=0º launches the strongest coupling signal, we can tentatively define the coupling factor as cos(α/2). Hence, the inverse of the coupling signal strength is better defined by the length of the shortcuts divided by cos(α/2) rather than by the length of the shortcuts alone (Fig. 15).

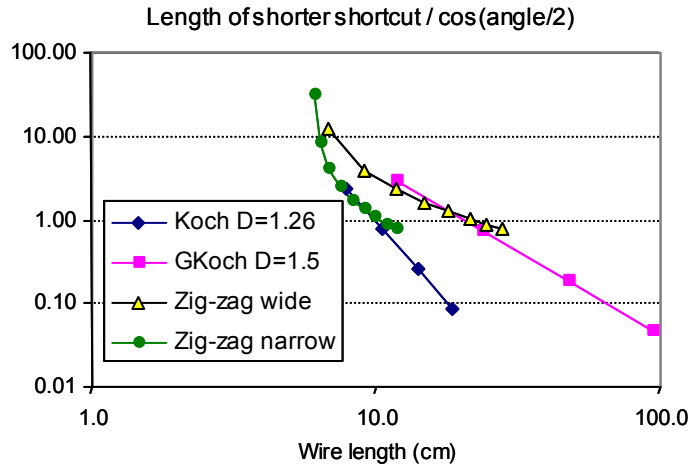

Figure 15: Length of shorter shortcut divided by the cosinus of half the curve angle α. The curve angle is α=60º for the Koch pre-fractal and α=90º for the generalized Koch. For the zig-zag configurations it is similarly defined.

Fig. 15 predicts similar performance for the generalized Koch and the wide zigzag, on the one hand, and for the Koch and the narrow zigzag on the other. However, the performance of the pre-fractals is better than expected from Fig. 15. In order to have a complete picture of the amount of coupling for a given monopole configuration, other factors have still to be accounted, like for instance the number of shortcuts and the length of wire bypassed by the shortcut.

6.7. Guidelines for the design of miniature monopoles

As a conclusion of the work in this report, the work in other FRACTALCOMS reports [Gómez-02] and very recent work available in the literature [Best-02b], the following guidelines can established for the design of miniature wire antennas:

1- In order to reduce signal coupling –or shortcuts- between wire angles, the distance between those angles must be as large as possible, and the angles α the larger possible.

2- In order to reduce the signal coupling between the feeder and the wire segments, the most possible wire length must be perpendicular to the electric field radiated by the feeder [Gómez-02].

3- In order to reduce coupling between wire segments, parallel wire segments with opposite currents very close to each other must be avoided [Best-02b].

An example of wire antenna that closely follows these guidelines is a two-arm spiral. Table II, extracted from [Cabot-02], shows that the resonant frequency of a square spiral is inversely proportional to the wire length, while keeping the wire enclosed by a small square.

Other possible configurations that, according to these guidelines, may be very interesting are slot and coplanar waveguide antennas, in which the coupling between antenna segments is very weak.

	1-turn	**2-turns**	**3-turns**	**4-turns**
Resonant frequency (GHz)	4.6	3.3	2.3	1.77
Wire length (cm)	6.66	10.53	14.44	17.94
Wire length incresase factor	------	1.59	2.16	2.69
Frequency compression	------	1.40	2	2.6

Table 3: Resonant frequency and wire length of a family of square two-arm spiral antennas [Cabot-02]. When increasing the number of turns, the frequency compression factor remains approximately equal to the wire length increase factor, while keeping the wire packed inside a small rectangle.

6.8. References

[Peitgen] Heinz-Otto Peitgen, et al., "Chaos and Fractals: New Frontiers of Science", Springer-Verlag, 1992.

[Puente-88] C. Puente, J. Romeu, R. Pous, J. Ramis, A. Hijazo, "Small but long Koch fractal monopole", IEE Electronics Letters, vol. 34, nº 1, pp. 9-10, January, 1998.

[Best-02a] Steven R. Best, "On the Resonant Properties of the Koch Fractal and Other wire Monopole Antennas", IEEE Antennas and Propagation Letters, Vol. 1, 2002, pp. 74-76.

[Best-02b] Steven R. Best, "The Effectiveness of Space-Filling Fractal Geometry in Lowering Resonant Frequency", IEEE Antennas and Propagation Letters, Vol. 1, 2002, pp. 112-115.

[Harrington] R.F. Harrington, Field computation by Moment Methods, New York, MacMillan, 1968.

[Burke] G.J. Burke, A.J. Poggio, J.C. Logan, J.W. Rockway, "NEC:-Numerical electromagnetics code for antennas and scattering", IEEE AP-S Int. Symp. Dig., Seattle, WA, pp. 147-150, June, 1979.

[Imbrialle] W.A. Imbrialle, "Applications of the method of moments to thin-wire elements and arrays", Cap. 2, *Numerical and Asymptotic Techniques in Electromagnetics*, editor R. Mittra, Springer-Verlag, 1975.

[Gómez-02] R. Gómez Martín, A. Rubio Bretones, M. Fernández Pantoja, F. García Ruiz , "Study of small prefractal antennas in the time domain", FRACTALCOMS project report WP4 T3.4 UGR T0+12.

[Cabot-02] E. Cabot, J.R. Mosig, "The square spiral antenna: benchmark for prefractal antenna performance", FRACTALCOMS project report WP1 T1.1 EPFL T0+12.

7. BENCHMARKS FOR PRE-FRACTAL ANTENNA PERFORMANCE. HIGH-GAIN LOCALIZED MODES: THE MEANDER LINE

7.1. Introduction

The convoluted shape of some fractals allows a size reduction of an antenna with this fractal geometry [1], because within the same surface it can be enclosed a larger perimeter. That is, the fractal shaped antenna will have the same surface/volume as its Euclidean equivalent but it will be much longer. The more iterated the fractal is, the longer it will be, but as iterations are increased high coupling between segments of wire/strip appears due to bending. For this reason the electric current instead of flowing following the fractal shape "jumps" following the shortest path. So which is the real efficient equivalent length from the electromagnetic point of view?

To study these phenomena some simulations have been made with a meander line, and the deformation of this structure to a patch (which is a meander without separation between arms) and a line, which is an unwrapped meander. The analysis technique being used is a Method of Moments (MoM) code based on the Mixed Potential Integral Equation (MPIE).

7.2. Study of a meander line structure

Description of the structure under study

The structure under study is a patch on which there have been made some gaps of infinitesimal width parallel to the shortest side of the patch, that is the collapsed form of a meander type antenna, see Figure 1.

The length of the structure is $L=50$mm and the width is $W=36.5$mm. It is over an infinite ground plane, and the dielectric is air of thickness $h=1$mm. The width of the gaps is $W_g=0.1$mm and the length is L_g=31.5mm. As it is seen in Figure 1 the meander is excited on the left-down side of the structure by means of a generator of internal impedance $Z_g=50\Omega$.

When we take both extremes of meander and we unwrap it we obtain a line, whose length is the middleway in the arms of the meander, $L=365$mm in our case. Resonances in the line, f_n , for an analysis in free space occur when:

$$L = n\frac{c_o}{2f_n}, \quad \text{with } n = 1, 2...$$

so the resonance frequencies are

$$f_n = n\frac{c_o}{2L}.$$

On the other hand, if gaps are removed from the meander what we obtain is a patch with the same length and width as the meander. For the patch resonances occur for

$$fmn = \frac{c_o}{2\pi}\sqrt{\left(\frac{m\pi}{L}\right)^2 + \left(\frac{n\pi}{W}\right)^2}, \quad \text{with } m = 0,1,2... \text{ and } n = 0,1,2...$$

In the following paragraphs a frequency-domain study is made in order to extract similarities or differences in the behaviour of these three structures.

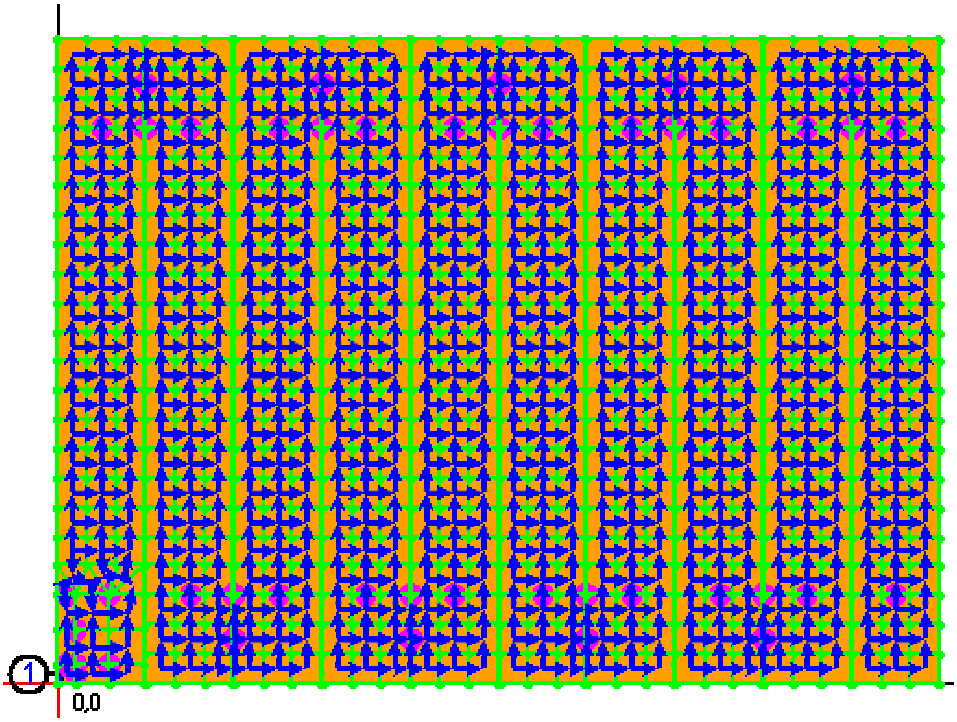

Figure 1. Mesh of the structure (green) , basis functions (blue arrows).

Analysis at low frequencies

It has been observed a different behaviour of the structure for frequencies lower than the first resonance of the patch (mode 1,0). So an analysis has been made for frequencies below first patch mode, that is what we mean with low frequencies. In Figure 2 we have the plot of imaginary part of input impedance for the meander and the equivalent line, which has been taken by simply unwrapping the meander, taking as effective length the middleway. The resonance frequencies for the line are f_1=*0.4110*GHz, f_2= *0.8219* GHz, f_3=*1.2329*GHz, f_4= *1.6438*GHz, f_5=*2.0548*GHz, f_6=*2.4658*GHz, f_7= *2.8767*GHz, as it can be checked in Figure 2.

From the picture we can see that line and patch have the same behaviour (same shape and same resonances), but with a frequency shift that is less remarkable for high frequencies. It can be due to the fact that the effective length as the middleway in the arms of the meander is more approximate in high frequencies, whereas for low frequencies the effective length should be maybe shorter. Equivalent length of line when unwrapping the meander changes with frequency.

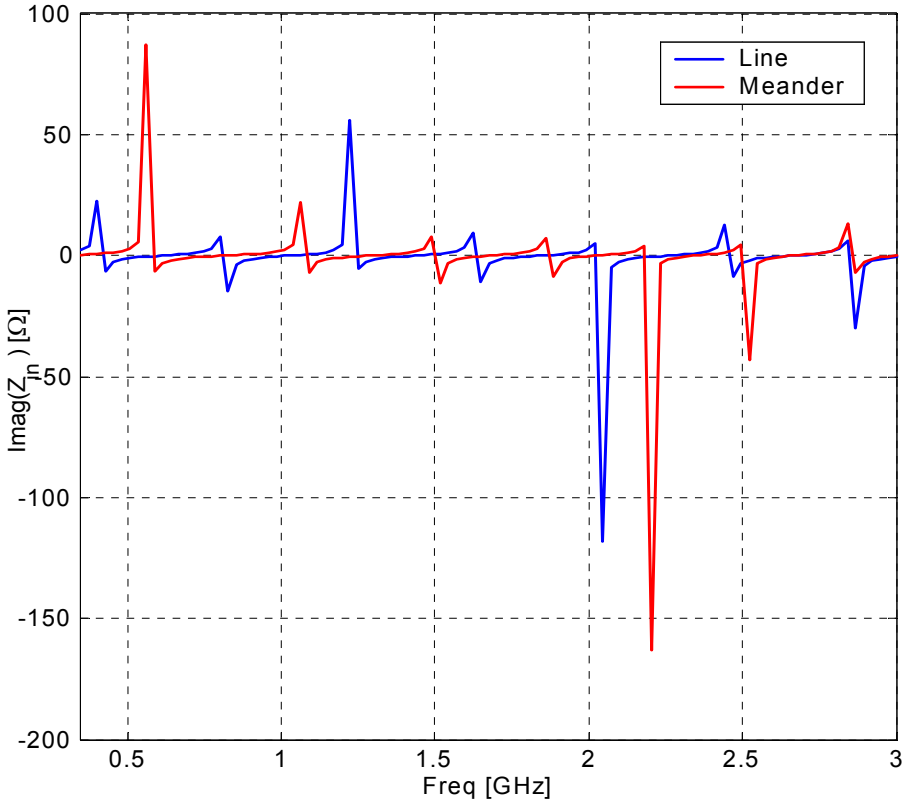

Figure 2. Imaginary part of input impedance of line (blue) and meander (red) .

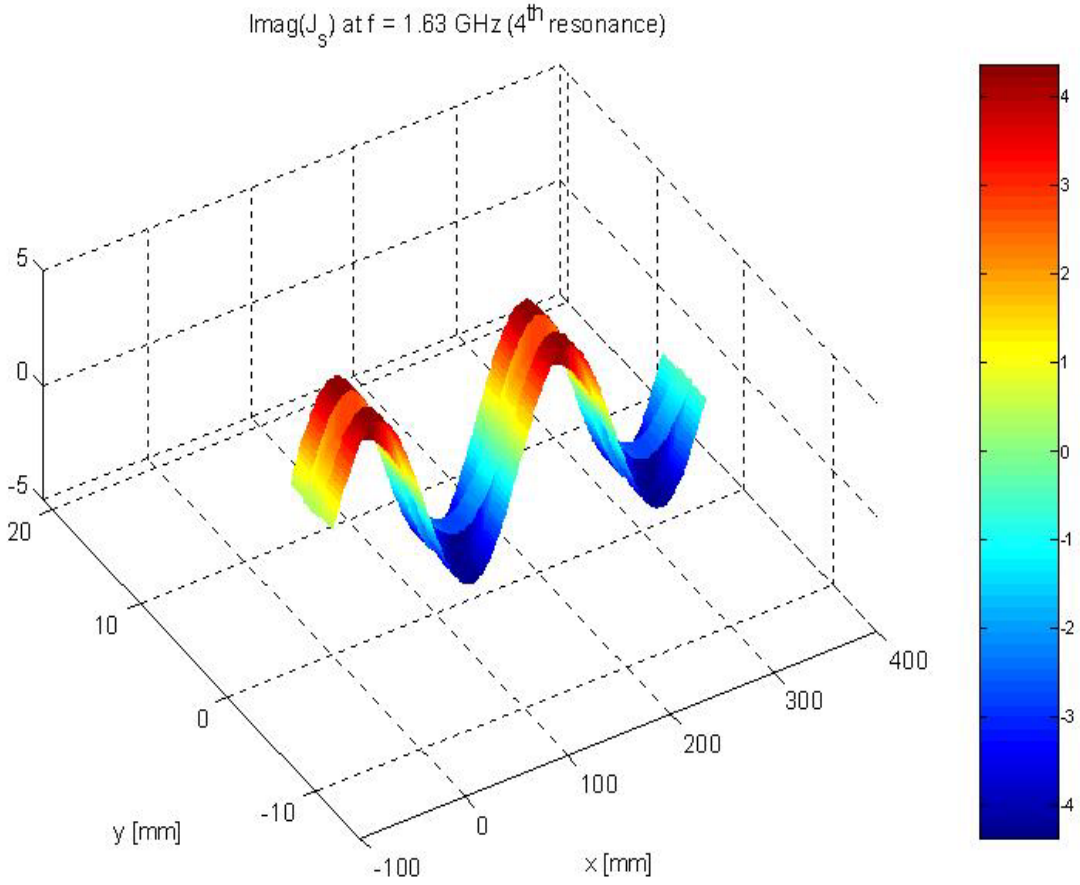

Figure 3. Imaginary part of surface current density (Js) for the four resonance of the line.

To illustrate that meander behaves as a line for frequencies below the first resonance of a patch, f_{10}, we have plotted imaginary part of current density, not affected by the feeding and so more adequate to see the shape of resonance, for the fourth resonance of the line and the meander. For the line there it is not a big deal, four half sinus or five zeros are counted, see Figure 3.

So if it is true that the meander behaves as a line it should present the same, that is, four half sinus or five zeros. For the sake of clarity, it has been plotted the phase of the imaginary part of the current in colours, going from blue (-90 degrees) to red (90 degrees), and also the magnitude of current in white arrows. When there is a change in the sense of the arrows there is a zero. If this change is produced in the same arm of the meander (an arm here is the metal part between two arms), phase changes from red for blue, or the other way round. It happens twice in Figure 4. Two zeros. If the change is produced in the boundary of two arms, there is no phase swapping, the sense change exists but phase remains the same. It happens once in the centre up of the structure, see Figure 4. We have to add the zeros at the beginning of the patch and at the end, so counting the total we get 5 zeros, which demonstrates that the meander for low frequencies has a line behaviour.

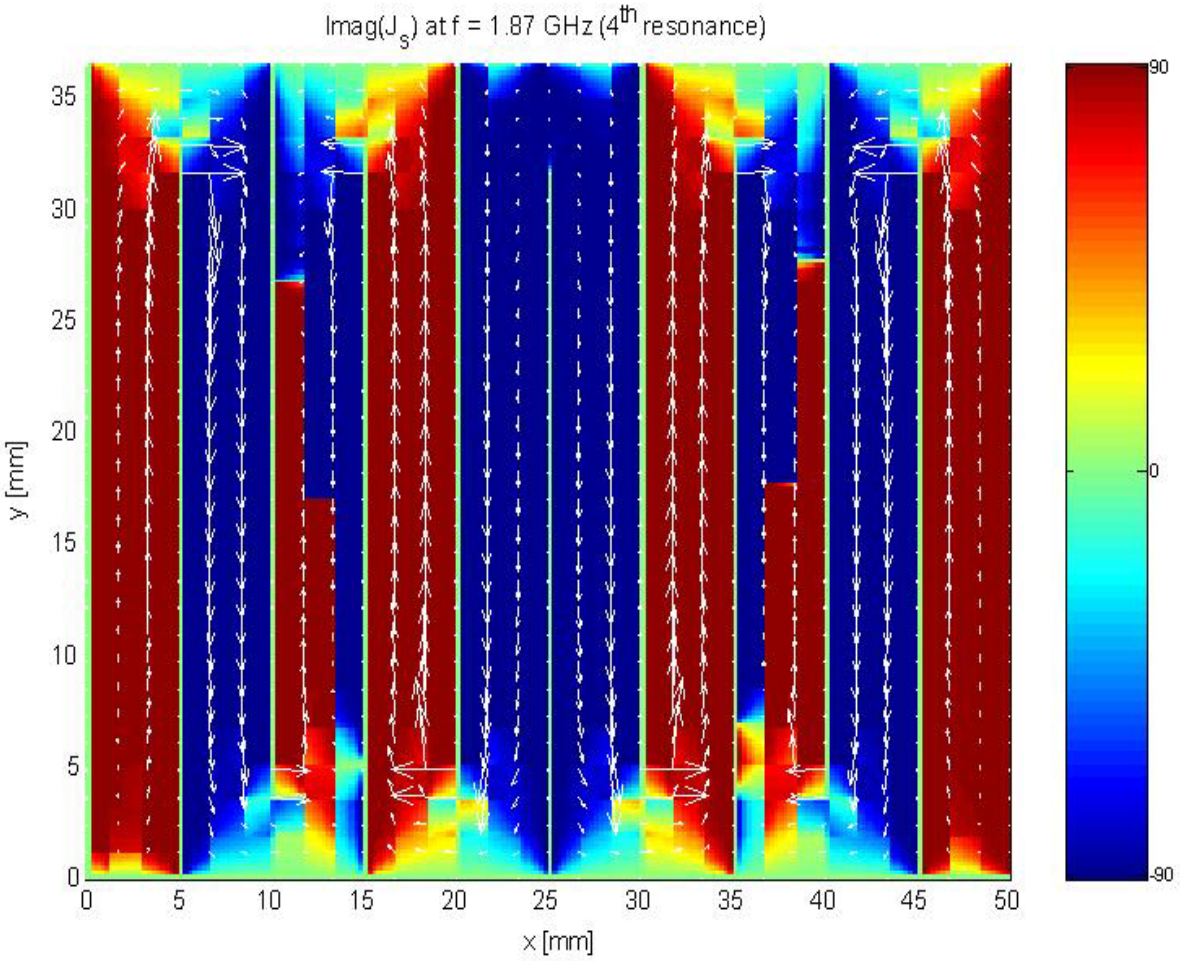

Figure 4. Imaginary part of surface current density over the meander (white arrows) and its phase (colours) for the meander at its fourth resonance.

Comparison patch-meander

For higher frequencies a comparison between patch and meander has been done. In Figure 5 we can see the S_{11} parameter of both structures. At first sight they are completely different. First of all it can be observed that the first resonance of the patch doesn't appear for the meander, as expected, because putting the gaps we have killed this resonance, as current is supposed to flow in the sense perpendicular to the gaps, see Figure 6 for a representation of currents in a patch for f_{10}, but there is not, so to say, a free way due to the presence of the gaps. So patch f_{10} resonance is not a meander resonance.

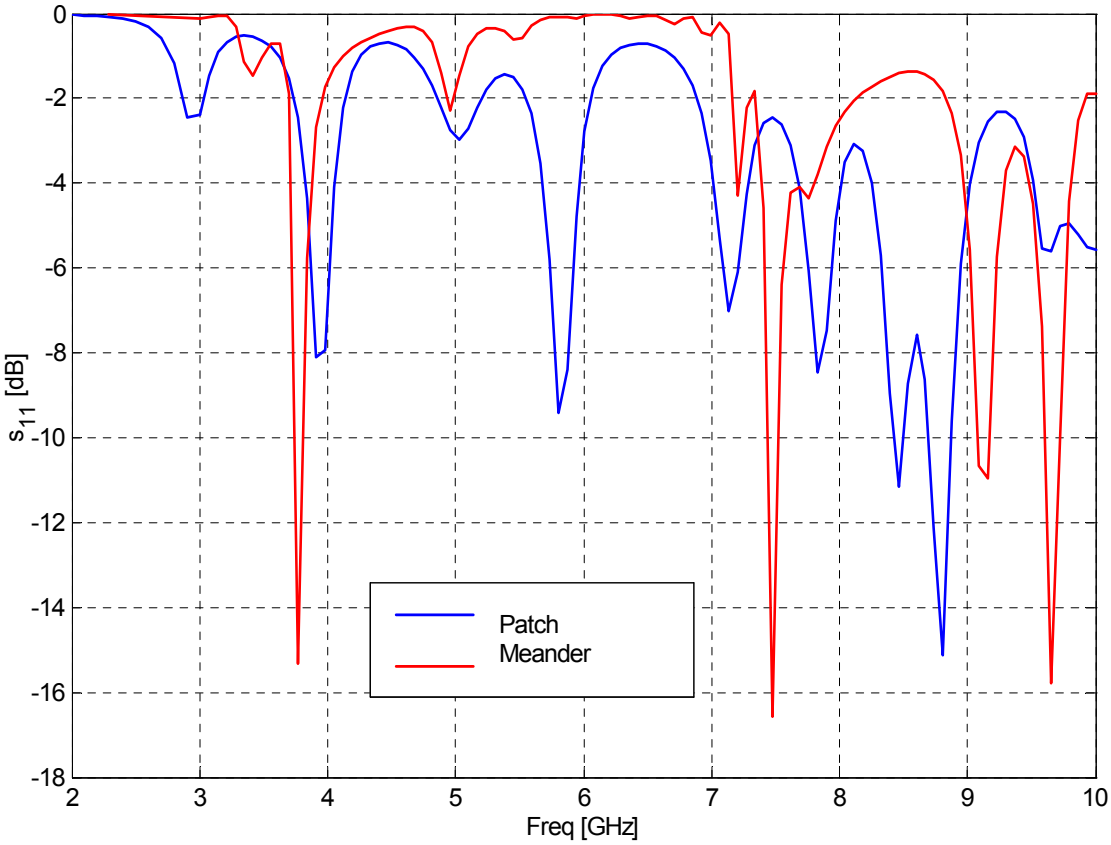

Figure 5. S11 parameter of patch (blue) and meander (red).

At f = 3.77GHz we find a meander mode that could be a modified mode(0,1) of a patch. As gaps are parallel to the direction of the current for this mode, it is allowed in the meander, but when we plot currents we see that in the meander currents have different levels in its left short side and in the right one, whereas in the patch this level is the same. Indeed, in Figure 7 we can see the currents for second resonance on a patch and on the meander, where arrow size is less important on the right side.

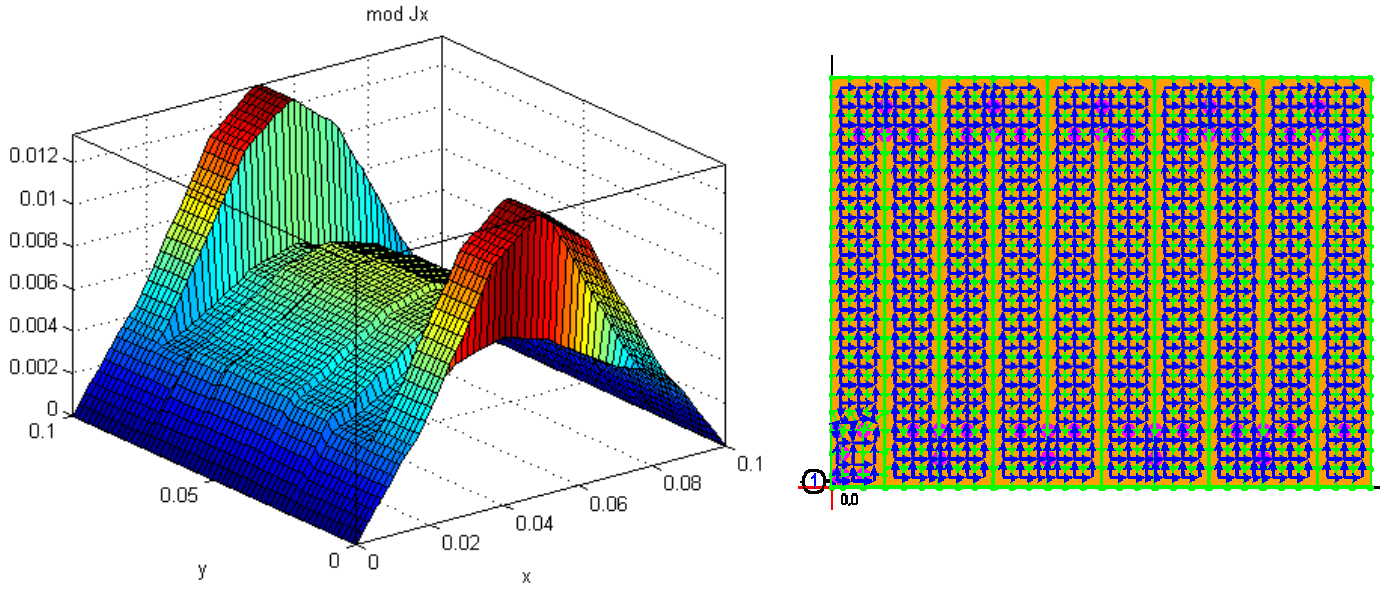

Figure 6. Currents for the first resonance of a patch (left), and the avoiding geometry of meander (right) .

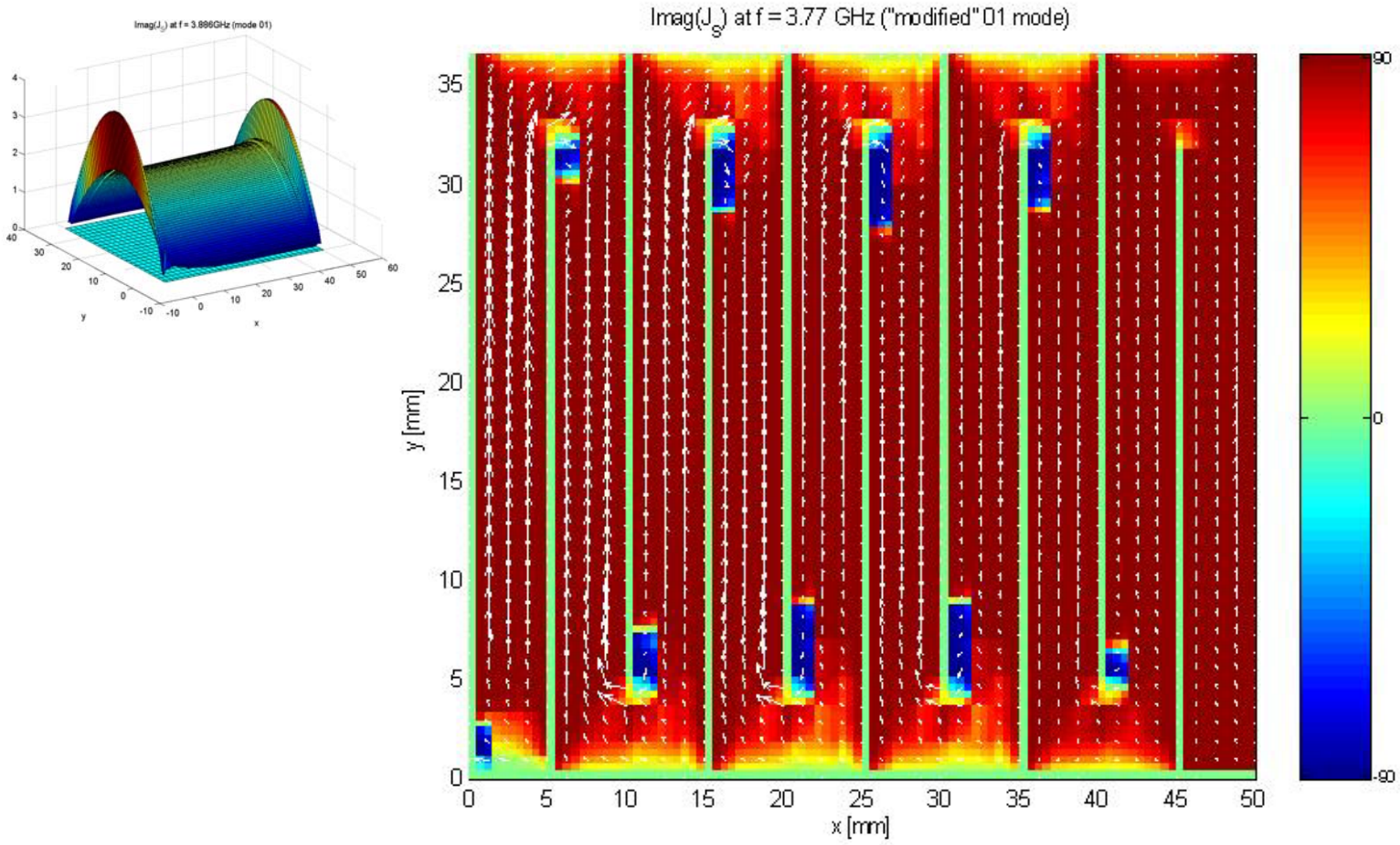

Figure 7. Currents for second resonance of the patch (left) and meander (right).

White arrows on the meander representing imaginary part of current are strongly y-directed, so phase is dominantly the same in all the arms of the meander, except some localized focus in the extremes of the gaps, where there are high "turbulences", and it seems as if current wanted to flow following the labyrinth formed by gaps, but the natural second resonance of the patch does not allow it. This could explain the difference of level in both sides of the patch, due to this kind of leakages.

For higher modes it is not that evident to discern whether the meander behaves as a patch or not, the truth is that the more the frequency is increased the more the meander creates its own modes and recognizing there some similarities with a patch behaviour becomes impossible, because the coupling between the arms of the meander turns out to be higher and this creates the new behaviour in the structure.

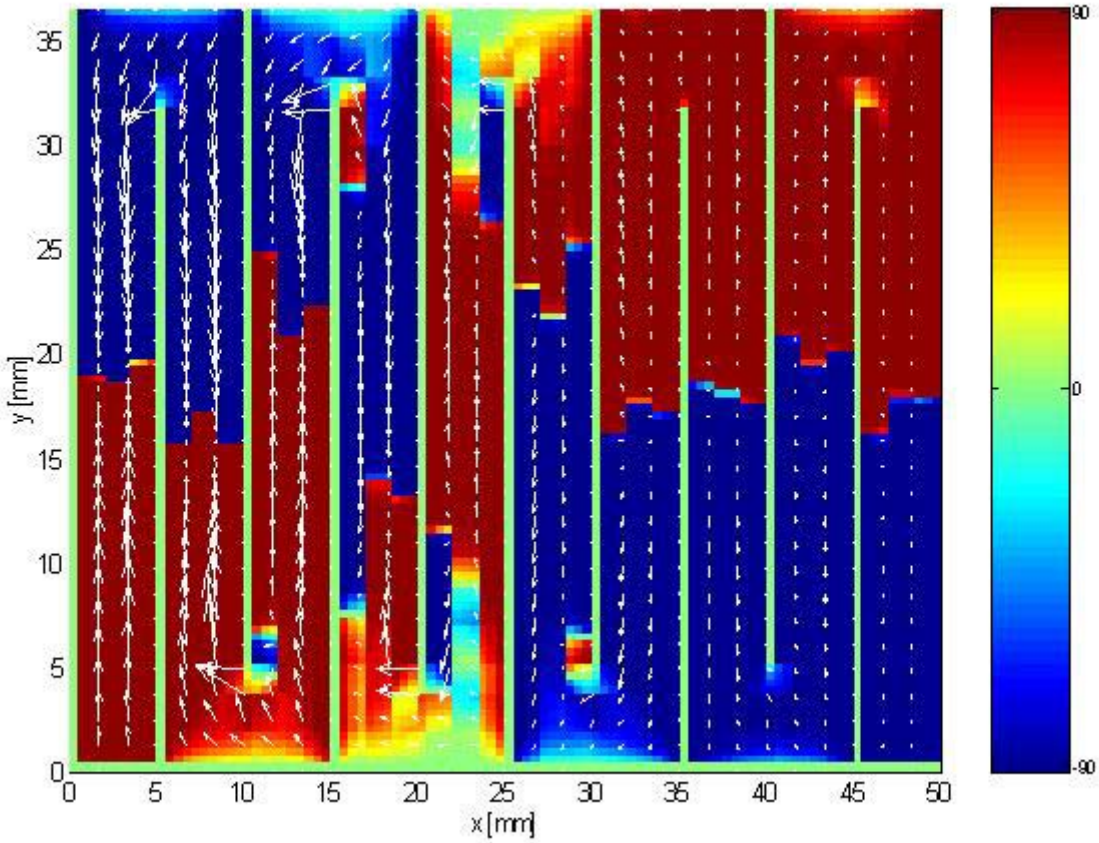

Figure 8. Currents (white arrows) and phase (colorbar) for a higher order meander mode.

In some fractal structures as the Koch island or the Sierpinski microstrip patch antennas for high frequencies there are some hot spots on the surface which are in phase and benefit a broadside radiation [2]. In this case we observe some hot spots at the end of the gaps, and the ones in the upper side are in phase, and so they are the ones in the down part, but up and down spots are in counter phase. So the radiation pattern is not broadside, as it can be seen in Figure 9.

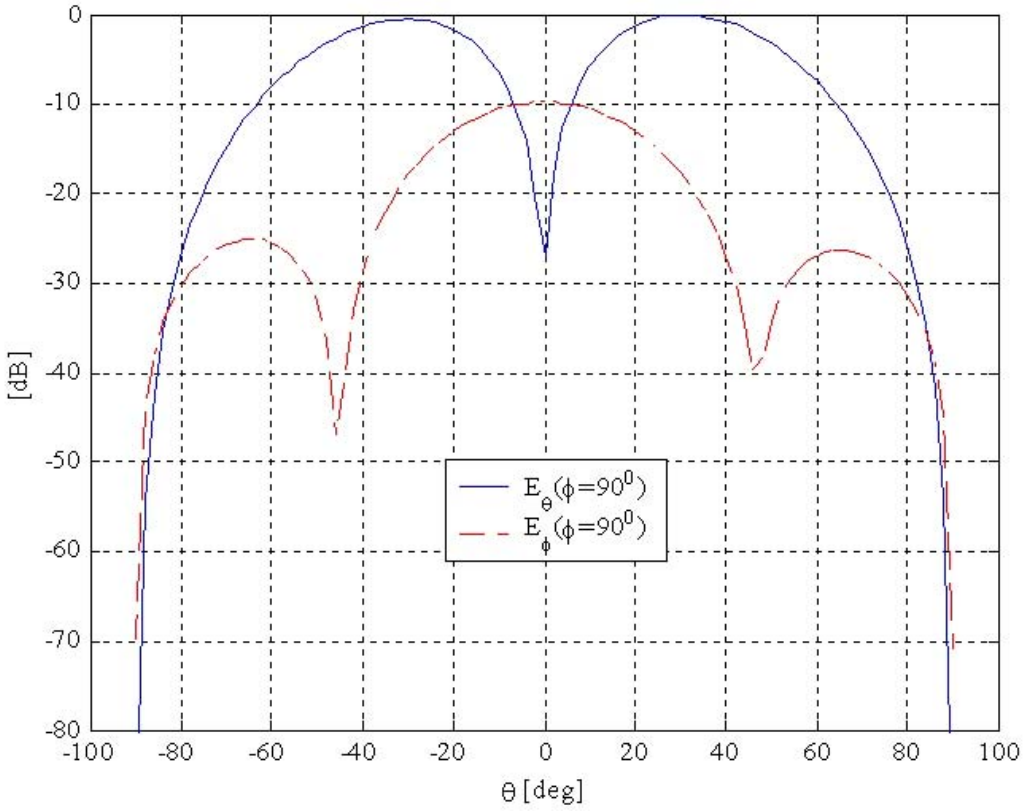

Figure 9. Radiation pattern for the higher mode.

7.3. Conclusions

A meander type antenna has been studied as an example of pre-fractal structure. Below first resonance of a patch having the same surface that encloses the meander, the meander behaves as a line resulting of unwrapping the structure. But a miniaturisation effect exists in meanders, because it presents almost the same resonance frequency that unwrapped line, but much more radiation at these frequencies (higher $Re(Z_{in})$).

Meander also show some patch-like resonances and specific resonances. Therefore size reduction doesn't require fractal shapes and can be very effective with simple meanders. However non-fractal shapes seem to lack the "superdirectivity" property. "Hot spots" of current also appear in meanders but they are not equiphase. Therefore we don't expect broadside radiation.

The last fractal-like feature which must be investigated in other highly convoluted shapes is the stability of the radiation pattern.

For higher frequencies complex resonance phenomena appear due to EM coupling between the parallel lines. Further studies are needed in order to understand these complex phenomena.

7.4. References

[1] Puente C., Romeu, J., Cardama, A. « The Koch monopol : a small fractal antenna« , Antennas and Propagation, IEEE Transactions on, Vol.48 No 11, Nov.2000.
[2] Borja, C., Romeu, J. «Fracton vibration modes in the Sierpinski microstrip patch antenna « Antennas and Propagation Society, 2001 IEEE International Sym , Vol. 3 , 2001.

8. BENCHMARKS FOR PRE-FRACTAL ANTENNA PERFORMANCE. MINIATURE ANTENNA: THE TWO-ARM SPIRAL

8.1. Introduction

Fractal geometry is interesting from the electromagnetic point of view due to some characteristics as having infinite length in a finite surface, and as self similarity. In order to develop accurate numerical tools for pre-fractal antennas, well defined benchmarks must be first considered. One interesting possibility is the spiral shape which has been known since long time by antenna engineers as a source of compact antennas. From the electromagnetic point of view spirals share with fractals the interesting properties of infinite length in a finite surface, allowing antenna miniaturization keeping reasonably low resonance frequency as well as fractals, and self-similarity, indeed in each turn they make they are repeating themselves with a scale factor. Moreover some of spirals have shapes that would make an antenna to be self complimentary, that is to say, an antenna with this shape would have a constant behaviour in frequency. This is a behaviour that should be sought in fractal shapes.

8.2. Geometry of spirals

One possible class of objects which defies length measurements are spirals, as well discussed in [1]. Spirals can conceal any arbitrary length into a finite surface. The two more interesting types of spiral to our purposes are the Archimedean and the logarithmic spirals.

Archimedean spiral: The characteristic feature of an Archimedean spiral is that the distance between its windings is constant. In polar coordinates an Archimedean spiral can be modeled by the equation: $r(\phi) = q\phi$, so $\phi = 2\pi$ is one turn, $\phi = 4\pi$ corresponds to two turns, and so on.

Figure 10. Logarithmic spiral (left) archimedean spiral (right).

Logarithmic spiral: Replacing $r(\phi)$ by the natural logarithm we obtain the formula for the logarithmic spiral. It has a remarkable property which is related to fractals, namely self-similarity.

The polygonal spiral, on the other hand, has the property of being easier to build and that it fits better the surface where it is plotted. To build it we first choose a decreasing

sequence $a_1, a_2, a_3, \ldots$ of positive numbers. We construct a polygon in the following way: draw a_1 vertically from bottom to top. At the end make a right turn and draw a_1 again from left to right. At the end of that line start to draw a_2 from left to right, then make a right turn and plot a_2 again from top to bottom, taking a_3 at the end of this line, and continue on using the same principles.
How long is this polygon? The answer is that it depends on the sequence of numbers we have taken as generating system. Each segment appears twice, so the length is $2(a_1 + a_2 + a_3 + \ldots)$. In Figure 11 the chosen sequence is $a_k = \frac{1}{k}$, so the length is a series which is known not to have a limit, that is, this spiral has infinite length.

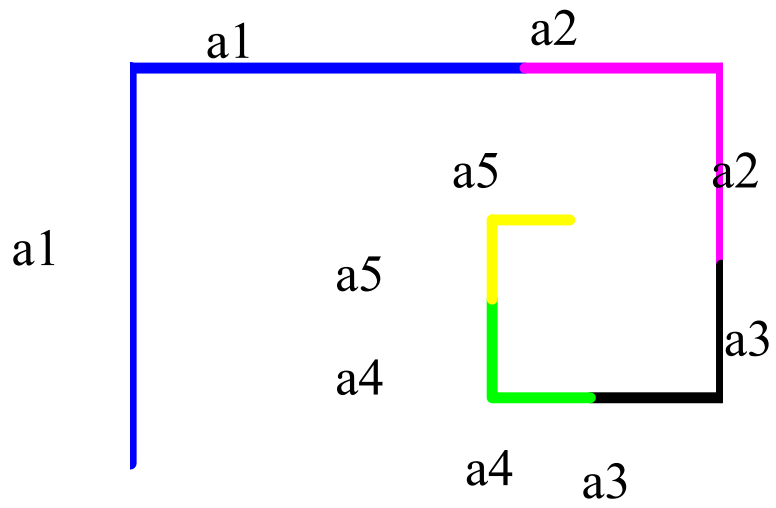

Figure 11. Polygonal spiral.

8.3. Square spiral

In the following sections a study of a printed two arms square spiral will be done, as appeared in [2]. The square spiral presents advantages to a circular Archimedean design for reasons of simplicity of construction and more efficient utilization of a limited area mounting plane.

Specification parameters

The construction of a Square Spiral antenna **backed by a ground plane** can be fully specified with only four parameters [2], namely:

Order: A measure of the spiral winding density.
d: Substrate thickness.
SL: Side length.
ε_r: Substrate relative Permittivity.

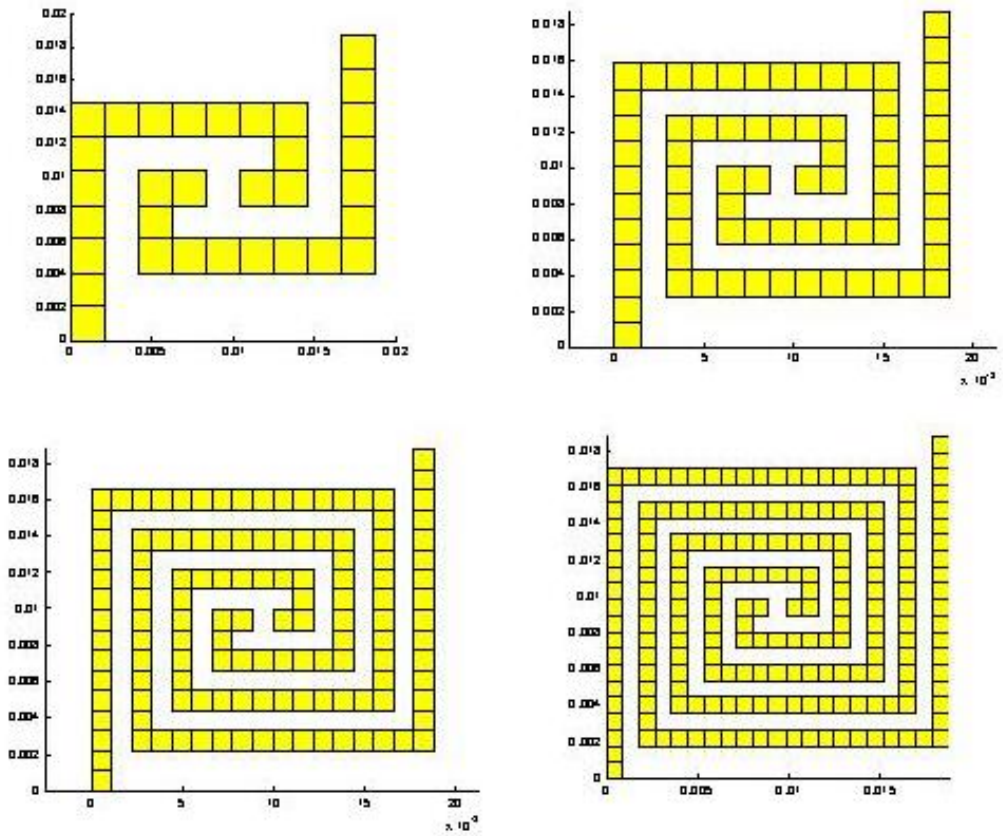

Figure 12. Metallization layer of the four first iterations of a two arm square spiral.

The mesh for the first four iterations can be found in Figure 12. The gap between the two arms is set to be equal to the strip width. So there is the same space with metal than without it. Extrapolating towards infinity we have a self-complimentary antenna. All the iterations fit in a square of side SL=1.875cm, so the width of the lines changes for each iteration. A size of $2cm^2$ would allow the antenna to fit in a watch, for instance.

The excitation of the antenna is modeled as an **E** field that produces a 1 V differential across the gap between the two spiral arms, see Figure 13.

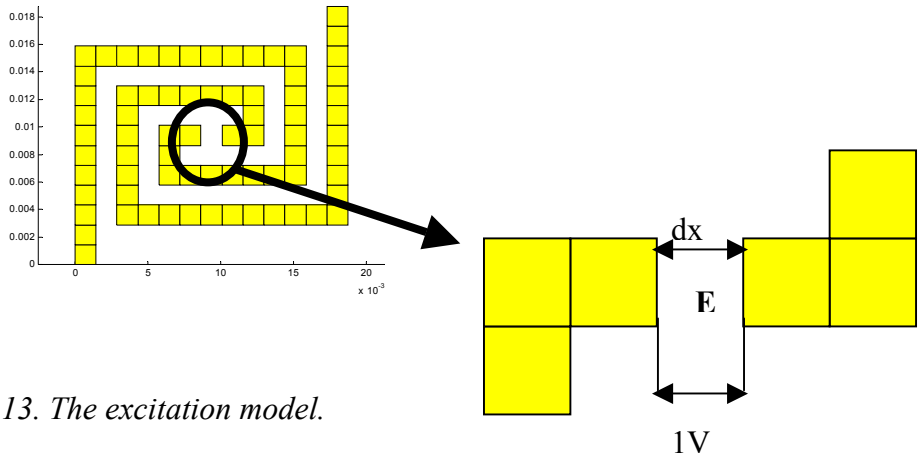

Figure 13. The excitation model.

Input impedance of spiral antennas.

In this section the input impedance for the four iterations of the spiral antenna is computed. The highest frequency of resonance is expected for the lowest iteration, and as the number of iterations increases the resonant frequency is expected to be smaller, because the equivalent length is bigger.

	1st Iteration	2nd Iteration	3rd Iteration	4th Iteration
1st F_{res} (GHz)	4.6	3.3	2.3	1.77
Lequivalent (cm)	6.66	10.53	14.44	17.94
Size compression	------	1.59	2.16	2.69
Frequency compression	------	1.40	2	2.6

Table 1. Simulated spiral antennas. First resonance for the four iteration, equivalent length of an unwrapped spiral, size compression from each iteration compared with the first one and frequency compression of the first mode of each iteration compared with the first one.

In Figure 14 it can be seen that the expected pattern is accomplished by the four first iterations, indeed, the more convoluted the shape is, the lower the resonance frequency is. It has been computed the size compression, which is the ratio between the equivalent length of the first iteration and all the other. It has been also computed the compression factor in frequency with respect to the first iteration, so for the third other iterations. All these data are represented in Table 1. It can be seen that frequency and size compression are of the same order of magnitude for all the cases.

Iterations 3 and 4 have first and second modes for a lower frequency than the first mode of the first iteration.

Another characteristic of spiral antenna that must be mentioned and that can be observed in Figure 14 is the self-similarity. For self-similar antennas as it is the case here, a constant behaviour in frequency is expected. For low frequencies we have the normal resonances but as we go higher in frequency the input impedance seems not to vary that much with frequency, so it is achieving a constant behaviour. It can be explained by the fact that to be self-similar the size of the antenna side must be λ, so the input impedance begins to be constant from a certain value of frequency.

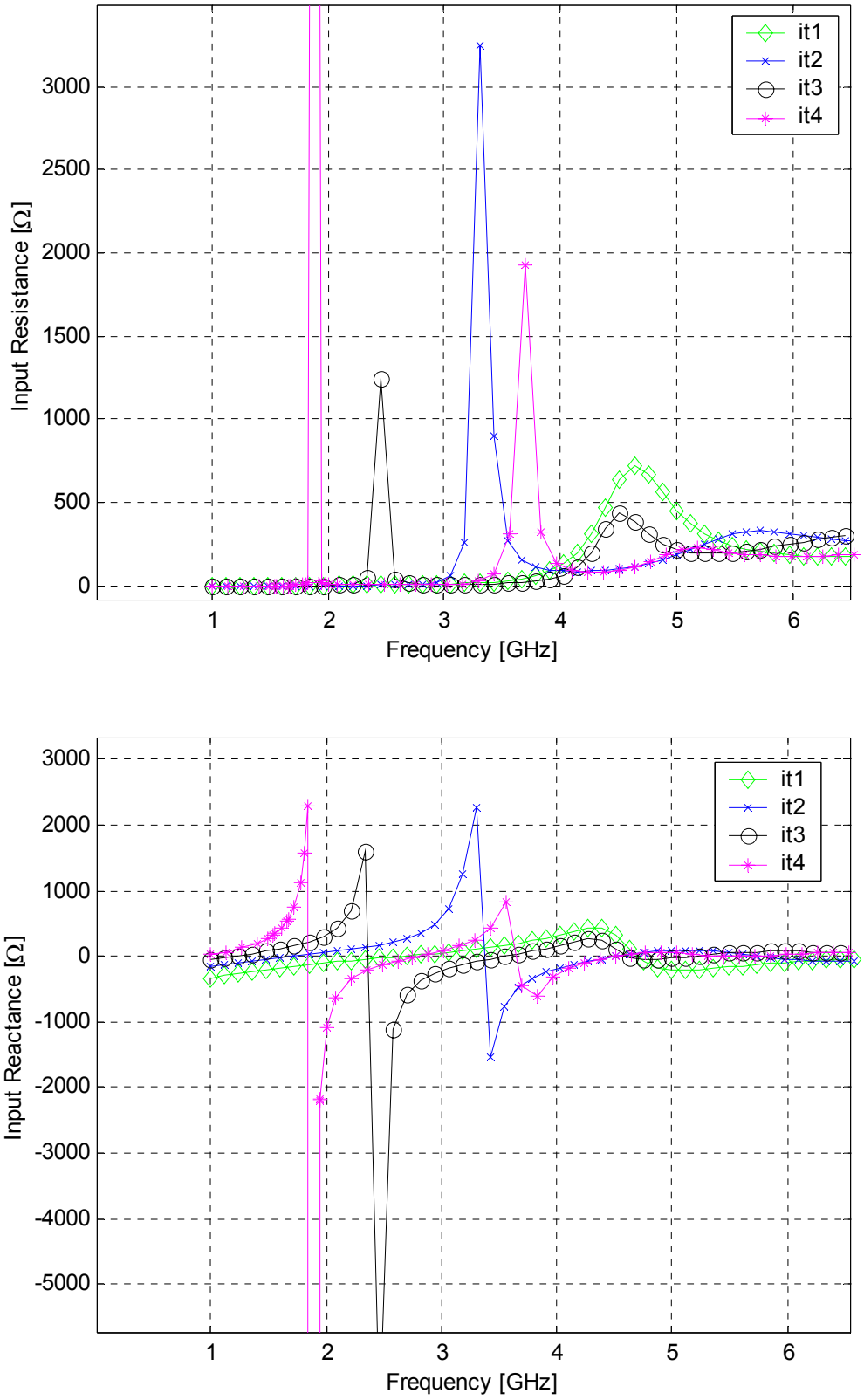

Figure 14. Real and imaginary parts of Input Impedance for the four spiral iterations.

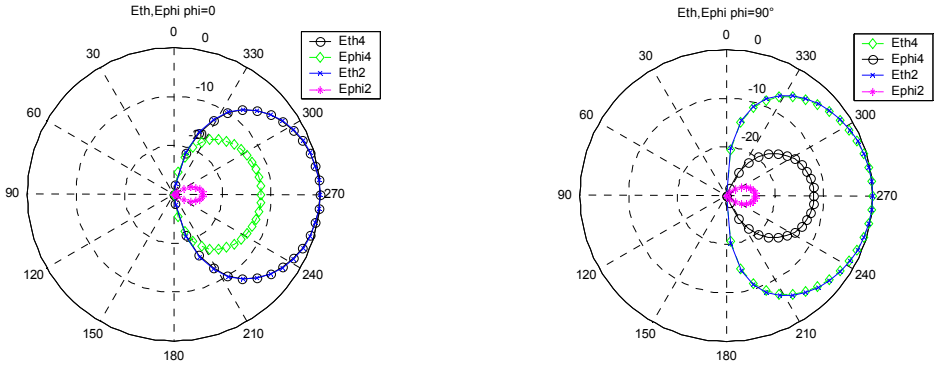

Figure 15. Radiation pattern for order2 and order4 spiral antennas, in the phi=0 plane (left) and the phi=90° plane (right).

Taking two of the spirals, let us say 2 and 4, and making a comparison of their radiation patterns, it can be seen that in the E-plane (phi=0), the co-polar is of the same level, but the level of cross-polar is much bigger for order 2 (to the order of 10 dB). The same happens in the H-plane, as it can be seen in Figure 15.

Comparison between spiral antennas and straight dipoles

Let us suppose that for a given application we need to build an antenna which must fit in a square of side $SL = 1.875cm$. In this section we are going to study which are the advantages, if any, of filling the given surface with a spiral rather than with a straight dipole having as length the maximum length suiting in the square surface, that is to say, $L = \sqrt{2}SL$, to justify the use of convoluted shapes. It will be done for the second and fourth iteration of the spiral and for the frequency range 1-13GHz.

Iteration 2

Input impedance for a spiral of order 2 and a line of length $L = \sqrt{2}SL$ is shown in Figure 16. The self-complementary behaviour can be seen for frequencies bigger than 6GHz.

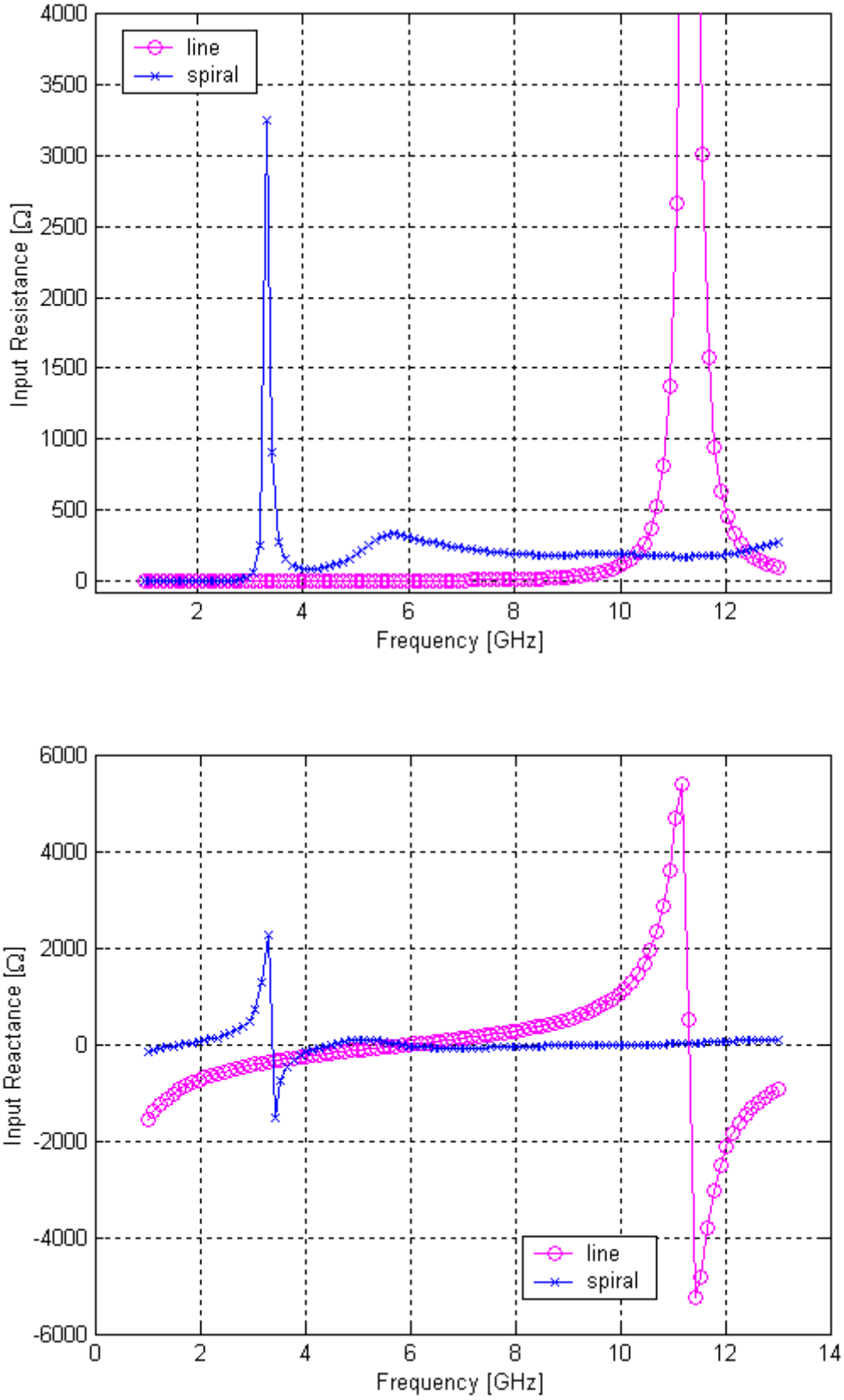

Figure 16. Input impedance of iteration 2 spiral vs dipole of length equal to the diagonal of the circunscribed square.

The order 2 spiral has two resonances and the dipole has a resonance in the range from 1 to 13 GHz. To see if it is the same mode the coefficients of currents (solutions to the MoM) are plot as a function of the basis function number. In the case of the spiral the numeration of the basis functions is done from the external part of one of the arms to the centre, and from the centre to the final of the second arm, it doesn't matter which one, as it is a symmetric structure.

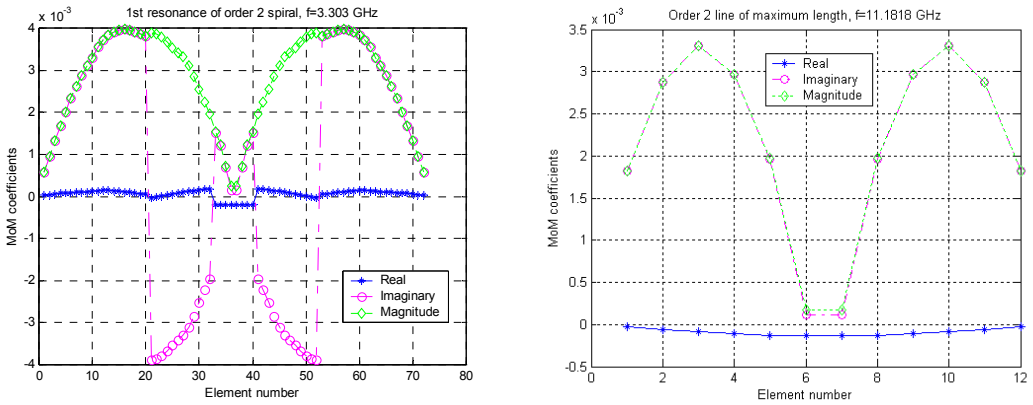

Figure 17. Current coefficients vs. basis function for spiral (left) and dipole (right).

It can be seen in
Figure 17 that the first mode is not appearing either for the spiral or for the dipole as the excitation is in the middle, but the second mode. For the line it appears at f=11.1818GHz, whereas for the spiral we have the resonance at 3.303GHz, which means that the convoluted shape of the spiral introduces a frequency compression factor of 3.38.

Iteration 4

Input impedance for a spiral of order 4 and a line of length $L = \sqrt{2}SL$ is shown in Figure 18. Again for the order 4 spiral a self-complementary behaviour can be observed from 4GHz, which means that the order 4 spiral begins to have a "constant" behaviour in frequency for a frequency 2 GHz lower than the order 2.

The order 4 spiral has four resonances and the dipole has a resonance in the range from 1 to 13 GHz. To see if it is the same mode the coefficients of currents (solutions to the MoM) are plotted as a function of the basis function number. As it can be seen in
Figure 19 the order 4 spiral presents a resonance for fres=1.77GHz, whereas the dipole presents it for 11.6GHz, what means a frequency compression factor of 6.55.

Comparing this result with the one for the spiral 2, the increment of frequency compression is 1.94, which means that resonance frequency is almost reduced the double with respect to a dipole than for the order 2 case.

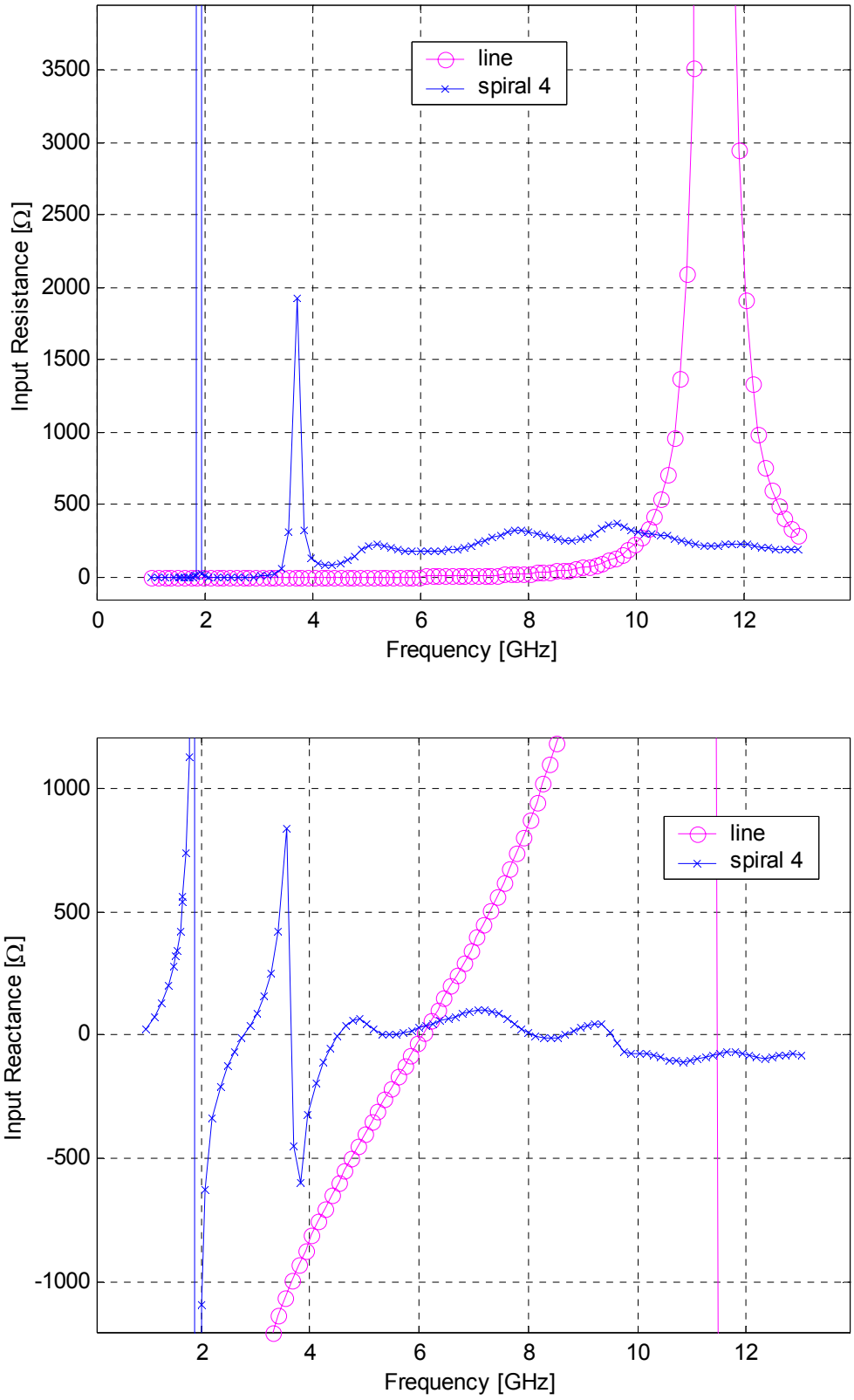

Figure 18. Input impedance of iteration 4 spiral vs. dipole of length equal to the diagonal of the circumscribed square.

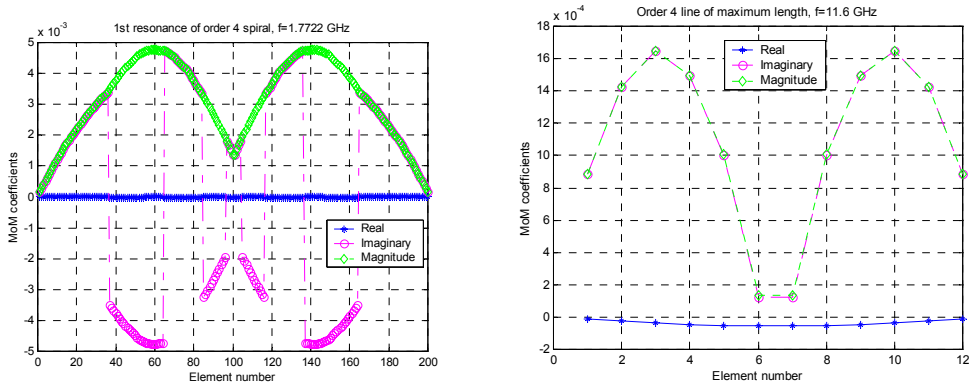

Figure 19. Current coefficients vs. basis function for spiral 4 (left) and dipole (right).

Identification of modes.

In this section current distribution is going to be plotted to have an overview of current location over the structure. It is going to be done for spiral order 2, for its first and second mode, and order 4 for its first and fourth mode.

Order 2

Again the numeration of basis functions begins in one extreme of the spiral and goes towards the centre of the spiral and for the other arm it goes from the centre to the extreme. One arm goes from element one to element 36 and the other arm goes from element 37 to 72.

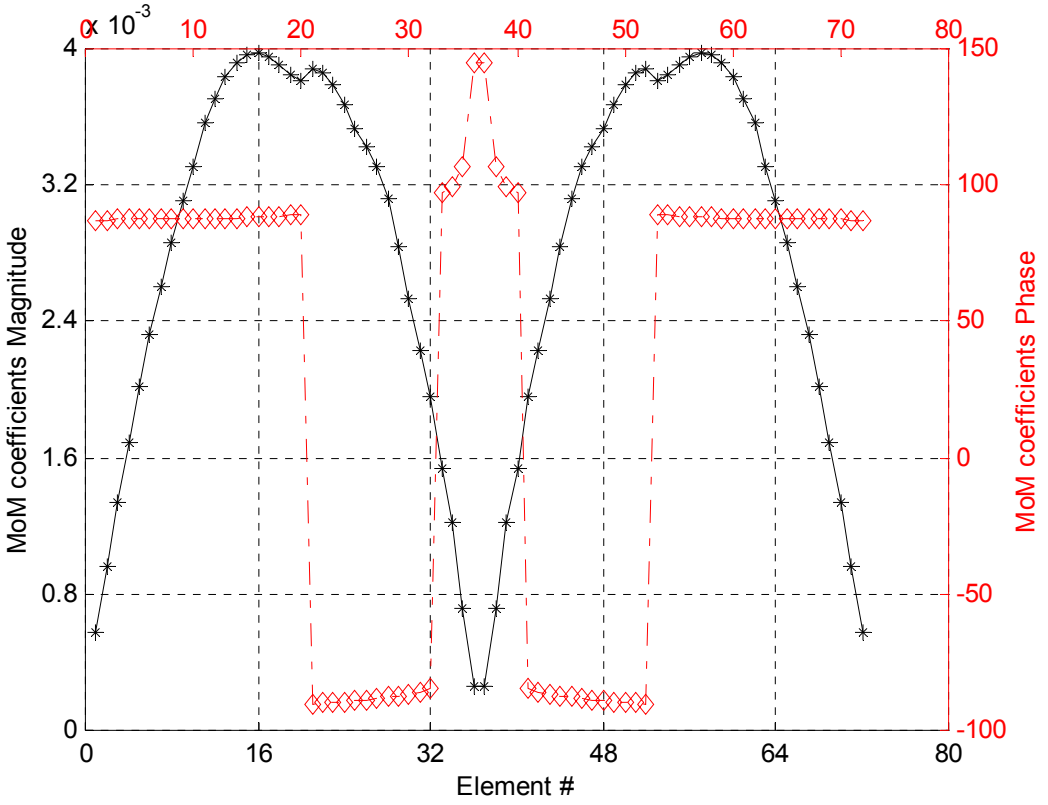

Figure 20. Magnitude and phase of current coefficients for order 2 spiral at f=3.3GHz.

In Figure 20 can be seen, for the first mode of spiral 2, in black and according to the y-axis on the left the magnitude of the MoM coefficients [A/m^2], and in red according to

the y-axis on the right the phase of the MoM coefficients in degrees. The phase switches from 90° to –90°, so it can be said that all the elements are in phase.

Plotting the magnitude of surface current density (Figure 21) it can be seen that for the first mode of order 2 spiral there is a concentration of currents on the corners of the more external bendings of the structure, which is in fact reproducing the half sine shape we have observed for current magnitude in Figure 20.

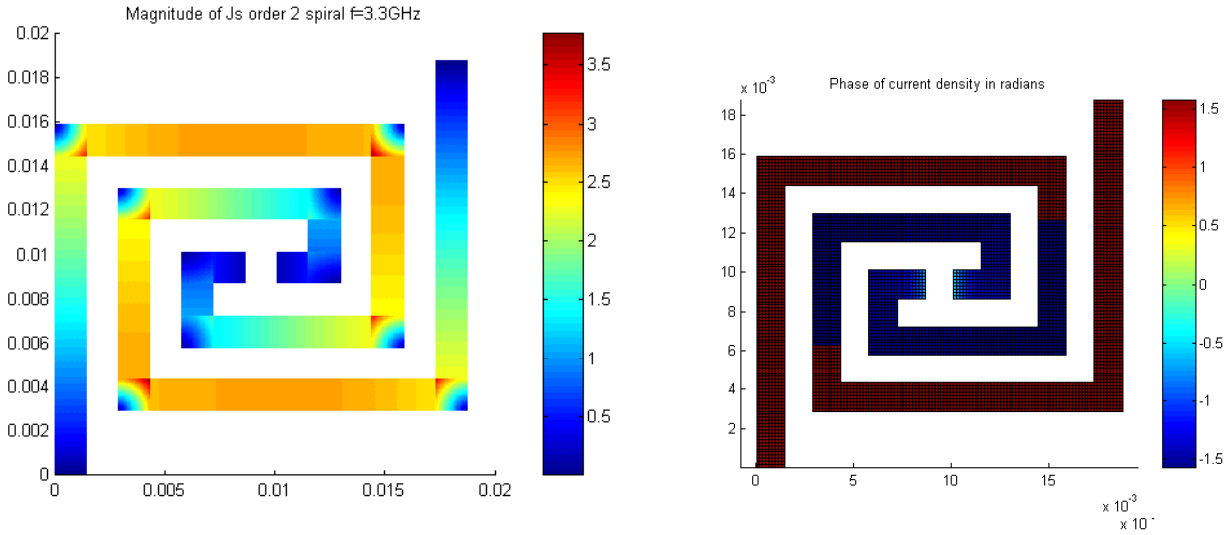

Figure 21. Magnitude of the surface current density [A/m^2] (left) and phase [rad] for the first mode of order 2 spiral.

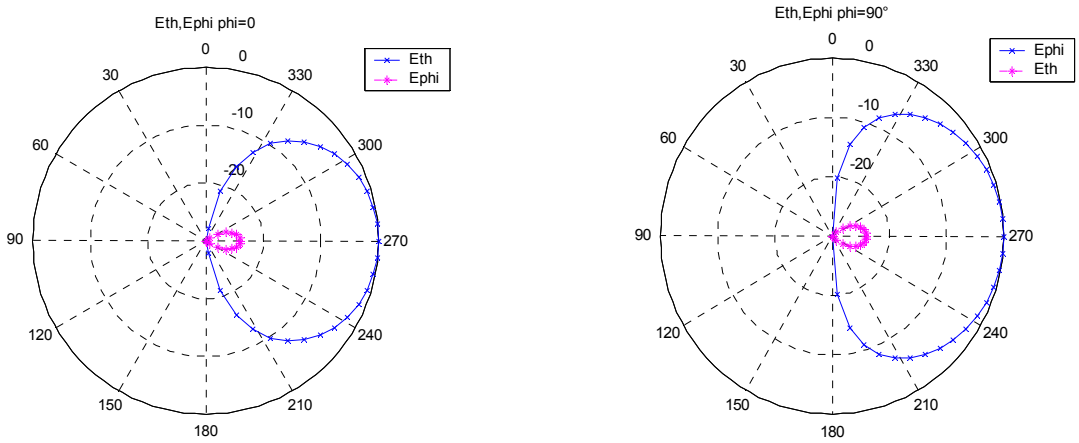

Figure 22. Radiation pattern for first mode of spiral 2, phi=0 (left) , phi=90° (right).

The radiation patterns for both planes E and H are plotted in Figure 22. Spiral 2 for its first mode has a dipole-type radiation pattern, with the characteristic of having the cross-polar much lower than the co-polar in both planes.

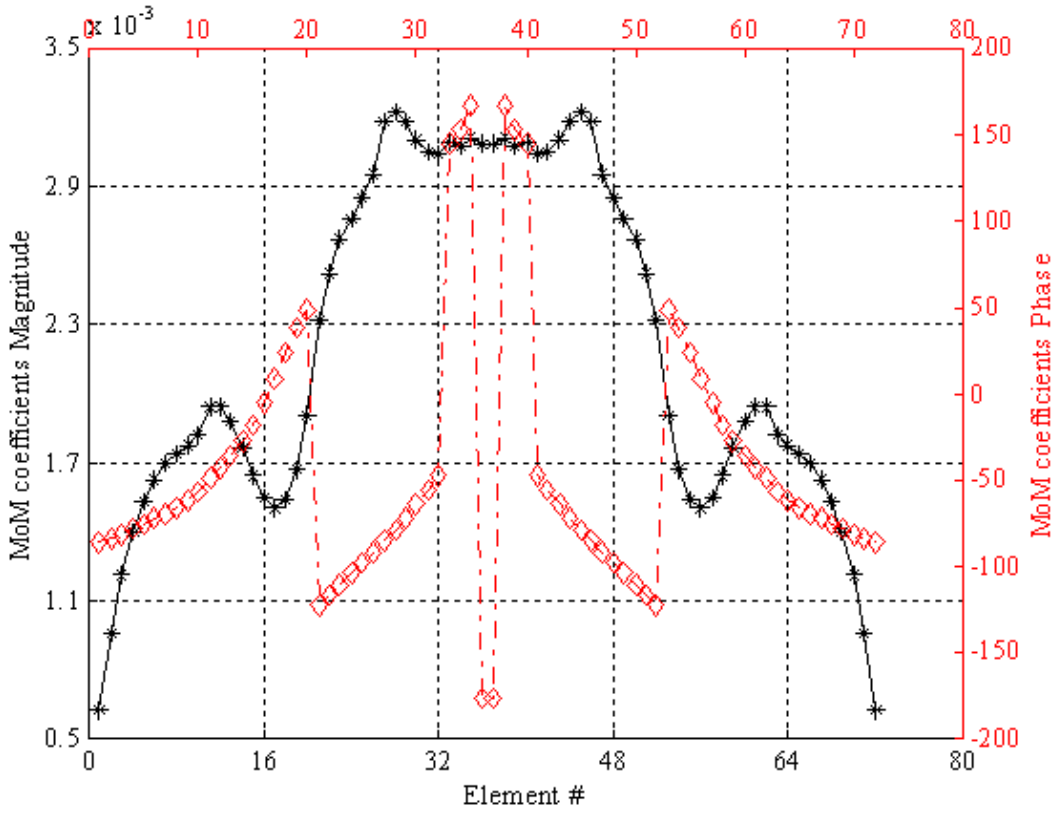

Figure 23. Magnitude and phase of current coefficients for order 2 spiral at f=3.3GHz.

For the second mode of spiral 2, which occurs at 5.84 GHz, currents do not have the typical shape of a straight dipole mode, fact that is showing this mode is an own mode of the spiral. In Figure 23 again it is plotted in black and according to the y-axis on the left the magnitude of the MoM coefficients [A/m^2], and in red according to the y-axis on the right the phase of the MoM coefficients in degrees, for the second mode of spiral 2. This time the phase is varying along the arm of the spiral, so currents are not in phase.

Plotting the magnitude of surface current density (Figure 24) it can be seen that for the second mode of order 2 spiral there is a concentration of currents on the corners of the more internal bendings of the structure, which is in fact reproducing the shape we have observed for current magnitude in Figure 14.

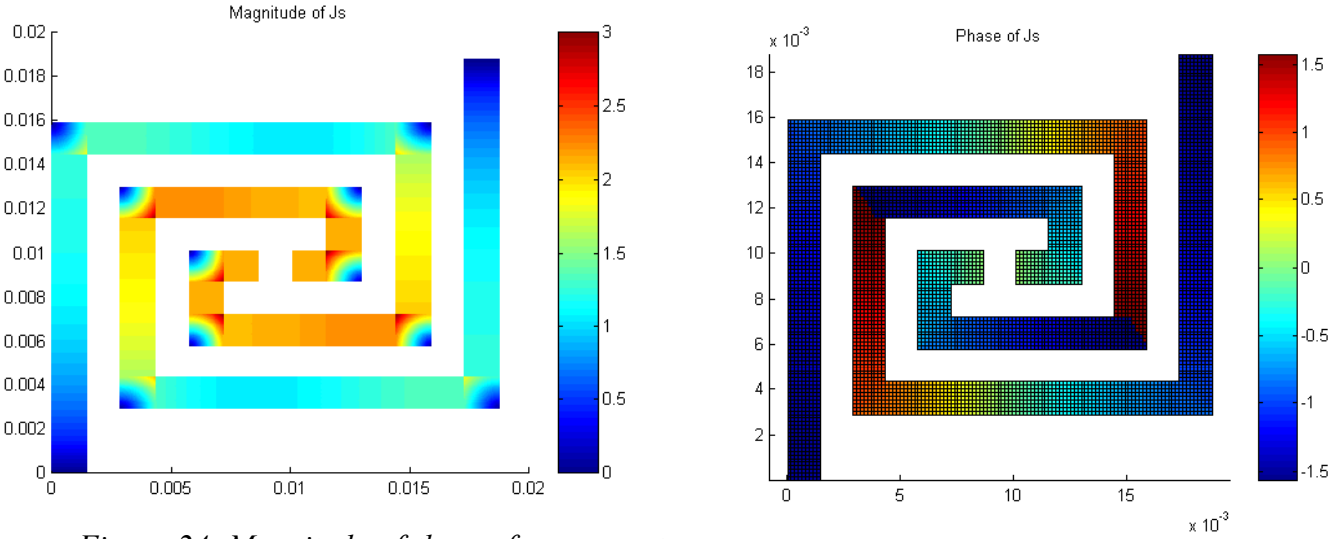

Figure 24. Magnitude of the surface current density [A/m˜] (left) and phase [rad] for the second mode of order 2 spiral.

As localised currents are not in phase, radiation pattern is not expected to be directive. Indeed, looking at Figure 25 it can be seen that the pattern lobe in both planes is even wider that for the first mode. But on the other hand, E_{th} and E_{ph} have the same level, so for higher modes than the first mode spiral order two is having a circular polarization.

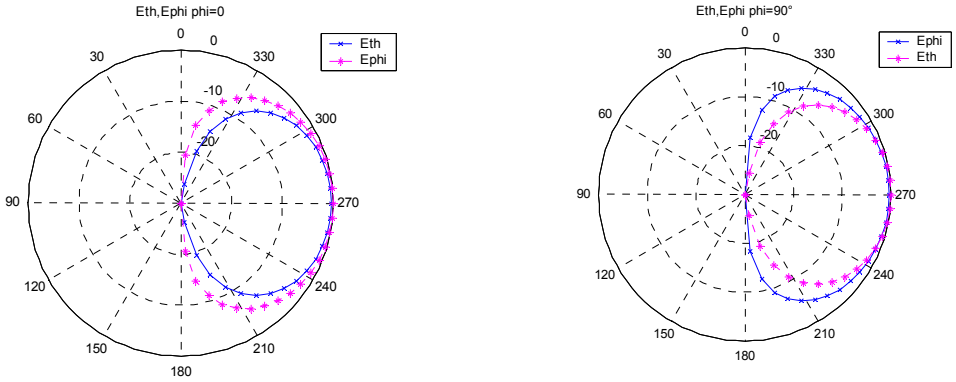

Figure 25. Radiation pattern for the second mode of order 2 spiral, phi=0 (left), and phi=90° (right).

Order 4

The same analysis will be now made for spiral 4 in the first and fourth modes.
For the first mode at 1.77GHz, it can be seen in Figure 26 in black and according to the y-axis on the left the magnitude of the MoM coefficients [A/m^2], and in red according to the y-axis on the right the phase of the MoM coefficients in degrees. The phase switches from 90° to –90°, so it can be said that all the elements are in phase.

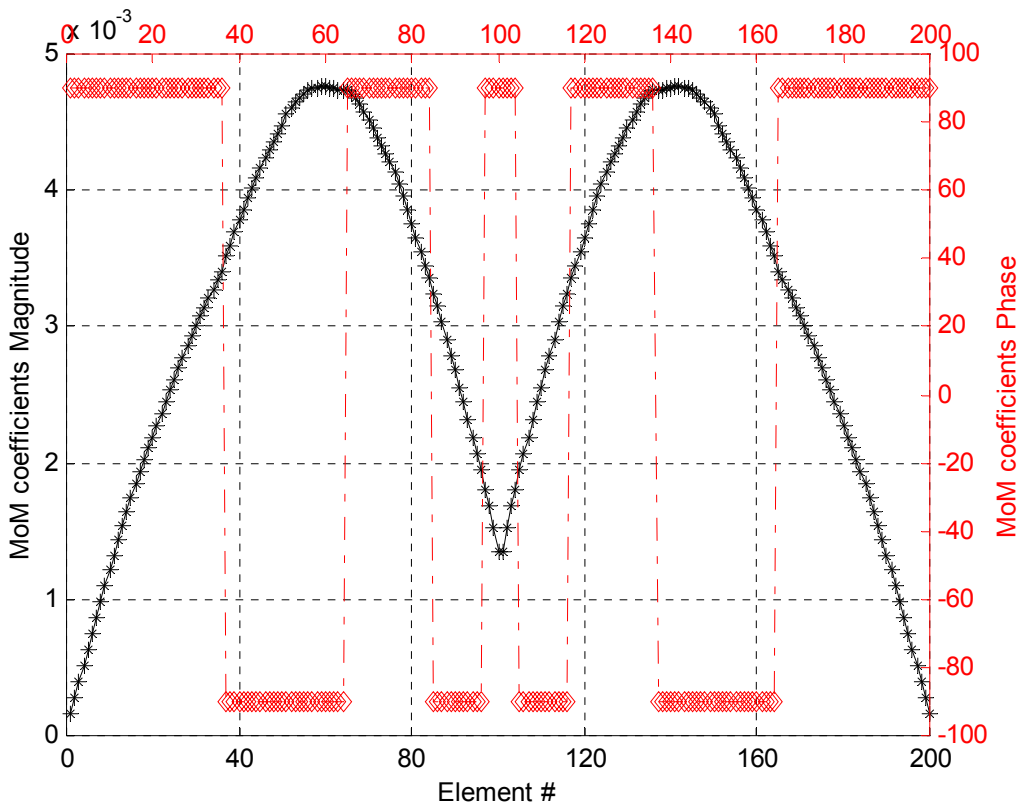

Figure 26. Magnitude and phase of MoM coefficients of order 4 spiral for f=1.77GHz.

Plotting the magnitude of surface current density (Figure 27) it can be seen that for the first mode of order 4 spiral the behaviour of currents is similar to the first mode of order 2 spiral, that is there is a concentration of currents on the corners of the more external bendings of the structure, which is in fact reproducing the half sine shape we have observed for current magnitude in Figure 26.

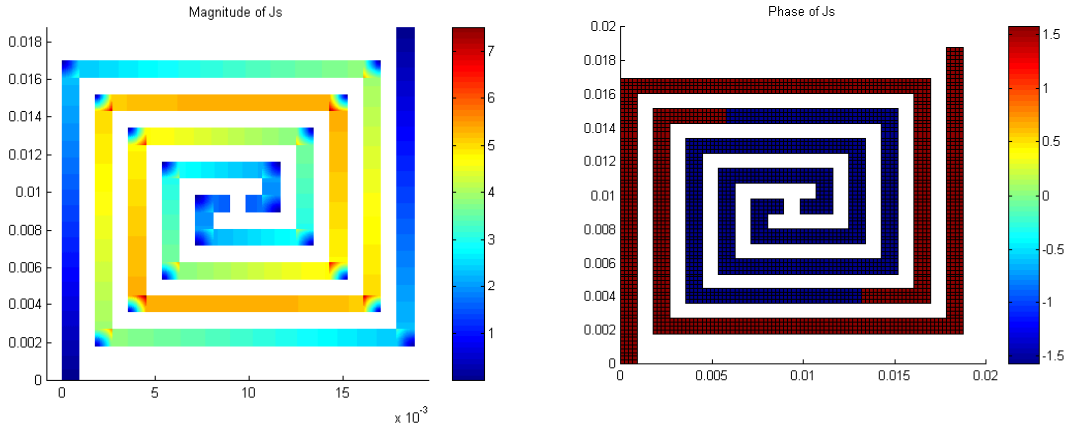

Figure 27. Magnitude of the surface current density [A/m^2] (left) and phase [rad] for the first mode of order 4 spiral.

Looking at the radiation patterns in Figure 28 it can be seen it is a dipole-like pattern, but the difference between the cross-polarization and the co-polarization is not as big as for the spiral 2 first mode case.

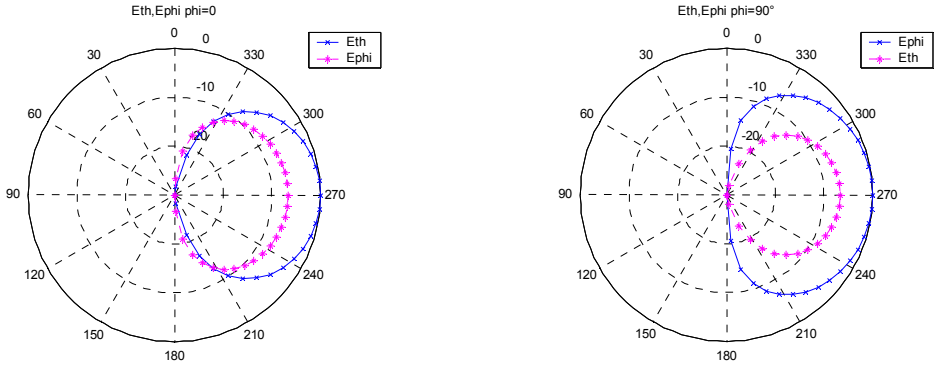

Figure 28. Radiation pattern for first mode of spiral 4, phi=0 (left), phi=90° (right).

For the fourth mode of spiral 4, which occurs at 7.33 GHz, again currents do not have the typical shape of a straight dipole mode, fact that is showing this mode is an own mode of the spiral. In Figure 23 again it is plotted in black and according to the y-axis on the left the magnitude of the MoM coefficients [A/m^2], and in red according to the y-axis on the right the phase of the MoM coefficients in degrees, for the second mode of spiral 2. This time the phase is varying along the arm of the spiral, so currents are not in phase.

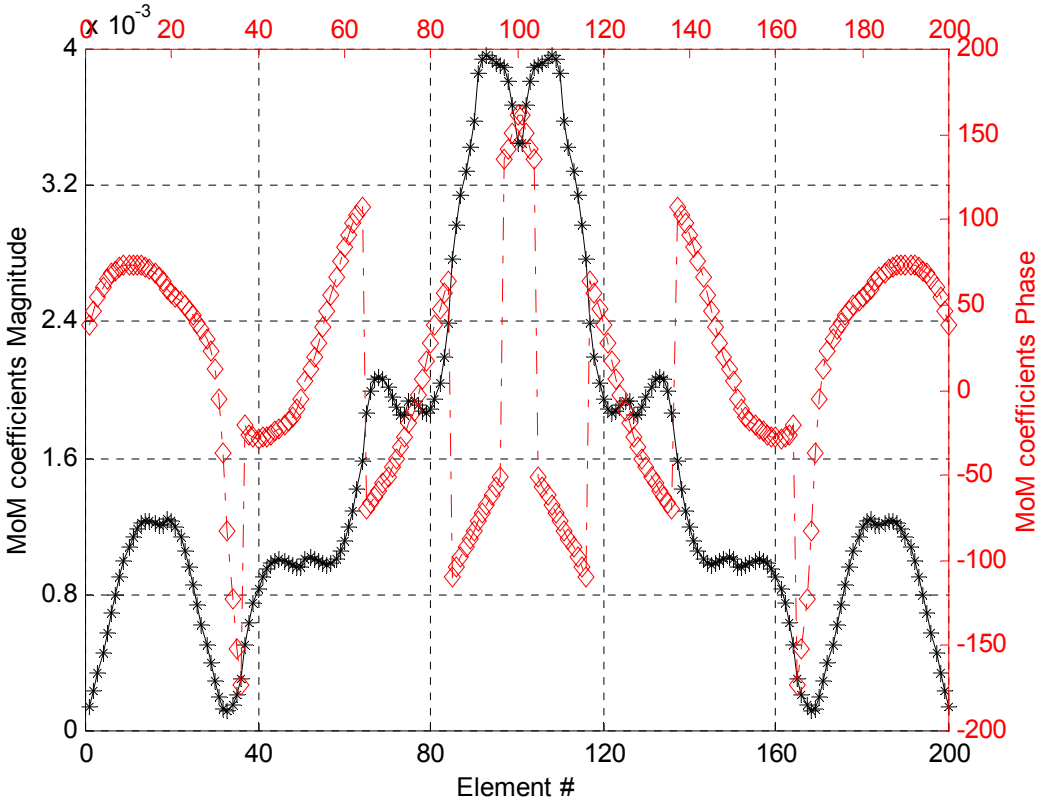

Figure 29. Magnitude and phase of current coefficients for order 4 spiral at f=7.33GHz.

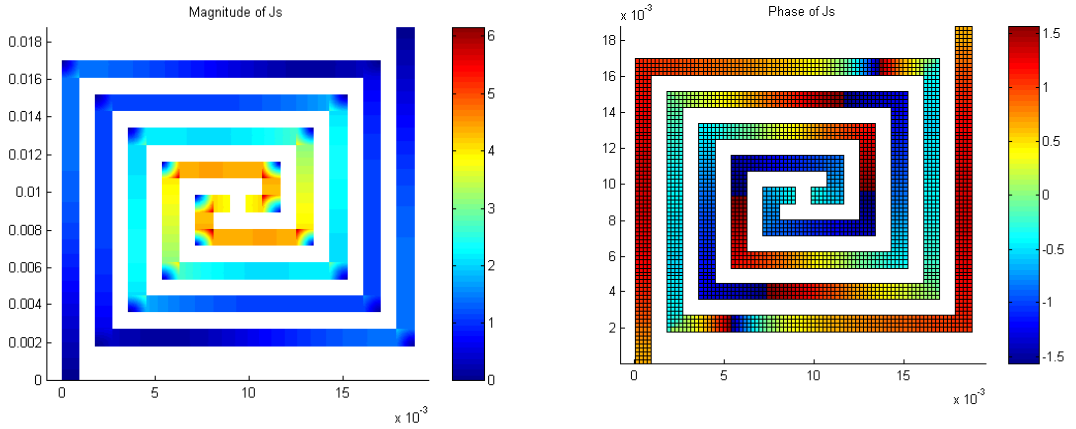

Figure 30. Magnitude of the surface current density [A/m^2] (left) and phase [rad] for the fourth mode of order 4 spiral.

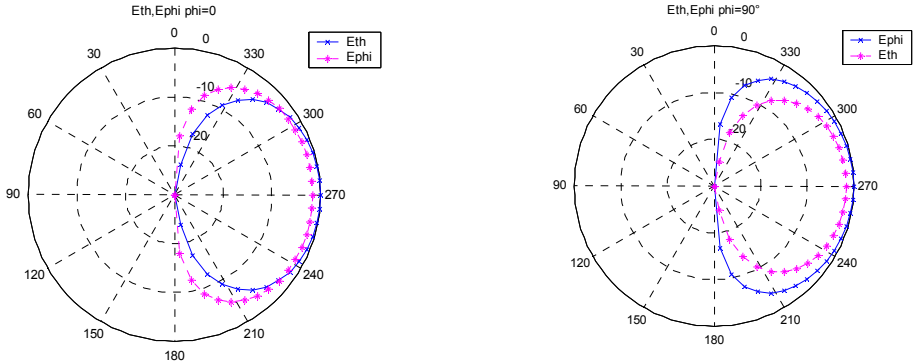

Figure 31. Radiation pattern for fourth mode of spiral 4, phi=0 (left), phi=90° (right).

As localised currents are not in phase, radiation pattern is not expected to be directive. Looking at Figure 31 it can be seen that the pattern lobe in both planes is even wider that for the first mode. As for the spiral 2 in its second mode, E_{th} and E_{ph} have the same level, so again for the case of spiral 4 we have a circular polarization for higher modes.

8.4. Conclusions

A study of a two arm square microstrip spiral antenna backed by a ground plane has been made.

A spiral presents interesting properties from the geometric point of view, namely self-similarity and infinite length in a finite surface, properties shared by fractal objects. Having chosen a polygonal spiral rather than a Archimedean one is due to the fact that polygonal spiral fits better in a given surface, achieving a more efficient utilization of given area, a principle to take into account when miniaturizing antennas.

Taking as working surface a square of side SL=1.875cm, different iterations of a spiral have been studied and compared with the equivalent "straight" case, that is a dipole, both the dipole build from the unwrapped spiral and the maximum length dipole that would fit in the reference square, thus a dipole having as length the diagonal of the square. All these data are summarized in Table 2.

	Fres1 [GHz]	**Fres2 [GHz]**	**Fres3 [GHz]**	**Fres4 [GHz]**	**Fres5 [GHz]**	**Fres6 [GHz]**	**Fres7 [GHz]**
Spiral 2	3.303	5.8485					
Spiral 4	1.7722	2.8876	4.6404	7.3371			
UWSpiral2	2.8182	5.6061	8.5152	11.3030			
UWSpiral4	1.6	3.3	5	6.6	8.3	10	11.5
Diag 2	11.1818						
Diag 4	11.6						

Table 2. In the range 1-13GHz resonances for: spirals order 2 and 4, unwrapped spirals order 2 and 4 and dipoles of length equal to the diagonal of the square where the spiral is inscribed.

Spiral 2 in the range of 1-13GHz has two resonances, if we increase the number of bendings in a factor of 2 we increase the number of resonances in the same factor. The unwrapped spiral with the same length as spiral 2 has four resonances, so it can be said that we are loosing resonances when making it curly. Besides, the first resonance of the dipole is slightly lower than for the spiral, but all this backwards are highly compensated with the size reduction: simply, if we have a surface limitation the dipole does not fit into. And the maximum dipole fitting in the given surface has so reduced length that it achieves the first resonance at a very high frequency (11.18 for a strip width of spiral 2 and 11.6 with a strip width of spiral 4).

A high size reduction has been achieved with a low frequency of resonance (1.77GHz for order 4), which can even be reduced by increasing the number of turns because order 4 does not reach the limit of technical possibilities.

Summarizing, these spirals constitute a very good benchmark to judge pre-fractal antennas as they provide a tough challenge offering excellent miniaturization while keeping a reasonable frequency behaviour. However, they do not show flexibility to shape a radiation pattern and this is a point where pre-fractal antennas can have a cutting edge.

8.5. References

[1] Heinz-Otto Peitgen, Hartmut Jürgens, Dietmar Saupe,"Chaos and Fractals", Springer Verlag.

[2] Ely J., Christodoulou C., Shively D., "Square Spiral Microstrip Antennas: Analysis for different sizes and substrate parameters using a personal computer", Southcon/95, Conference record, 1995.

DISCLAIMER

The work associated with this report has been carried out in accordance with the highest technical standards and the FRACTALCOMS partners have endeavoured to achieve the degree of accuracy and reliability appropriate to the work in question. However since the partners have no control over the use to which the information contained within the report is to be put by any other party, any other such party shall be deemed to have satisfied itself as to the suitability and reliability of the information in relation to any particular use, purpose or application.

Under no circumstances will any of the partners, their servants, employees or agents accept any liability whatsoever arising out of any error or inaccuracy contained in this report (or any further consolidation, summary, publication or dissemination of the information contained within this report) and/or the connected work and disclaim all liability for any loss, damage, expenses, claims or infringement of third party rights.